

**Impacts of Climate Change and Upstream Intervention on the Hydrology of the
Meghna River Basin using SWAT**

by

Afiya Narzis
1014162011P

In partial fulfillment of the requirements for the Degree of
MASTER OF SCIENCE IN WATER RESOURCES ENGINEERING



Department of Water Resources Engineering

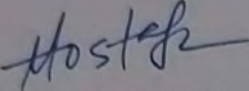
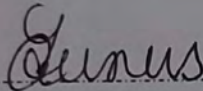
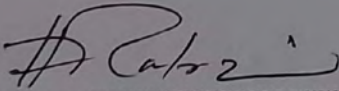
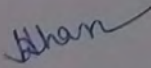
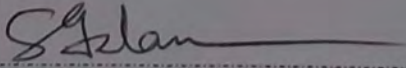
BANGLADESH UNIVERSITY OF ENGINEERING AND TECHNOLOGY

October, 2020

CERTIFICATION OF APPROVAL

The thesis titled "Impacts of Climate Change and Upstream Intervention on the Hydrology of The Meghna River Basin using SWAT" submitted by Afiya Narzis, Roll No: 1014162011, Session: October 2014, has been accepted as satisfactory in partial fulfillment of the requirement for the degree of Master of Science in Water Resources Engineering on October 03, 2020.

BOARD OF EXAMINERS

1. 
.....
Dr. Md. Mostafa Ali
Professor, Department of Water Resources Engineering
Bangladesh University of Engineering and Technology
Chairman
(Supervisor)
2. 
.....
Dr. Anika Yunus
Professor and Head,
Department of Water Resources Engineering
Bangladesh University of Engineering and Technology
Member
(Ex-officio)
3. 
.....
Dr. Md. Ataur Rahman
Professor, Department of Water Resources Engineering
Bangladesh University of Engineering and Technology
Member
4. 
.....
Dr. Nasreen Jahan
Associate Professor,
Department of Water Resources Engineering
Bangladesh University of Engineering and Technology
Member
5. 
.....
Dr. A. K. M. Saiful Islam
Professor, Institute of Water and Flood Management
Bangladesh University of Engineering and Technology
Member
(External)

DECLARATION

I hereby declare that this thesis is my original work and it has been written by me entirely. I have duly acknowledged all the sources of information which have been used in the thesis. This thesis has also not been submitted for any degree in any university previously.

Afiya Narzis

ACKNOWLEDGEMENT

All praise to Almighty Allah, the most beneficent and merciful who gave me enough courage and patience in this endeavor. This dissertation would not have been possible without the guidance, help, and contribution of several individuals by their valuable assistance in the preparation and completion of this study. First and foremost, I would like to express my sincere gratitude to my supervisor Prof. Dr. Md. Mostafa Ali for the continuous support of my M.Sc. study and related research, for his patience, motivation, and immense knowledge. His guidance helped me in all the time of research and writing of this thesis.

I would also like to thank Prof Dr. A. K. M. Saiful Islam and Associate Prof. Dr. Nasreen Jahan for their valuable suggestion regarding the climate change analysis part of this research. Without their significant input, the analysis could not have been successfully conducted.

I would also like to acknowledge Prof Dr. Md. Ataur Rahman and Prof. Dr. Anika Yunus as the member of the board of examiner, and I am gratefully indebted to them for their invaluable comments on this thesis.

Finally, I must express my very profound gratitude to my beautiful family for providing me with unfailing support and continuous encouragement throughout my years of study and through the process of researching and writing this thesis. This accomplishment would not have been possible without them.

Thank you.

Afiya Narzis

ABSTRACT

The Meghna river basin is expected to suffer from the adverse impacts of climate change according to the IPCC 5th assessment report and other hydrological studies. Previous studies and models indicated that the Meghna river basin area may experience frequent floods, high variability in rainfall patterns, and an increase in surface temperature which will disrupt the haor ecosystem. Moreover, any human-made intervention (dam/barrage) in the upstream part of the basin, may pose a great threat to the downstream country like Bangladesh. The present study developed a semi-distributed hydrological model for the Meghna river basin using SWAT to simulate the impact of changing climate and upstream intervention on the hydrologic cycle of the basin area. The model was set up using the topographic data, land cover data, soil property, and meteorological data. The simulated and observed hydrographs of the daily discharge showed a good agreement during calibration (2000-2008) and validation (2009-2018) and the results are NSE: 0.60, PBIAS: 23.55, RSR: 0.39, R²:0.71, and NSE: 0.64, PBIAS: 19.19, RSR: 0.36, R²: 0.68 respectively.

Initially, projected future precipitation and temperature from four RCM model outputs were analyzed under RCP 4.5 and RCP 8.5. Maximum changes in rainfall (-14.49% to +26.16%) and in average temperature (+2.20⁰C to +4.25⁰C) were observed under the dry-cold and wet-warm scenario. Predicted maximum changes (-250% to >400%) in mean monthly discharge is observed under wet-warm scenario (the 2080s, RCP 8.5). Whereas, the least changes in flow volume was observed (-100% to +100%) under the dry-cold scenario (in 2050s, RCP 4.5). Analyses of seasonal flow variation show that river flow will decrease (-7% to >50%) in every season under both RCP scenarios if the dry-cold scenario prevails. Contributions from the lateral flow and percolation losses will be much higher in future.

The probable impact of an upstream intervention (reservoir) on the Surma-Kushiyara river system at Amalshid was simulated for the present state (1998-2018) and near future (2049-2069). Results reveal that peak flow at Amalshid could be greatly affected in the monsoon and post-monsoon (> -60%) and may increase in the dry season (> +200%). The study will assist researchers to understand the hydrological changes and to study further how the chnages will impact the nature and the wetlands of the basin area.

Table of Contents

ACKNOWLEDGEMENT	iii
ABSTRACT.....	iv
List of Figures.....	viii
List of Tables	xii
1 INTRODUCTION.....	1
1.1 Background and Present State of the Problem.....	1
1.2 Objectives of the Study	2
1.3 Organization of the Thesis	3
2 LITERATURE REVIEW AND THEORETICAL BACKGROUND	4
2.1 Physiography.....	4
2.2 Hydrometeorology of Meghna River Basin.....	5
2.3 Major River System	6
2.3.1 The Barak river system.....	6
2.3.2 The Surma-Kushiyara river system	7
2.4 Review of Previous Studies	8
2.4.1 Application of SWAT model for large basin hydrologic responses.....	8
2.4.2 Climate change studies using SWAT model	10
2.4.3 Impact analysis of upstream intervention using SWAT.....	13
2.4.4 Previous studies on upper Meghna river basin	17
2.5 Theoretical Background.....	20
2.5.1 Overview of the SWAT model.....	20
2.5.2 Climate change modeling for hydrological impact assessment.....	29
3 METHODOLOGY	37
3.1 General	37
3.2 Data Collection.....	37
3.2.1 Digital elevation model, stream network, land use, and soil data	37

3.2.2	Weather, discharge, and water level data	41
3.3	Methodological Framework	44
4	MODEL SETUP AND SELECTION OF SCENARIOS	46
4.1	Model Setup	46
4.1.1	Watershed configuration.....	46
4.1.2	HRU analysis	47
4.1.3	Bias correction of rainfall data.....	48
4.1.4	Weather data input	50
4.1.5	Point source discharge data input	51
4.2	Model Simulation.....	51
4.3	Model Calibration and Validation.....	52
4.3.1	Selection of calibration parameters.....	53
4.4	Sensitivity Analysis.....	56
4.5	Calibration Outputs	59
4.6	Evaluation of Model Performance	59
4.6.1	Model evaluation statistics.....	59
4.7	Selection of Climate Change Scenario.....	65
4.7.1	Shortlisting of GCMs/RCMs	65
4.8	Selection of Upstream Intervention Scenario	69
4.8.1	Secondary data and information collected from the previous study.....	69
5	ANALYSIS AND RESULTS	74
5.1	Model Outputs.....	74
5.1.1	Daily and monthly discharge	74
5.1.2	Water balance components	75
5.2	Climate Change Analysis	78
5.2.1	Projected precipitation	78
5.2.2	Projected temperature	79

5.2.3	Impact on discharge	80
5.2.4	Impact on water balance components	95
5.3	Impact on flow due to upstream intervention	109
5.3.1	Reservoir/Dam location	110
5.3.2	Reservoir/Dam operation	111
5.3.3	Post-Dam river flow at Amalshid (Present State).....	112
5.3.4	Post-Dam river flow at Amalshid (2050s).....	115
5.3.5	Summary of the results	116
6	CONCLUSION AND RECOMMENDATIONS	120
6.1	Conclusion.....	120
6.2	Limitations	121
6.3	Recommendations	121
7	References	123

List of Figures

Figure 2.1 Location of Meghna River basin inside and outside Bangladesh (Water Resources Information System (WRIS), India,2014).....	4
Figure 2.2 Location of Meghna River Basin in GBM Delta (Joint River Commission Bangladesh, 2018)	6
Figure 2.3 Barak River System.....	7
Figure 2.4 Schematic representation of the hydrologic process in the SWAT model....	21
Figure 2.5 All forcing agents' atmospheric CO ₂ -equivalent concentrations according to the four RCPs (https://en.wikipedia.org/wiki/Representative_Concentration_Pathway)	33
Figure 3.1 Digital Elevation Model (DEM) of the Meghna Basin	38
Figure 3.2 Stream network of the Meghna Basin	39
Figure 3.3 Land cover type and land use pattern map of Meghan river basin.....	40
Figure 3.4 Soil Classification Map of Meghan River Basin.....	41
Figure 3.5 Schematic of SWAT model development and scenario analysis	45
Figure 4.1 Delineated watershed of the Meghna river basin	47
Figure 4.2 HRU definition within the study area.....	48
Figure 4.3 Bias correction at Sylhet.....	49
Figure 4.4 Bias correction at Srimangal	49
Figure 4.5 Location of satellite-derived weather data station.....	50
Figure 4.6 Linkage between SWAT and five optimization programs [67]	53
Figure 4.7 Graph of statistical index values: “t-stat”; and “p-value” vs calibrated parameters.....	58
Figure 4.8 Scatter plot of simulated vs observed discharge at Sheola for the calibration and validation period of the model	62
Figure 4.9 Daily observed discharge (at Sheola) and simulated discharge (at Sheola) hydrograph for calibration and validation of the model	64
Figure 4.10 Projected changes in mean air temperature (ΔT) and annual precipitation sum (ΔP) between the historic period and 2080s for four RCP 4.5 RCMs.....	67
Figure 4.11 Projected changes in mean air temperature (ΔT) and annual precipitation sum (ΔP) between the historic period and 2080s for four RCP 8.5 RCMs.....	68
Figure 4.12 Area-Elevation curve collected for Dam Reservoir [59].....	70

Figure 4.13 Capacity-Elevation curve collected for Dam Reservoir [59]	70
Figure 4.14 DPR suggested or desired rule curve (for June to October) and assumed rule curve for the rest of the period [59]	71
Figure 4.15 Day average discharge at dam site on the Barak River [59]	72
Figure 4.16 Possible withdrawal of water from the Barak River for an irrigation project [59].....	72
Figure 5.1 Observed and simulated mean monthly discharge at the catchment outlet station near Sheola (SW 173) for 2000-2018	75
Figure 5.2 Mean monthly water balance components of the basin (2000- 2018)	76
Figure 5.3 Spatial distribution of average annual rainfall, evapotranspiration, surface runoff, potential evapotranspiration, water yield, percolation, groundwater in the basin area.....	77
Figure 5.4 Changes in annual precipitation under RCP 4.5 and RCP 8.5	79
Figure 5.5 Changes in average annual temperature under RCP 4.5 and RCP 8.5	80
Figure 5.6 Mean monthly discharge under RCP 4.5 (wet-warm scenario)	81
Figure 5.7 Changes in monthly discharge in the 2020 under RCP 4.5 (wet-warm scenario)	82
Figure 5.8 Changes in monthly discharge in the 2050s under RCP 4.5 (wet-warm scenario).....	83
Figure 5.9 Changes in monthly discharge in the 2080s under RCP 4.5 (wet-warm scenario).....	83
Figure 5.10 Mean monthly discharge under RCP 4.5 (dry-cold scenario).....	85
Figure 5.11 Changes in monthly discharge in the 2020s under RCP 4.5 (dry-cold scenario)	86
Figure 5.12 Changes in monthly discharge in the 2050s under RCP 4.5 (dry-cold scenario)	86
Figure 5.13 Changes in monthly discharge in the 2080s under RCP 4.5 (dry-cold scenario)	87
Figure 5.14 Mean monthly discharge under RCP 8.5 (wet-warm scenario)	88
Figure 5.15 Changes in monthly discharge in the 2020s under RCP 8.5 (wet-warm scenario).....	88
Figure 5.16 Changes in monthly discharge in the 2050s under RCP 8.5 (wet-warm scenario).....	89
Figure 5.17 Mean monthly discharge under RCP 8.5 (dry-cold scenario).....	90

Figure 5.18 Changes in mean monthly discharge in the 2020s under RCP 8.5 (dry-cold scenario).....	91
Figure 5.19 Changes in mean monthly discharge in the 2050s under RCP 8.5 (dry-cold scenario).....	91
Figure 5.20 Changes in mean monthly discharge in the 2080s under RCP 8.5 (dry-cold scenario).....	92
Figure 5.21 Changes in seasonal flow under RCP 4.5 (wet-warm scenario)	93
Figure 5.22 Changes in seasonal flow under RCP 4.5 (dry-cold scenario)	93
Figure 5.23 Changes in seasonal flow under RCP 8.5 (wet-warm scenario)	94
Figure 5.24 Changes in seasonal flow under RCP 8.5 (dry-cold scenario)	95
Figure 5.25 Percent changes in evapotranspiration (ET mm) under RCP 4.5 (wet-warm scenario).....	96
Figure 5.26 Percent changes in evapotranspiration (ET mm) under under RCP 4.5 (dry-cold scenario).....	97
Figure 5.27 Percent changes in evapotranspiration (ET mm) under RCP 8.5 (wet-warm scenario).....	97
Figure 5.28 Percent changes in evapotranspiration (ET mm) RCP 8.5 (dry-cold scenario)	98
Figure 5.29 Percent changes in water yield (WYLDmm) under RCP 4.5 (wet-warm scenario).....	99
Figure 5.30 Percent changes in water yield (WYLDmm) under RCP 4.5 (dry-cold scenario).....	99
Figure 5.31 Percent changes in water yield (WYLDmm) under RCP 8.5 (wet-warm scenario).....	100
Figure 5.32 Percent changes in water yield (WYLDmm) under RCP 8.5 (dry-cold scenario).....	101
Figure 5.33 Percent changes in groundwater contribution (GWmm) under RCP 4.5 (wet-warm scenario).....	101
Figure 5.34 Percent changes in groundwater contribution (GWmm) under RCP 4.5 (dry-cold scenario).....	102
Figure 5.35 Percent changes in groundwater contribution (GWmm) under RCP 8.5 (wet-warm scenario).....	103
Figure 5.36 Percent changes in groundwater contribution (GWmm) under RCP 8.5 (dry-cold scenario).....	103

Figure 5.37 Percent changes in percolation (PERCmm) under RCP 4.5 (wet-warm scenario).....	104
Figure 5.38 Percent changes in percolation (PERCmm) under RCP 4.5 (dry-cold scenario).....	105
Figure 5.39 Percent changes in percolation (PERCmm) under RCP 8.5 (wet-warm scenario).....	105
Figure 5.40 Percent changes in percolation (PERCmm) under RCP 8.5 (dry-cold scenario).....	106
Figure 5.41 Percent changes in lateral flow (LAT_Qmm) under RCP 4.5 (wet-warm scenario).....	107
Figure 5.42 Percent changes in lateral flow (LAT_Qmm) under RCP 4.5 (dry-cold scenario).....	107
Figure 5.43 Percent changes in lateral flow (LAT_Qmm) under RCP 8.5 (wet-warm scenario).....	108
Figure 5.44 Percent changes in lateral flow (LAT_Qmm)	108
Figure 5.45 Location map of Tipaimukh dam, Fulertal barrage site and Amalshid [57]	109
Figure 5.46 Hypothetical reservoir/dam location in the Meghna basin.....	110
Figure 5.47 Simulated discharge at Amalshid and reservoir/dam location	111
Figure 5.48 Simulated target release from the reservoir/dam.....	112
Figure 5.49 Post-dam Amalshid flow (1998-2018)	113
Figure 5.50 Average discharge at Amalshid in driest monsoon year (2005)	113
Figure 5.51 Average discharge at Amalshid in average monsoon year (1998).....	114
Figure 5.52 Post-dam Amalshid flow (2040-2069) under wet-warm scenario	115

List of Tables

Table 3.1 Generic Codes of Land Cover Types Used in SWAT	40
Table 3.2 Collected input data for model setup and development.....	42
Table 4.1 Calibration parameters reported in various watershed studies [17].....	54
Table 4.2 Calibration parameters generally used for SWAT model [50].....	55
Table 4.3 Initial range of the calibration parameters	56
Table 4.4 Ranking of sensitive parameter based on t-stat and p-value.....	57
Table 4.5 Final adjusted intervals and calibrated value for each parameter.....	59
Table 4.6 Classification of statistical indices.....	61
Table 4.7 Model performance evaluation	62
Table 4.8 List of experiments by CORDEX-SA initially considered for climate change analysis.....	66
Table 4.9 List of RCM models classified based on projection scenario.....	69
Table 5.1 Monthly observed and simulated discharge at the catchment outlet station near Sheola (SW 173).....	74
Table 5.2 Percent changes in annual precipitation sum.....	78
Table 5.3 Percent changes in average annual temperature	79
Table 5.4 Available discharge in the Surma-Kushiyara river system at Amalshid during monsoon, post-monsoon and dry season for pre and post dam condition	114
Table 5.5 Summary of the results of scenario analyses	116

1 INTRODUCTION

1.1 Background and Present State of the Problem

Bangladesh is most vulnerable to the challenges associated with the impact of climate change. This is due to the diversified climate in the Ganges-Brahmaputra-Meghna (GBM) river basin. The GBM river basin is a trans-boundary river basin distributed between India (64 percent), China (18 percent), Nepal (9 percent), Bangladesh (7 percent), and Bhutan (3 percent) [57]. Nepal is located entirely in the Ganges river basin and Bhutan is located entirely in the Brahmaputra river basin. Bangladesh and the eastern part of West Bengal in India are formed at the confluence of the Ganga, Brahmaputra, and Meghna (GBM) rivers and their tributaries. Climate change may alter the distribution and quality of GBM river basin water resources. The occurrence of more intense rains, changed the spatial and temporal distribution of rainfall, higher runoff generation, low groundwater recharge, melting of glaciers, changes in evaporative demands, and water use patterns in agricultural, municipal, and industrial sectors, etc. may be the possible impacts of climate change. These impacts will lead to severe natural hazards in Bangladesh. Therefore, understanding the hydrologic characteristics of the three river basins of GBM is one of the important concerns of this country for effective river basin management.

Meghna river basin (also known as Upper Meghna river basin), located in the south of one of the rainiest regions in the world, has an annual rainfall of up to 5,800 mm [58]. It occupies a total area of 82,000 km², distributed between India (57%) and Bangladesh (43%)[62]. Meghna River Basin includes six administrative districts, that is, Kishoreganj, Netrokona, Habiganj, Moulvibazar, Sunamgang, and Sylhet. Meghna river is estimated to have a peak flood flow of 19,800 m³/sec and receives a huge amount of sediment inflow (approximately 13 million tons is deposited in the basin every year), resulting in extremely harsh natural conditions. Furthermore, since much of the basin is located in India the area is highly vulnerable to the impacts to be imparted by any upstream intervention on the Indian side [19],[29],[48]. Besides, the anticipated climate change is likely to have a major impact on the overall hydrology of the Meghna river basin and will ultimately lead to an increase in the frequency of water-induced disasters in Bangladesh.

Research studies focusing on climate change responses of the Meghna river basin are very limited in our country. Most of the studies investigated the climate change impacts on stream flow and cannot represent how climate change stresses will affect the existing water balance components of the basin [65]. Research studies of the Meghna river basin addressing the inevitable challenges of climate change also includes very limited application of IPCC AR4 [43] and AR5 scenarios. But climate change also brings about substantial alternatives of precipitation and temperature in the spatial and temporal patterns. These changes affect evaporation, snowmelt, infiltration, and runoff, altering the hydrological cycle and causes flood or drought events. This requires ensemble climate-hydrology modeling consisting of multiple climate ensembles and RCP scenarios by IPCC assessment report 5 to predict long term streamflow. Previous studies that include RCPs did not consider the uncertainties involved in the projection of different GCM and RCM model output. Hence, the current study aims at filling the above mentioned research gaps by developing a semi-distributed hydrologic model in conjunction with climate scenarios (IPCC AR5 scenarios, climate ensemble of RCM outputs) to understand the behavior of hydrologic systems of Meghna river basins to make better predictions and to address the major challenges in the basin area. SWAT is a river basin scale hydrological model that can assess the water balance of catchments, potential future climatic changes, impact of the reservoir or flow-regulating structures, etc. Therefore, the present study intends to develop a hydrological model for the Meghna river basin area using SWAT to investigate the probable scenario of future climate on the hydrologic cycle of the basin and probable impacts of the upstream intervention on the Barak river at Manipur on the basin area.

1.2 Objectives of the Study

The specific aims of the study are-

- (a)** To develop a baseline hydrological model for the Meghna river basin using SWAT to simulate the hydrology and water balance.
- (b)** To evaluate the hydrologic condition and water balance of the study area under projected future climate extreme and moderate scenarios.
- (c)** To assess the hydrological impacts of upstream intervention at Manipur on the Surma-Kushiyara river system.

1.3 Organization of the Thesis

Chapter 1 includes the introduction of the present study. Background and present state of the study along with the specific objectives.

Chapter 2 comprises the literature review and the theoretical background. This chapter describes the hydro morphology, topography, and major river system of the Meghna river basin. A review of previous studies has been conducted in several categories- application of the SWAT model to compute large basin hydrology, the impact of climate change and upstream intervention studies, and previous works on the Meghna river basin.

Chapter 3 discusses the steps followed in the present thesis to set up and develop the SWAT model, from data collection to the methodological framework of the thesis.

Chapter 4 includes calibration/validation of total discharge, sensitivity analysis, selection of climate change scenario, and reservoir scenario to assess the impact of climate change and upstream intervention on the hydrology of the Meghna River Basin.

Chapter 5 is the results and analysis chapter where projected future climate extreme and moderate scenarios have been analyzed. Model outputs are discussed for different climate scenarios under RCP 4.5 and 8.5 and reservoir operation. Changes in the water balance of the Meghna river basin has also been discussed here.

Chapter 6 is the conclusion and recommendations. This chapter gives a summary of the results obtained in this study and also includes recommendations for further study.

2 LITERATURE REVIEW AND THEORETICAL BACKGROUND

2.1 Physiography

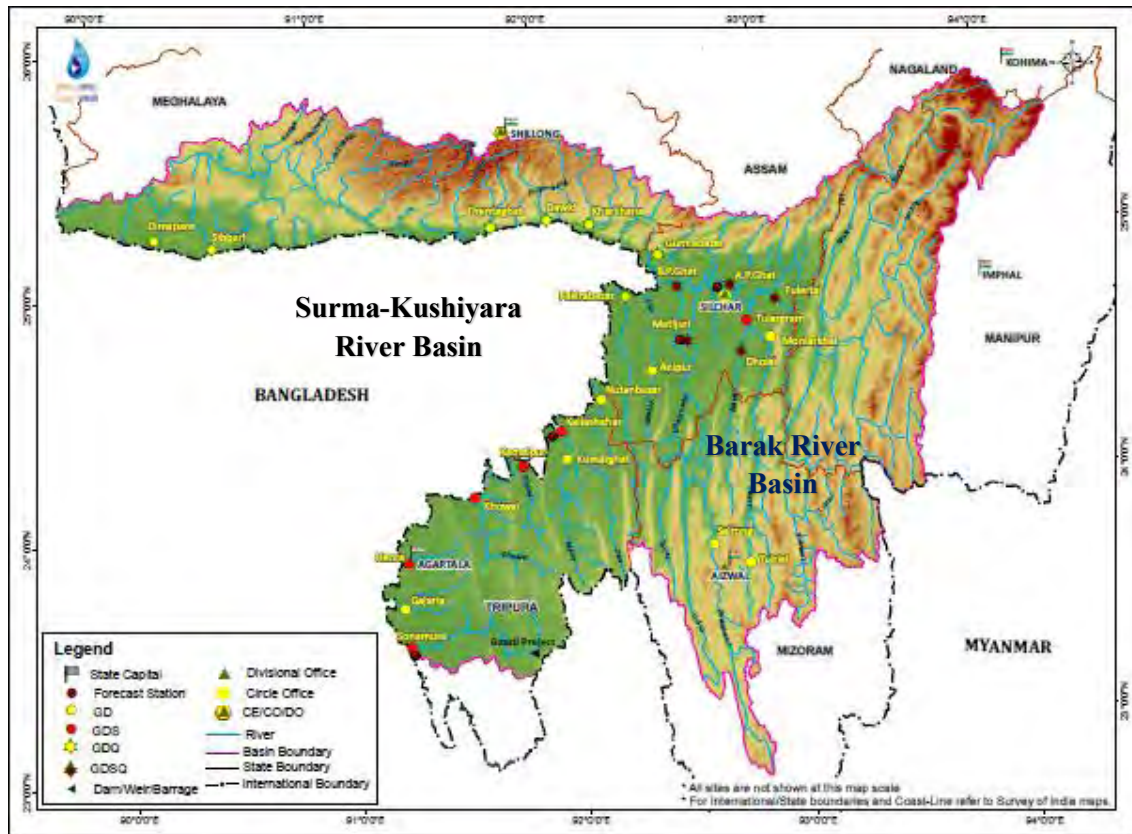


Figure 2.1 Location of Meghna River basin inside and outside Bangladesh (Water Resources Information System (WRIS), India,2014)

Meghna river basin is a significant part of the greater Ganges-Brahmaputra-Meghna (GBM) basin. The basin is less than 5 percent of the total GBM basin, but the area is more than half of the country, and discharge is nearly 20 percent. Meghna basin covers partial land of two countries, India and Bangladesh. About 43 percent (35,000 sq km) of the total Meghna basin area lies within Bangladesh. The upper part of the basin consists of hills, forests, cultivated lands, and tea gardens. From the view of the Bangladesh side, the total basin is constituted of four parts- (a) The Barak (b) The Surma (southern part of Meghalaya mountains) (c) The Kushiyara (northern Tripura hill), and (d) Sylhet, inner region.

Meghna basin outside Bangladesh, known as the Barak basin (Figure 2.1), covers the larger part eastern India including the partial area of Meghalaya, Assam, Tripura,

Mizoram, Nagaland, and Manipur province. The Barak sub-basin drains areas in India, Bangladesh, and Myanmar. The drainage area of the sub-basin lying in India is 41,723 sq. km. which is nearly 1.38% of the total geographical area of the country [60]. It is bounded on the north by the Barail range separating it from the Brahmaputra sub-basin, on the east by the Naga and Lushai hills, and on the south and west by Bangladesh. The sub-basin lies in the States of Meghalaya, Manipur, Mizpra, Assam, Tripura, and Nagaland.

The total basin system of Meghna inside the Bangladesh boundary, including upper tributaries known as the Surma-Kushiyara-Meghna river system. It covers the northeastern haor region of Sylhet district and southeastern Bangladesh. The physical setting and hydrology of this Sylhet (haor) region have created innumerable opportunities as well as constraints for the inhabitants of the haor. The region has distinctive hydrological characteristics. Annual rainfall ranges from 2200 mm along the western boundary to 5800 mm in its northeast corner and is as high as 12000 mm in the headwaters of some catchments extending to India [60]. The region receives water from the catchment slopes of the Shillong Plateau across the borders in India to the north and the Tripura Hills in India to the south-east.

2.2 Hydrometeorology of Meghna River Basin

River Meghna is mainly formed due to the confluence of the Surma and Kushiyara rivers originating from the hilly regions of eastern India as the Barak River. Barak River rises from the Manipur hills, south of Mao in Senapati district of Manipur at an elevation of 2,331 m. It enters Bangladesh at Amalshid, the easternmost village of the country, where it is subdivided into Kushiyara (south) and Surma (north) and meets again at Markuli, where it is named as Meghna. Down to Chandpur (above Bhairab Bazar), the Meghna river is hydrographically referred to as the Upper Meghna (Figure 2.2).

The Basin system centered on this Upper Meghna River, as well as the Surma River and Kushiyara River, is known as the Meghna river basin. It is also called as Upper Meghna basin, Barak-Kushiyara, or Surma-Meghna basin. The basin lies in India (57%), Myanmar, and Bangladesh (43%). It is bounded on the north by the Barail range, on the east by the Naga and Lushai hills. The basin area covers almost 23 % of the total area of

Bangladesh and includes six administrative districts that are Kishoreganj, Netrokona, Habiganj, Moulvibazar, Sunamgang, and Sylhet. The total drainage area of the basin is 82,000 sq.km, and the total length is more than 800 km [58]. The average annual rainfall and peak flood flow of the basin are 5800 mm and 19800 m³/sec respectively.

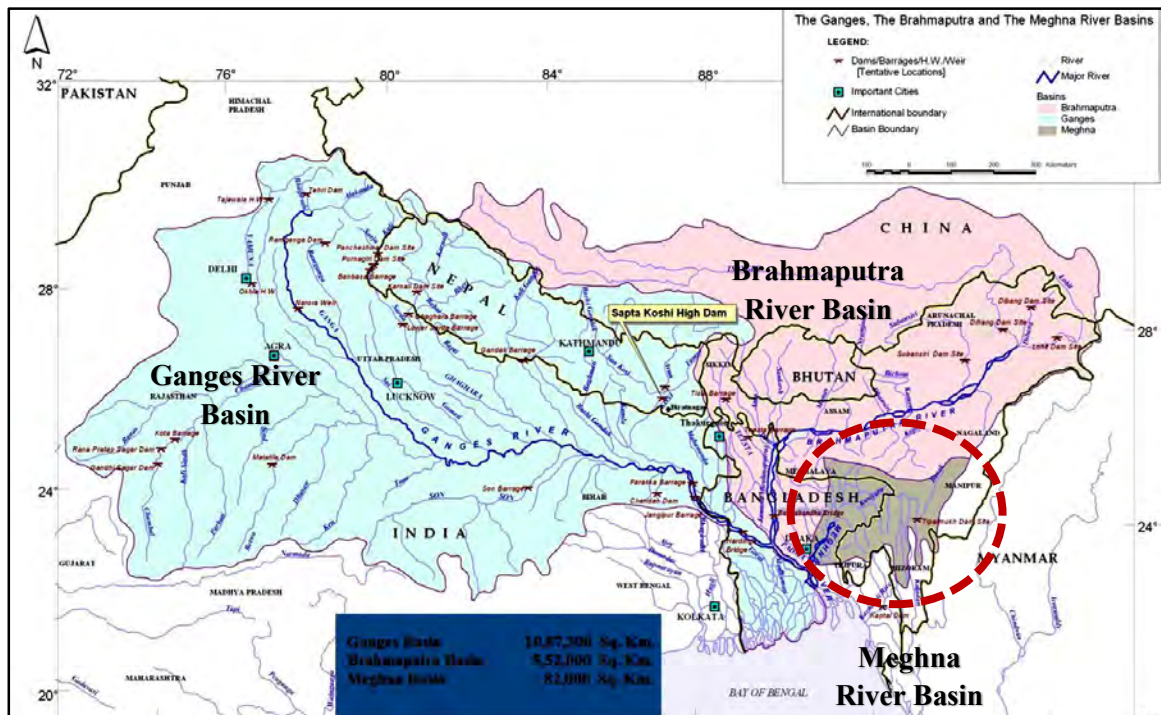


Figure 2.2 Location of Meghna River Basin in GBM Delta (Joint River Commission Bangladesh, 2018)

2.3 Major River System

2.3.1 The Barak river system

Meghna river basin outside Bangladesh is mainly known as the Barak River basin. This basin system is centered on the Barak river. It rises on the southern slope of the lofty Barail Range near the border of Manipur and Nagaland and forms a part of the northern boundary of the Manipur State with Nagaland where it is known as Kirong. From there it flows a westerly and southerly course to Tipaimukh, where it sharply turns to the north, and for a considerable distance, forms the boundary line between the Cachar district of Assam and Manipur. Thereafter, it turns westward at Jirimukh and runs through the Cachar plain sluggishly. Near Karimganj, it is bifurcated into the northern branch of Surma and the southern branch of Kushiyara (Figure 2.3). The river with a total length of

900 km from source to mouth drains an area of 52,000 sq. km [1]. The river drains the southern part of the Assam which includes the districts of Cachar, Karimganj, Hailakandi, and the southern part of the North Cachar Hills.

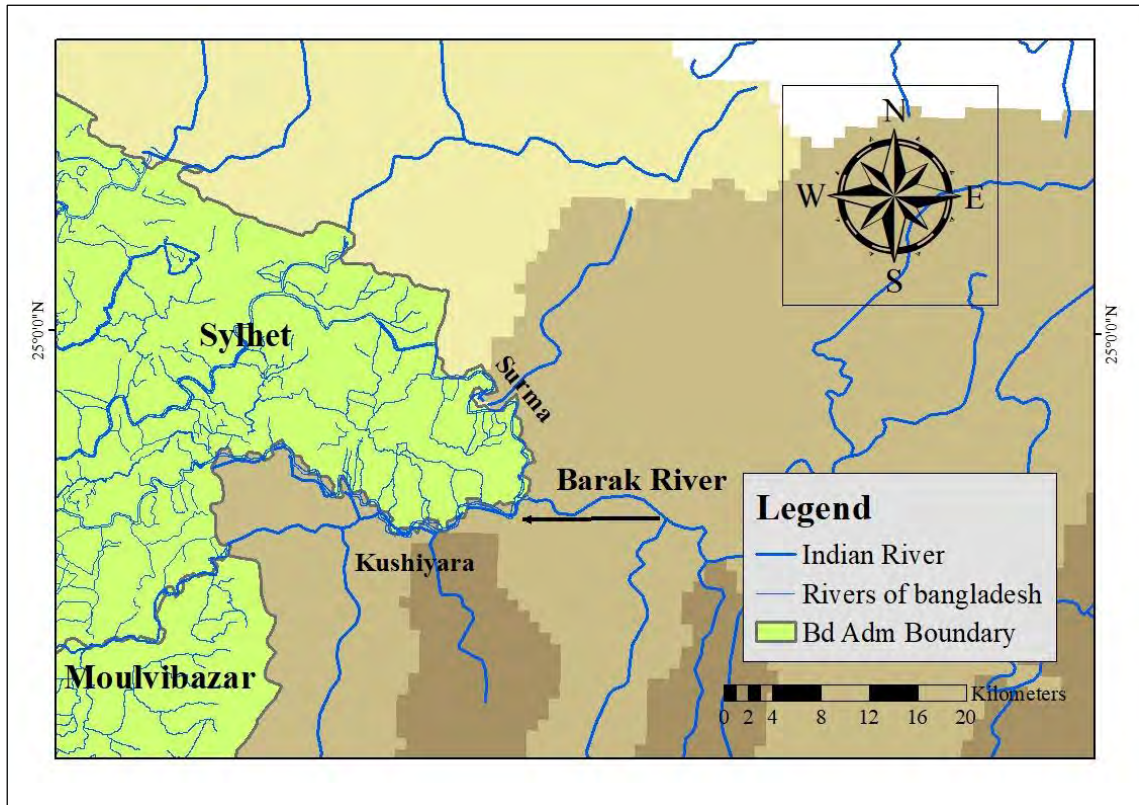


Figure 2.3 Barak River System

2.3.2 The Surma-Kushiyara river system

The major rivers and representative basins inside Bangladesh in the Upper Meghna Basin can be classified into the following two-

- a. Basin system centered on the Surma River and Kushiyara River, where the central lowland haors are vulnerable to damage from flash floods and monsoon floods.
- b. River and basin systems near to sloping land around the border regions, for example, the Khowai River in the south and Khankusha River in the north, which are vulnerable to damage from flash floods.

Surma River flows west and then southwest to Sylhet town. From there it flows northwest and west to Sunamganj town. Then it maintains a course southwest and then south to Markuli to meet Kushiyara. The joint course flows up to Bhairab Bazar as the Kalni. Flowing north of the Sylhet basin, Surma receives tributaries from Khasi and Jaintia Hills

of Shillong plateau. East to west, they are Lubha, Hari, Goyain Gang, Piyain, Bogapani, Jadukata, Shomeshwari, Kangsa, and Mogra. Surma bifurcates south of Mohanganj soon after it receives Kangsa and further south the Mogra. The western channel is known as Dhanu in its upper course, Boulai in the middle, and Ghorautra lower down. It joins Kalni near Bhairab Bazar of Kishoreganj district and the name Meghna is given to the course from this confluence to the Bay of Bengal. Meghna receives Old Brahmaputra on its right-bank at Bhairab Bazar and on the way to the Bay it carries the water of Padma from Chandpur [1]. Kushiya receives left bank tributaries from Tripura hills, the principal ones being Manu, north of Maulvi Bazar town and bifurcates into the northern channel, the Bibiyana, and a southern one, which resumes the original name, Barak [2]. Bibiyana changes its name to Kalni lowering down its course and joins Surma near Ajmiriganj. Barak receives Gopla and Khowai from Tripura Hills and falls into Surma at Madna [3]. Unlike Surma, the tributaries of Kushiya are less violent although prone to producing flash floods in part due to lesser elevations and rainfall of Tripura Hills.

Between Surma and Kushiya, there lies a complex basin area comprised of depressions. Most of the Surma system falls in the Haor basin, where the line of drainage is not clear or well defined. In the piedmont tract from Durgapur to Jaintiapur, the network of streams and channels overflows in the rainy season and creates vast sheets of water that connect the haors with the rivers.

2.4 Review of Previous Studies

2.4.1 Application of SWAT model for large basin hydrologic responses

To understand the hydrologic processes within a catchment area, it is necessary to acquire a large amount of detailed quantitative measurements at different spatial and temporal scales. The strength of the hydrological model is that it can provide an output at high temporal and spatial resolutions, and for hydrological processes, those are difficult to observe in the case of large basins. Hydrological models (SWAT, HEC-HMS, VIC, etc.) therefore enable us to gain insight into hydrologic processes using a limited number of measurements in large basins.

SWAT has been successfully applied to simulate the hydrologic response of the hilly parts of a Himalayan river basin in [30]. The basin receives a contribution from snow/glaciers

and rainfall. The study was mainly conducted for the Ganga River Basin up to Devprayag. The catchment area is about 18,728 km² and elevation varies from 427 m to 7785 m. The study developed a hydrologic model using SWAT employing a larger amount of observed data to determine various water balance components for a better understanding of the hydrologic response of the watershed. The water balance components that have been considered are- the total amount of precipitation, actual evapotranspiration, snowmelt runoff, and water yield. The model results indicate that the overall shape of the simulated hydrograph is well representative of the observed hydrograph and the recession behavior is also well simulated by the SWAT model. Contribution from direct surface runoff is found to be small in the water yield and the main contribution to water yield is through lateral flow and groundwater flow. As Ganga river up to Devprayag is a comparatively less snow-covered area, evapotranspiration found to be of a higher rate. The statistical performance of the model R² and NSE for calibration and validation vary between 0.69 and 0.64 and can be considered as good. Thus, the SWAT model can be considered to be a good tool to model the discharge hydrograph and various water balance components for a large basin-like Himalayan river basin.

To evaluate the water cycle situation and to verify the adaptability of the China Meteorological Assimilation Driving Datasets for the (CMADS) for large basins a hydrological model has been developed in [38] using SWAT. The Manas River Basin (MRB) which is located between the northern foothills of the Tian-shan mountain chain and the north of the Junggar Basin, China has been chosen as the study area. The length of the basin is 260,8 km from south to north and 198,7 km from east to west, and the total area is 31.000 km². The SWAT model was firstly built to simulate water resources of the MRB, then the model was calibrated with CMADS dataset and finally, the simulated runoff was calibrated with observed data using SWAT-CUP (SWAT Calibration and Uncertainty Programs). Also, parameter sensitivity analysis, parameter calibration, and validation have been included in the study. Model results demonstrate that the SWAT model could well reproduce the runoff process of multiple (two) stations (Kenswat and Hongshanzui) in the research area by using data from CMADS. The simulation performed well on a monthly scale in both stations, where R² ranges between 0.56-0.99 and NSE in between 0.84-0.99. Finally, the study suggests that the SWAT model can show satisfactory results through parameter calibration in areas with a high glacial recharge

rate. Moreover, CMADS can provide necessary meteorological data for SWAT simulations and support parameter calibration and historical surface data analysis.

Integration of remote sensing or satellite-derived products i.e. gridded precipitation and temperature data, with the Soil and Water Assessment Tool (SWAT) to evaluate the hydrology, sediment yield and water balance have been tested in a study. The study has been conducted for the Ken basin (28,672 km²) area of Central India in [7]. The entire basin area has been divided into 10 sub-basins comprising 143 hydrological response units based on unique land cover, soil, and slope classes using the SWAT model. The runoff simulation is good on daily basis ($R^2 = 0.766$ and 0.780 for calibration and validation period respectively) and further improved (very good) on monthly basis ($R^2 = 0.946$ and 0.959 for calibration and validation period respectively). The sediment simulation is considerable on daily basis ($R^2 = 0.429$ and 0.379 for calibration and validation period respectively) and also further improved (good) on monthly basis ($R^2 = 0.748$ and 0.721 for calibration and validation period respectively). From the calibration and validation results, the study concluded that the SWAT model is capable of simulating hydrology and sediment concentration of the study area accurately and can be applied for large catchment areas as well.

2.4.2 Climate change studies using SWAT model

Hydrologic models have gained widespread attention to understand the implication of climate change on water availability. The Soil and Water Assessment Tool (SWAT) has widely been used to assess the impact of climate change on hydrological variables, water resources, and water balance components. For instance, in [9] SWAT was used to investigate the variability and trend of hydrological variables, i.e., precipitation, temperature, evapotranspiration, soil moisture, deep aquifer recharge, and water yield under the impacts of climate change in Alberta, Canada. The calibrated model was used to generate these variables. Future changes were investigated under two representative concentration pathways, i.e., RCP 2.6 and RCP 8.5, projected by nine global climate models (GCM).

The impact of future climate change on Tekeze basin hydrology was investigated in [14] using bias-corrected ensembles of CORDEX-Africa RCP 4.5 and RCP 8.5 climate scenarios projections of precipitation and temperature. Soil and Water Assessment Tool (SWAT) used to simulate streamflow Results from the simulation showed an increase in mean temperature up to 1.07 °C for RCP 4.5 and 2.21 °C for RCP 8.5 climate scenarios in all periods. The long rain and dry season's precipitation also showed an increasing trend up to 48%, whereas the short rain season showed a decreasing trend up to 52% under both RCP scenarios for all future periods annually. For this study, SWAT performs well with values of Nash-Sutcliffe efficiency and R^2 greater than 0.7 for simulating streamflow with reasonable accuracy. Results from this study indicated that the SWAT model gives better simulation results for future prediction and shows that climate changes will affect the basin hydrology and water resources.

In [18] Soil and Water Assessment Tool (SWAT) was used for future projection of changes in the hydrological regime of the Kaligandaki basin based on Representative Concentration Pathways Scenarios (RCP 4.5 and RCP8.5) of ensemble downscaled Coupled Model Intercomparison Project's (CMIP5) General Circulation Model (GCM) outputs. It is predicted to be a rise in the average annual temperature of over 4 °C and an increase in the average annual precipitation of over 26% by the end of the 21st century under the RCP 8.5 scenario. Modeling results show these will lead to significant changes in the basin's water balance and hydrological regime. In particular, a 50% increase in discharge is expected at the outlet of the basin. Snowmelt contribution will largely be affected by climate change. Water availability in the basin is not likely to decrease during the 21st century. The study demonstrates that the important water balance components of snowmelt, evapotranspiration, and water yield at higher elevations in the upper and middle sub-basins of the Kaligandaki Basin will be most affected by the increasing temperatures and precipitation.

SWAT model was used in [10] to estimate the impacts of climate change on floods and low flows in Bangladesh at three different increasing temperature scenarios of 1.5°C, 2°C, and 4°C. The study simulated daily flows of the GBM Rivers for future climate projections using SWAT. A 13-member ensemble of projected daily precipitation and daily maximum/minimum temperature data was used as input in the calibrated and validated SWAT model for future climate change analysis. The possible changes in future

riverine floods were analyzed and the results revealed that flood magnitudes in Bangladesh are projected to increase in the future compared to the present. According to the researchers, at the three global warming levels of 1.5°C, 2°C, and 4°C, 100-year return period floods predicted to be increased by 27%, 29%, and 54% for the Ganges; 8%, 24%, and 63% for the Brahmaputra; and 15%, 38%, and 81% for the Meghna, respectively, concerning the baseline of 1986–2005. The study showed that the duration of future floods may also increase.

Another study by [40] explored the effects of climate change on streamflow in the Bheri River using the Soil and Water Assessment Tool (SWAT) model. Three General Circulation Models (GCMs) under two Representative Concentration Pathways (RCPs; 4.5 and 8.5) for the periods of 2020–2044, 2045–2069, and 2070–2099 were used to investigate the impact of climate change. Based on the ensemble of the three models, they found an increasing trend in maximum and minimum temperatures at the rate of 0.025 °C/year and 0.033 °C/year respectively, under RCP 4.5, and 0.065 °C/year and 0.071 °C/year under RCP 8.5 in the future. Similarly, annual rainfall will increase by 6.8–15.2% in the three future periods. The study also stated that the model may not be useful for flood estimation and forecasting.

Soil and Water Assessment Tool (SWAT) model has been used in [34] for daily streamflow and its extreme value modeling of two watersheds located on the Island of Oahu (Hawaii). The study aimed to assess how climate change impacts watershed-wide streamflow and its extreme values and to provide an overview of the impacts of different climate change scenarios (RCP 4.5 and 8.5) on streamflow and hydrological extremes when compared with the baseline values. Following successful calibration and validation of SWAT at three USGS flow gauging stations, researchers simulated the impact of climate change by the 2050s (2041–2070) and the 2080s (2071–2100). SWAT adequately reproduced the observed daily streamflow hydrographs and their temporal evolution at three USGS flow gauging stations as the calculated NSE values were greater than 0.5 for both calibration and validation periods. Besides, the model bracketed more than 80% of observed streamflow data at 95% model prediction uncertainty with a narrow uncertainty band, indicating the suitability of the model for future daily streamflow prediction.

SWAT model has been applied in [13] to northeast Iraq at monthly time steps to calculate blue and green waters. The research projects future climatic scenarios of the region based on six oft-used General Circulation Model (GCM) ensembles, namely CCSM4, CSIRO-Mk3.6.0, GFDL-ESM2M, MEROC5, HadGEM2-ES, and IPSL-CM5A-LR. According to model outputs, the region may experience a precipitation reduction of about 12.6% and 21% in near (2049–2069) and distant (2080–2099) futures respectively under RCP 8.5. Precipitation changes under RCP 4.5 are 15% and 23.4% respectively and under RCP 2.6 are 12.2% and 18.4% respectively. The study further investigated how the population is adapting to already changed climates and how they are expected to cope in the future when the shift in climate is expected to be much greater.

Another study has been done in [49] which evaluates surface runoff generation under climate change scenarios considering RCP 4.5 and 8.5 for the Ilala watershed in the Northern highlands of Ethiopia. Hydrological response to climate change has been evaluated using the Soil and Water Assessment Tool model. The Soil Water Analysis Calibration and Uncertainty Program of Sequential Uncertainty fitting version 2 algorithm has also been used to compute the uncertainty analysis, calibration, and validation process. The results show that the minimum and maximum temperature increases for the future of 1.7 and 4.7 °C respectively. The 95% prediction uncertainty brackets the average values of observation by 71 and 74% during the calibration and validation processes respectively. Similarly, R-factor equals 0.5 and 0.6 during calibration and validation periods. The simulated and observed hydrographs of the total river yield showed a good agreement during calibration (NSE = 0.51, $R^2 = 0.54$) and validation (NSE = 0.54, $R^2 = 0.63$). Due to an increasing trend in temperature and evaporation loss for the future, the surface runoff also declined from 1.74% in RCP4.5 near-term to 0.36% in RCP8.5 end-term periods. This implies proper planning and implementation of appropriate water management strategies are needed for sustainable water resources management in the region.

2.4.3 Impact analysis of upstream intervention using SWAT

Modern mathematical models have been developed for studying the complex hydrological processes of a watershed and their direct relation to weather, topography, geology, and land use. In [27], the researcher studied the hydrology of Simly Dam

watershed located in Saon River basin at the north-east of Islamabad using the Soil and Water Assessment Tool (SWAT). The study simulated the streamflow, established the water balance, and estimated the monthly volume inflow to Simly Dam to help the managers to plan and handle this important reservoir. The model has been calibrated from 1990 to 2001 and evaluated from 2002 to 2011. Based on four recommended statistical coefficients, the evaluation indicates a good performance for both calibration and validation periods and acceptable agreement between measured and simulated values of both annual and monthly scale discharge. The water balance components have been correctly estimated and the Simly Dam inflow was successfully reproduced with Coefficient of Determination (R^2) of 0.75. These results revealed that if properly calibrated, the SWAT model can be used efficiently in semi-arid regions to support water management policies.

A continuous hydrological model has been developed in SWAT to individually simulate regulated and unregulated daily streamflows entering the Paldang Dam, which is located at the outlet of the Han River basin. In [33] it was aimed to evaluate the impacts of the upstream Soyanggang and Chungju multi-purpose dams on the frequency of downstream floods in the Han River basin, South Korea through this research. The simulation of the regulated flows by the Soyanggang and Chungju dams was calibrated with observed inflow data to the Paldang Dam. The estimated daily flood peaks were used for frequency analysis. From the results, the two upstream dams were found to be able to reduce downstream floods by approximately 31% compared to naturally occurring floods without dam regulation. Furthermore, an approach to estimate the flood frequency based on the hourly extreme peak flow data, obtained by combining SWAT simulation and Sangal's method, was proposed and then verified by comparison with the observation-based results. The increased percentage of floods estimated with hourly simulated data for the three scenarios of dam regulation ranged from 16.1% to 44.1%. The reduced percentages were a little higher than those for the daily-based flood frequency estimates. The developed approach allowed for a better understanding of flood frequency, as influenced by dam regulation on a relatively large watershed scale.

The primary limiting eutrophication factor (total phosphorus (TP) concentration) in the Mahabad Dam reservoir in Iran was studied by Sharabian et al. in [42]. They also considered the combined impacts of climate change as well as the scenarios on changes

in upstream TP loadings and downstream dam water allocations. Downscaled daily projected climate has been used under moderate (RCP4.5) and extreme (RCP8.5) scenarios. A Calibrated (SWAT) model of the watershed has been used to determine the effects of climate change on runoff yields in the watershed from 2020 to 2050. The SWAT model was calibrated/validated using the SUFI-2 algorithm. Moreover, to model TP concentration in the reservoir and to investigate the effects of upstream/downstream scenarios, along with forecasted climate-induced changes in streamflow and evaporation rates, the System Dynamics (SD) model was implemented. The scenarios covered a combination of changes in population, agricultural and livestock farming activities, industrialization, water conservation, and pollution control.

For adequate and effective implementation of erosion control measures to reduce reservoir sedimentation, distributed erosion modeling has been used by [28] for the Upper Tana basin (Kenya). The study included bathymetric surveys of the main reservoirs and point measurements of suspended sediment loads, despite the availability of a large data set of historic streamflow measurements. Calibration and validation results for SWAT showed that these multiple sources of data provided relatively good results allowing its use for scenario analysis. With the methodology applied in their study, it has been observed that erosion rates are highest in the cultivated areas (coffee, maize, and other cereals) on steep slopes. The study also predicted that if erosion control measures have been implemented and maintained properly, the sediment yield in reservoirs could be reduced significantly by up to around 25%, depending on the level of adoption. The methodology and the model results indicate that distributed erosion and sediment yield modeling with SWAT, supported by sufficient data on discharge and sediment yields of different points in time and space, can provide quantitative insight into the effectiveness of erosion control measures and their downstream impact on reservoir sedimentation and other off-site effects.

Small and large dams and soil and water conservation works (i.e. contour ridges) have been periodically constructed in the Merguellil catchment (central Tunisia) to alleviate the drought-induced regular water shortage problem. The effect of these water-harvesting systems on the water balance components of this semi-arid basin has been investigated by [15] using the soil and water assessment tool model (SWAT). Large dams have been modeled as reservoirs, small dams as ponds, and contour ridges as potholes that are filled with water and increase the percolation into the aquifer. The model predicts that contour

ridges produce annually a reduction of 32 and 21% in surface run-off and river discharge, respectively, and an increase in aquifer recharge of 50%. At the same time, the retention of a large proportion of entrained sediment (26%) has been modeled. Researchers identified the SWAT model as a useful tool to identify the most appropriate location for the soil water conservation works and their impact on water balance and sediment yield at the basin scale.

Soil and Water Assessment Tool, SWAT, and SUFI-2 algorithm were used in [16] for runoff simulation for the Karaj dam basin. The Karaj reservoir is 100 km northwest of Tehran and supplies a major part of the Iranian capital drinking water. This reservoir collects water from 849 km² catchment which is undergoing accelerated changes due to deforestation and urbanization. The study developed a catchment model platform that includes ongoing land-use changes, soil data, precipitation, and evaporation into the surface runoff of the river discharging into the reservoir. A variety of statistical indices have been used to evaluate the simulation results for both calibration and validation periods. Among them, the Nash–Sutcliffe coefficients are 0.58 and 0.62 in the calibration and validation periods respectively. According to the researchers, the SWAT model reproduced surface runoff in the Karaj River reliably for both calibration and validation periods using the entire records of the years 1997–2011.

In [55], the researcher investigated future changes in runoff and fish habitat quality of the Yalong River basin attributed to the individual and combined effects of construction of cascade dams and climate change. The study used bias-corrected and spatially downscaled CMIP5 GCM projections to drive the Soil and Water Assessment Tool hydrological model and to simulate and predict runoff responses under diverse scenarios. The physical habitat simulation model is established to describe the relationship between river hydrology and fish habitat qualities and to assess the individual and combined effects of cascade dam construction and climate change. From the results, the mean annual temperature and precipitation of the Yalong River in 2020–2100 are predicted to increase at a rate of 0.016–0.487 °C/10a and 4.55–10.13 mm/10a, with an increase of 1.63–3.25 °C and 0.66–3.34% in comparison with those in 1957–2012 respectively. While the mean annual runoff of the middle and lower reaches is increased by 11.77%–16.63% and 14.02%–19.02% compared with that in history respectively. The construction of cascade dams found to be effective to significantly improve the fish habitat quality of

the Yalong River basin, especially in dry seasons, and consequently, the ecological conservation degree is increased by about 2%. In the middle reaches, changes in runoff from February to October are mainly determined by cascade dam construction, but the effect of climate change becomes more pronounced from November to January. Similarly, cascade dam construction has a more significant effect on runoff of the lower reaches than climate change except in November and December.

2.4.4 Previous studies on upper Meghna river basin

A semi-distributed hydrological model has been developed in [41] using HEC-HMS to simulate the precipitation-runoff process for both events, based and continuous precipitation. 30S resolution of Digital Elevation Model (DEM) has been used to delineate the watershed and river network using HEC-Geo HMS. SCS curve method has been used to simulate the rainfall-runoff process, and the Muskingum method has been used for flood routing. They run the model for the year of 2005 and calibrated against the observed data at Bhairab Bazar station. Furthermore, the model has been validated for the year 2006. The effects of climate change scenarios were simulated by running the calibrated model using the future precipitation data found from Global Climate Models (CSIRO-30 and CCCMA-31). Results from those model data were used to predict flow hydrographs for 2050 and 2080.

Another model for the upper Meghna Basin was developed in [65] using HEC-HMS in 2016. The study used Soil Moisture Accounting (SMA) method was used to simulate the rainfall-runoff process and the Muskingum method used for flood routing. Calibration and validation for long term (1983-96) simulation have been done for both Kushiyara and Surma point. The calibrated hydrological model of the upper Meghna basin then has been used to assess the impact of climate change on water availability of the upper Meghna basin by applying different climate change scenarios of selected General Circulation Models (GCM). The selection of GCM was based on the Representative Concentration Pathways (RCPs) scenarios of two GCMs for the 21st century. Two climate change scenarios BCC-CSM1.1 RCP 4.5 and RCP 8.5 were used to compare future flow with the base flow. HEC-HMS simulated seasonal streamflow of the upper Meghna Basin for 2040-2069 (the 2050s) and 2070-2099 (2080s) of the 21st century were compared with the corresponding climate normal (1981-2010) base flow.

In the study in [8], the researcher presented the outcome of a research study conducted to analyze the propagation time of the flash floods in the Upper Meghna river basin in Bangladesh and corresponding socio-economic impacts. A numerical model set-up in the general river model system named MIKE 11 was applied to simulate flash floods in the river basin and the travel time of their flood peak from the border towards India (only limited information is available from inside India) and into North East region. The results reveal that there is only little warning time from the time the flood passes the border towards India and until the flood impacts the rural people in the North East region of Bangladesh. The corresponding socio-economic impacts were quantified and found to be substantial.

In [12] researchers assessed various aspects of the future projections of rainfall and temperature extremes (magnitudes and frequencies) of haor basin area which is in the northeast region of the Bangladesh. The impacts of extreme events are evaluated using Hadley Centre's higher resolution regional climate model known as PRECIS. The study found that upper part of the haor basin Surma-Kushiyara Basin is anticipated to be significantly wetter during the end of the century. The study also revealed the seasonal variation by analyzing rainfall and temperatures. The monsoon months shows high magnitude of increase according to the study. Highest variability in rainfall was found by the study during the month of May of pre-monsoon when flash floods in the haor region normally occur. Least changes were observed during the winter season and decrease in the end of the post monsoon season

How the flood peaks will change along the Ganges, Brahmaputra and Meghna rivers due to changing climate was evaluated in the study [11]. The study also provided an guideline on RCM models well that can be a used for climate change analysis and reveals which one is the best match ensemble for the GBM basin area. Researchers used a multi-model simulation approach that includes three models which are SWAT, Delft3D and HEC-RAS. For climate change analysis, projections of REMO 2009 RCM coupled with MPI-MPI-ESM-LR GCM was used for the Brahmaputra River, the model results provided the best match between the observed and simulated discharge. For the Ganges River, the study suggested best sync was with the RCA4 RCM coupled with IPSL-CM5A-MR

GCM. For the Meghna River, model simulates the best results when RCA4 RCM coupled with NOAA-GFDL-GFDL-ESM2m.

Another study compared the data of BMD and CanESM2 GCM predictors. Performed Climate projections followed by analysis of climate anomalies, shifting of season and long term drought severity for future periods 2030s (2016-2045), 2050s (2046-2065) and 2080s (2066-2095). Both average maximum and minimum temperature has been found to be increased in future making southern part of Bangladesh hotter gradually. The study reports that the seasonal average maximum temperature increase is found higher in monsoon (4.5°C) and post-monsoon season (4.0°C) considering all scenarios. The study also revealed that Bangladesh will face highest increment of average minimum temperature (5.2°C) in post-monsoon season. Mean annual average rainfall increase may increase about 8%, 9% and 19% for 2030s, 2050s and 2080s respectively under RCP8.5, whereas maximum increase is found 11% for 2080s under RCP 4.5. The study observed that the highest increase in occurrence of pre-monsoon rainfall is found to be 5%-6% in in north-eastern region, which clearly depicts that haor area of Bangladesh will be more prone to early rainfall as well as early flash floods in future period.

In [66], a hydraulic principles based wetland model for the Upper Meghna River Basin was developed using the SWAT_{Trw}. The model was manually calibrated and validated against 21 years (1990–2010) of observed stream flow and river stage at 18 gauging stations. The study investigated climate change impacts on the hydrological conditions of the basin area and used RCP 4.5 projections from four CMIP5 GCMs which are- CCSM4, GFDL-CM3, MIROC-ESM and NorESM1-M. Model results revealed that the monsoonal streamflows of the basin area may increase by 12% for 2021–2040 and 42% for 2061–2080. Whereas, lean season low flows may decrease by 58%. Researchers also investigated the flooding risk of intensively Boro rice cultivated haor wetlands in the lower Sylhet Basin of the UMRB in response to future climate change. The study reported that, the average flooding risk in haors in April is likely to decrease as per the findings of the study which may impose a serious threat to crop cultivation.

2.5 Theoretical Background

2.5.1 Overview of the SWAT model

The Soil and Water Assessment Tool (SWAT) is a river basin or watershed scale model developed by Dr. Jeff Arnold for the USDA Agricultural Research Service (ARS) to quantify the impact of land management practices in large, complex watersheds in [25]. It is a process-based and spatially semi-dispersed hydrological and water quality model designed to calculate and route water, sediments, and nutrient from individual sub-watersheds all through the mainstream watersheds towards its outlet. This public domain hydrology model SWAT has the following components: weather, surface runoff, return flow, percolation, evapotranspiration, transmission losses, pond and reservoir storage, crop growth and irrigation, groundwater flow, reach routing, nutrient and pesticide loading, and water transfer.

SWAT allows several physical processes to be simulated in a watershed using a two-level disaggregation scheme [45]. First, preliminary sub-basin identification is carried out based on topographic criteria followed by further discretization using land use and soil type considerations. Areas with the same soil type and land use form a Hydrologic Response Unit (HRU), a basic computational unit assumed to be homogeneous in hydrologic response to land cover change. SWAT is a continuous-time model that operates on a daily time step and can be used to simulate at the basin scale long term water and nutrients cycle. It can also help in assessing the environmental efficiency of best management practices and alternative management policies.

2.5.1.1 Water balance concept in SWAT model

Water balance is the main driving force behind every process in the SWAT model as a result of its effects on plant development and the movement of sediments, nutrients, pesticides, and pathogens within the watershed region. To accurately predict the movement of pesticides, sediments, or nutrients, the hydrologic cycle as simulated by the model must conform to what is happening in the watershed. Thus, the simulation of the hydrology of a watershed can be separated into two major divisions. The first division is the land phase of the hydrologic cycle (Figure 2.4) which controls the amount of water, sediment, nutrient, and pesticide loadings to the main channel in each sub-basin. The

second division is the water or routing phase of the hydrologic cycle which can be defined as the movement of water, sediments, etc. through the channel network of the watershed to the outlet.

Land phase of the hydrologic cycle

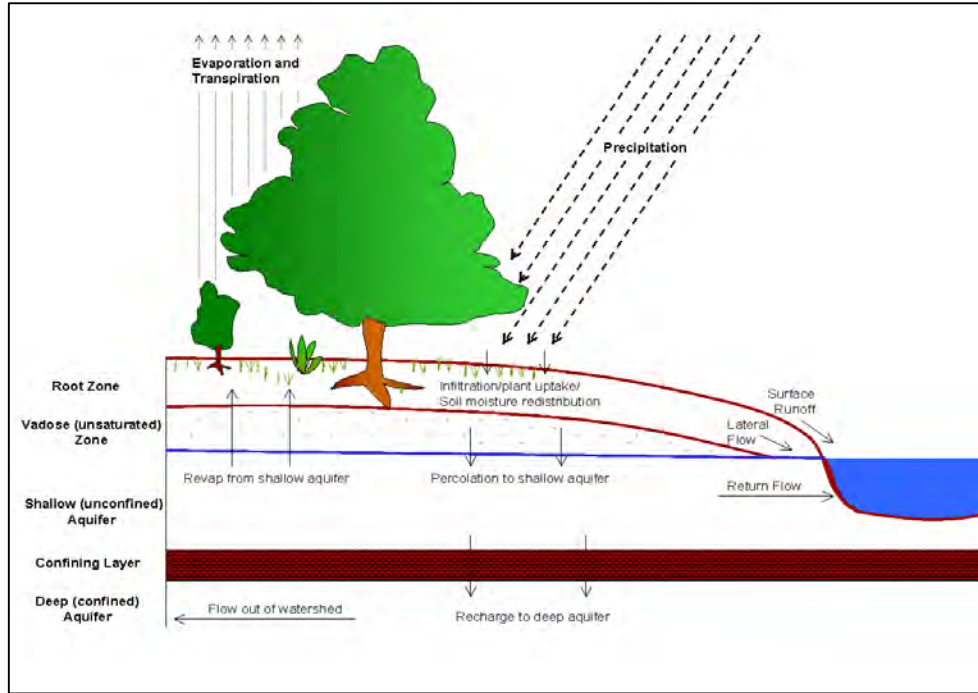


Figure 2.4 Schematic representation of the hydrologic process in the SWAT model

The SWAT model simulates the hydrological cycle according to equation (2.1)

$$SW_t = SW_0 + \sum_{i=1}^t (R_{day} - Q_{surf} - E_a - w_{seep} - Q_{gw}) \quad (2.1)$$

where SW_t is the final soil water content (mm H₂O), SW_0 is the initial soil water content on the day i (mm H₂O), t is the time (days), R_{day} is the amount of precipitation on day i (mm H₂O), Q_{surf} is the amount of surface runoff on day i (mm H₂O), E_a is the amount of evapotranspiration on day i (mm H₂O), w_{seep} is the amount of water entering the vadose zone from the soil profile on day i (mm H₂O) and Q_{gw} is the amount of return flow on day i (mm H₂O).

To simulate the hydrologic process using the above water balance equation, watershed subdivision provide aids to the model to reflect differences in evapotranspiration for various crops and soils. Runoff is generally predicted separately for each HRU and routed

to obtain the total runoff for the watershed. The input parameters and processes that are involved in this phase to estimate the flow and water balance are summarized below-

Climatic variables

The climatic variables required by the SWAT model consist of daily precipitation, maximum/minimum air temperature, solar radiation, wind speed, and relative humidity. The model allows values for daily precipitation, maximum/minimum air temperatures, solar radiation, wind speed, and relative humidity to be input from records of observed data or generated during the simulation.

Precipitation

The precipitation reaching the earth's surface on a given day may be read from an input file or generated by the model. SWAT recommends researcher to incorporate measured precipitation into their simulations any time the data is available. The ability of SWAT to reproduce observed stream hydrographs is greatly improved by the use of measured precipitation data. Unfortunately, even with the use of measured precipitation, some errors due to inaccuracy in precipitation data can be expected. Measurement of precipitation at individual gages is subject to error from several causes and additional error is introduced when regional precipitation is estimated from point values.

Point measurements of precipitation generally capture only a fraction of the true precipitation. The inability of a gage to capture a true reading is primarily caused by wind eddies created by the gage. These wind eddies reduce the catch of the smaller raindrops and snowflakes.

Temperature

Temperature influences many physical, chemical, and biological processes. Plant production is strongly temperature-dependent, as are organic matter decomposition and mineralization. Daily air temperature may be input to the model or generated from average monthly values. Soil and water temperatures are derived from air temperature. SWAT requires daily maximum and minimum air temperature. This data may be read from an input file or generated by the model. Swat recommends obtaining measured daily

temperature records from gages in or near the watershed if at all possible. The accuracy of model results is significantly improved by the use of measured temperature data.

Hydrology

As precipitation descends, it may be intercepted and held in the vegetation canopy or fall to the soil surface. Water on the soil surface will infiltrate into the soil profile or flow overland as runoff. Runoff moves relatively quickly toward a stream channel and contributes to short-term stream response. Infiltrated water may be held in the soil and later evapo-transpired or it may slowly make its way to the surface-water system via underground paths.

Canopy storage

Canopy storage is the water intercepted by vegetative surfaces (the canopy) where it is held and made available for evaporation. When using the curve number method to compute surface runoff, canopy storage is taken into account in the surface runoff calculations. However, if methods such as Green & Ampt are used to model infiltration and runoff, canopy storage must be modeled separately. SWAT allows the user to input the maximum amount of water that can be stored in the canopy at the maximum leaf area index for the land cover. This value and the leaf area index are used by the model to compute the maximum storage at any time in the growth cycle of the land cover/crop. When evaporation is computed, water is first removed from canopy storage.

Infiltration

Infiltration refers to the entry of water into a soil profile from the soil surface. As infiltration continues, the soil becomes increasingly wet, causing the rate of infiltration to decrease with time until it reaches a steady value. The initial rate of infiltration depends on the moisture content of the soil before the introduction of water at the soil surface. The final rate of infiltration is equivalent to the saturated hydraulic conductivity of the soil. As the curve number method used to calculate surface runoff operates on a daily time-step, it is unable to directly model infiltration. The amount of water entering the soil profile is calculated as the difference between the amount of rainfall and the amount of

surface runoff. The Green & Ampt infiltration method does directly model infiltration, but it requires precipitation data in smaller time increments.

Evapotranspiration

Evapotranspiration is a collective term for all processes by which water in the liquid or solid phase at or near the earth's surface becomes atmospheric water vapor. Evapotranspiration includes evaporation from rivers and lakes, bare soil and vegetative surfaces; evaporation from within the leaves of plants (transpiration); and sublimation from ice and snow surfaces. Potential soil water evaporation is estimated as a function of potential evapotranspiration and leaf area index (area of plant leaves relative to the area of the HRU). Actual soil water evaporation is estimated by using exponential functions of soil depth and water content. Plant transpiration is simulated as a linear function of potential evapotranspiration and leaf area index.

Potential evapotranspiration

Potential evapotranspiration is the rate at which evapotranspiration would occur from a large area completely and uniformly covered with growing vegetation which has access to an unlimited supply of soil water. This rate is assumed to be unaffected by micro-climatic processes such as advection or heat-storage effects. The model offers three options for estimating potential evapotranspiration: Hargreaves, Priestley-Taylor, and Penman-Monteith [45]. The Hargreaves method was originally derived from eight years of cool-season Alta fescue grass lysimeter data from Davis, California. Several improvements were made to the original equation (Hargreaves and Samani, 1982 and 1985) and the form used in SWAT was published in 1985 (Hargreaves et al., 1985):

$$\lambda E_0 = 0.0023 H_0 (T_{mx} - T_{mn})^{0.5} (T_{av} + 17.8) \quad (2.2)$$

where λ is the latent heat of vaporization (MJ kg^{-1}), E_0 is the potential evapotranspiration (mm d^{-1}), H_0 is the extraterrestrial radiation ($\text{MJ m}^{-2} \text{d}^{-1}$), T_{mx} is the maximum air temperature for a given day ($^{\circ}\text{C}$), T_{mn} is the minimum air temperature for a given day ($^{\circ}\text{C}$), and T_{av} is the mean air temperature for a given day ($^{\circ}\text{C}$).

Lateral subsurface flow

Lateral subsurface flow, or interflow, is streamflow contribution which originates below the surface but above the zone where rocks are saturated with water. A kinematic storage model is used to predict lateral flow in each soil layer. The model accounts for variation in conductivity, slope, and soil water content.

Surface runoff

Surface runoff or overland flow is the flow that occurs along a sloping surface. Using daily or sub-daily rainfall amounts, SWAT simulates surface runoff volumes, and peak runoff rates for each HRU. Surface Runoff Volume is computed using a modification of the SCS curve number method (USDA Soil Conservation Service, 1972) or the Green & Ampt infiltration method [45]. In the curve number method, the curve number varies non-linearly with the moisture content of the soil. The curve number drops as the soil approaches the wilting point and increases to near 100 as the soil approaches saturation. The Green & Ampt method requires sub-daily precipitation data and calculates infiltration as a function of the wetting front matric potential and effective hydraulic conductivity. Water that does not infiltrate becomes surface runoff. SWAT includes a provision for estimating runoff from frozen soil where the soil is defined as frozen if the temperature in the first soil layer is less than 0°C. The model increases runoff for frozen soils but still allows significant infiltration when the frozen soils are dry.

SWAT provides two methods for estimating surface runoff. The SCS runoff equation is an empirical model that came into common use in the 1950s. It was the product of more than 20 years of studies involving rainfall-runoff relationships from small rural watersheds across the U.S. The model was developed to provide a consistent basis for estimating the amounts of runoff under varying land use and soil type runoff: the SCS curve number procedure (SCS, 1972) and the Green & Ampt infiltration method [45].

The SCS runoff equation is an empirical model that came into common use in the 1950s. It was the product of more than 20 years of studies involving rainfall-runoff relationships from small rural watersheds across the U.S. The model was developed to provide a

consistent basis for estimating the amounts of runoff under varying land use and soil types (Rallison and Miller, 1981). The SCS curve number equation is (SCS, 1972):

$$Q_{surf} = \frac{R_{day} - I_a}{R_{day} - I_a + S} \quad (2.3)$$

Where Q_{surf} is the accumulated runoff or rainfall excess (mm H₂O), R_{day} is the rainfall depth for the day (mm H₂O), I_a is the initial abstractions which includes surface storage, interception, and infiltration before runoff (mm H₂O) and S is the retention parameter (mm H₂O). The retention parameter varies spatially due to changes in soils, land use management, and slope and temporally due to changes in soil water content. The retention parameter is defined as:

$$S = 25.4 \left(\frac{1000}{CN} - 10 \right) \quad (2.4)$$

Where CN is the curve number for the day. The initial abstractions, I_a , is commonly approximated as $0.2S$ and equation 2.11 becomes

$$Q_{surf} = \frac{R_{day} - 0.2S}{R_{day} + 0.8S} \quad (2.5)$$

The runoff will only occur when $R_{day} > I_a$.

Peak runoff rate

Peak runoff predictions are made with a modification of the rational method. In brief, the rational method is based on the idea that if rainfall of intensity i begins instantaneously and continues indefinitely, the rate of runoff will increase until the time of concentration, t_c , when all of the sub-basin is contributing to flow at the outlet. In the modified Rational Formula, the peak runoff rate is a function of the proportion of daily precipitation that falls during the subbasin t_c , the daily surface runoff volume, and the sub-basin time of concentration. The proportion of rainfall occurring during the sub-basin t_c is estimated as a function of total daily rainfall using a stochastic technique. The sub-basin time of

concentration is estimated using Manning's Formula considering both overland and channel flow.

Tributary channels

Two types of channels are defined within a subbasin: the main channel and tributary channels. Tributary channels are minor or lower order channels branching off the main channel within the subbasin. Each tributary channel within a subbasin drains only a portion of the subbasin and does not receive groundwater contribution to its flow. All flow in the tributary channels is released and routed through the main channel of the subbasin. SWAT uses the attributes of tributary channels to determine the time of concentration for the subbasin.

Transmission losses

Transmission losses are losses of surface flow via leaching through the streambed. This type of loss occurs in ephemeral or intermittent streams where groundwater contribution occurs only at certain times of the year or not at all. Water losses from the channel are a function of channel width and length and flow duration. Both runoff volume and peak rate are adjusted when transmission losses occur in tributary channels.

Return flow

Return flow or base flow is the volume of streamflow originating from groundwater. SWAT partitions groundwater into two aquifer systems: a shallow, unconfined aquifer that contributes return flow to streams within the watershed and a deep confined aquifer which contributes return flow to streams outside the watershed. Water percolating past the bottom of the root zone is partitioned into two fractions each fraction becomes recharge for one of the aquifers. In addition to return flow, water stored in the shallow aquifer may replenish moisture in the soil profile in very dry conditions or be directly removed by the plant. Water in the shallow or deep aquifer may be removed by pumping.

Routing phase of the hydrologic cycle

Once SWAT determines the loadings of water, sediment, nutrients, and pesticides to the main channel, the loadings are routed through the stream network of the watershed. In addition to keeping track of mass flow in the channel, SWAT models the transformation of chemicals in the stream and streambed.

Routing in the main channel or reach

Routing in the main channel can be divided into four components: water, sediment, nutrients, and organic chemicals.

Flood routing

As water flows downstream, a portion may be lost due to evaporation and transmission through the bed of the channel. Another potential loss is the removal of water from the channel for agricultural or human use. Flow may be supplemented by the fall of rain directly on the channel and/or addition of water from point source discharges. Flow is routed through the channel using a variable storage coefficient method or the Muskingum routing method.

Routing in the reservoir

The water balance for reservoirs includes inflow, outflow, rainfall on the surface, evaporation, seepage from the reservoir bottom, and diversions.

Reservoir outflow

The model offers three alternatives for estimating outflow from the reservoir. The first option allows the user to input measured outflow. The second option is designed for small, uncontrolled reservoirs and requires the users to specify a water release rate. When the reservoir volume exceeds the principle storage, the extra water is released at the specified rate. Volume exceeding the emergency spillway is released within one day. The third option is designed for larger and managed reservoirs, has the user specify monthly target volumes for the reservoir.

2.5.2 Climate change modeling for hydrological impact assessment

Climate change impact studies are largely based on climatic projections simulated by climate models. Hydrological models are used to simulate the impact of climate change on the water cycle as well as to project future hydrological regimes. To drive such a model, reliable information on climatological variables (e.g. temperature, precipitation, or evapotranspiration) and on their distribution in space and time is required. This information can be provided by different climate models. Climate models use quantitative methods to simulate the interactions of the important drivers of climate including the atmosphere, oceans, land surface, and ice. They are used for a variety of purposes from the study of the dynamics of the climate system to projections of future climate. All climate models take account of incoming energy from the sun as short wave electromagnetic radiation, chiefly visible and short-wave (near) infrared, as well as outgoing longwave (far) infrared electromagnetic.

Climate change scenarios

There are several types of climate change scenarios. They range from scenarios that are devised arbitrarily based on expert judgment (arbitrary climate change scenarios) to scenarios based on past climate (analog climate change scenarios) to scenarios based on climate model output.

Arbitrary climate change scenarios

Arbitrary climate change scenarios are changes in key variables selected to test the sensitivity of a system to possible changes in climate. These are often uniform annual changes in variables, such as temperature and precipitation. An example is combinations of 1°, 2°, and 4° increases in temperature combined with no change and increases and decreases of 10% and 20% in precipitation. Different changes can be assumed for different seasons. These scenarios are most useful for testing the sensitivity of systems to changes in individual variables and combined changes.

Analogue climate change scenarios

Analogue, or past climates, can be created from historical instrumental records of climate or paleoclimate reconstructions. The instrumental record will often be a complete multi-decadal record of often daily or sub-daily weather observations. The advantage of these data is that they will be recorded at each observation station and thus could provide better information on the regional distribution of climate than many climate models. Their disadvantages include inaccuracies in the estimation of past climates, low temporal resolution (e.g., they may estimate seasonal or annual climates), and incomplete coverage.

Climate model-based scenarios

Climate models are mathematical representations of the climate. Although there are many uncertainties with models such as climate models, they do enable us to simulate how global and regional climates may change as a result of anthropogenic influences on the climate.

Models of both global and regional climate exist. Global climate models range from simple, one-dimensional models such as MAGICC, which is briefly described below, to more complex models such as general circulation models (GCMs). GCMs model the atmosphere and oceans, and interactions with land surfaces. The model on a regional scale, typically estimating the change in grid boxes that are approximately several hundred kilometers wide. GCMs, provide only an average change in climate for each grid box, even though real climates can vary quite considerably within several hundred kilometers.

Downscaling from GCMs

Climate change scenarios often require higher resolution (smaller grid boxes) than GCMs can provide. To develop higher resolution outputs, results from GCMs are “downscaled”, that is, transformed into results at a smaller scale than GCM grid boxes. There are three basic options for downscaling:

- (a). GCM output combined with historical observations
- (b). Statistical downscaling
- (c). Regional climate models.

GCM output combined with historical observations

This approach, which has been used in several studies, involves combining average monthly changes from GCMs (typically averaged 30 years of simulated data) with a historical database. The observed record is changed by the change in GCM output from current (e.g., late 20th century conditions) to the CO₂ doubling or to a particular time in the transient run. The advantage of this approach is that it is relatively easy to apply and can provide a scenario at the spatial and temporal scales of the historical climate database. The disadvantage is that it assumes a uniform change within each grid box and uniform change within months. Using average GCM output does not account for possible changes in inter-annual variability.

Statistical downscaling

Statistical downscaling develops high-resolution changes in climate based on larger scale output from GCMs. Relative to modeling, it is a simpler method for developing high-resolution data. It is based on the presumption that the relationship between the large-scale variables (predictors) and the small-scale variables (predictands) remains the same under climate change as under the present climate. This may not always be the case.

Regional climate models

Regional climate models (RCMs) are much higher resolution models that focus on a region, typically at a continental or subcontinental scale. Their grid boxes are 50 km or less across. They are therefore able to capture many regional features that GCMs cannot. However, RCMs must be run with boundary conditions from GCMs (e.g., changes in pressure patterns, sea surface temperatures), so there are typically RCM runs for only a few GCMs. Some applications are for limited periods, e.g., a simulated decade. The advantage of RCMs is that they can provide a better spatial representation of climate change than GCMs, but they cannot correct for errors in boundary conditions.

Key drivers of future climate and the basis on which projections are made

The representative concentration pathways (RCPs)

Representative Concentration Pathway (RCP) is a greenhouse gas concentration (not emissions) trajectory adopted by the IPCC for its fifth Assessment Report (AR5) in 2014.

It supersedes Special Report on Emissions Scenarios (SRES) projections published in 2000. It describes four different 21st-century pathways of greenhouse gas (GHG) emissions, atmospheric concentrations, air pollutant emissions, and land use. RCPs include a stringent mitigation scenario (RCP 2.6), two intermediate scenarios (RCP 4.5 and RCP 6.0), and one scenario with very high GHG emissions (RCP 8.5). The four RCPs, namely RCP2.6, RCP4.5, RCP6, and RCP8.5 are labeled after a possible range of radiative forcing values in the year 2100 (2.6, 4.5, 6.0, and 8.5 W/m², respectively). The newly developed RCP scenarios help the climate research community in several ways. They provide more detailed and better-standardized greenhouse gas concentration inputs for running climate models than those provided by any previous scenario sets. The RCP scenarios explicitly explore the impact of different climate policies to allow the cost-benefit evaluation of long-term climate goals. They also allow a more detailed exploration of the role of adaptation and further integration of scenario development across the different disciplines involved in climate research.

RCP 2.6

This scenario might be described as the best case for limiting anthropogenic climate change. It requires a major turnaround in climate policies and a start to concerted action in the next few years in all countries, both developing and developed. Global CO₂ emissions peak by 2020 and decline to around zero by 2080. Concentrations in the atmosphere peak at around 440 ppm in midcentury and then start slowly declining. Global population peaks midcentury at just over 9 billion and global economic growth is high. Oil use declines but the use of other fossil fuel increases and is offset by the capture and storage of carbon dioxide. Biofuel use is high. Renewable energy (eg. solar & wind) increases but remains low. Cropping area increases faster than current trends while the grassland area remains constant. Animal husbandry becomes more intensive. Forest vegetation continues to decline at current trends.

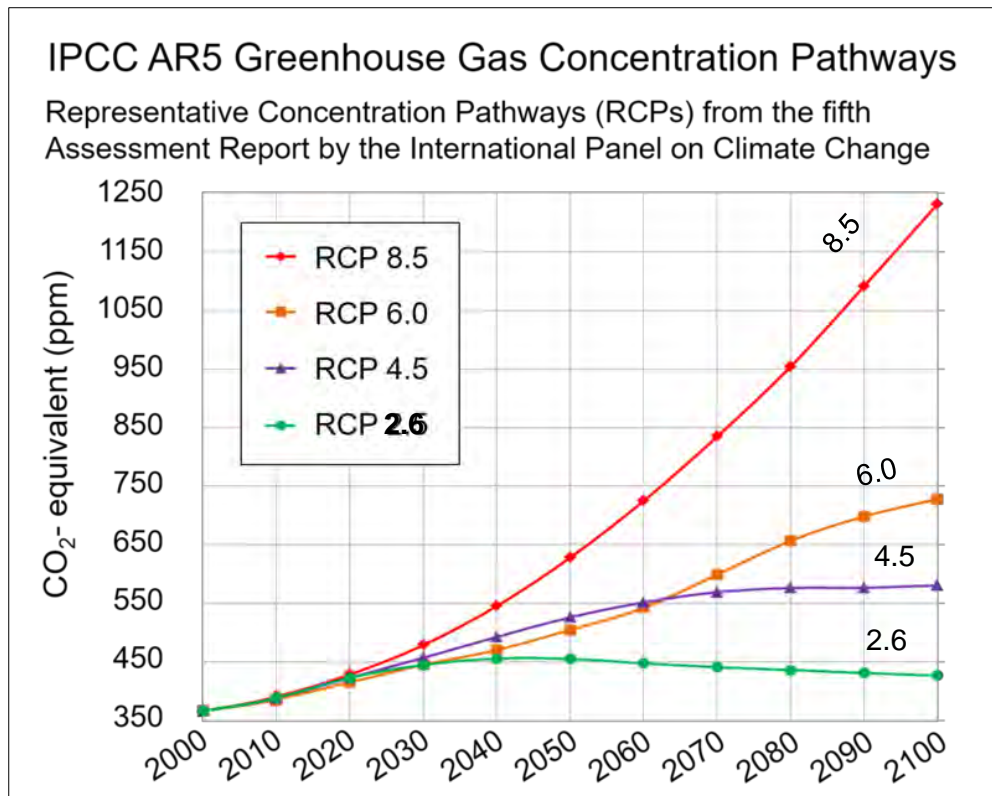


Figure 2.5 All forcing agents' atmospheric CO₂-equivalent concentrations according to the four RCPs (https://en.wikipedia.org/wiki/Representative_Concentration_Pathway)

RCP 4.5

Emissions peak around midcentury at around 50% higher than 2000 levels and then decline rapidly over 30 years and then stabilize at half of 2000 levels. CO₂ concentration continues on-trend to about 520 ppm in 2070 and continues to increase but more slowly. Population and economic growth are moderate but slightly lower than under scenario RCP 2.6. Total energy consumption is slightly higher than RCP 2.6 while oil consumption is fairly constant through to 2100. Nuclear power and renewables play a greater role. Significantly, cropping and grassland area declines while reforestation increases the area of natural vegetation.

RCP 6

In this scenario, emissions double by 2060 and then dramatically fall but remain well above current levels. CO₂ concentration continues increasing, though at a slower rate in the latter parts of the century, reaching 620 ppm by 2100. Population growth is slightly higher peaking at around 10 billion. This scenario assumes the lowest GDP growth of the four. Energy consumption increases to a peak in 2060 then declines and levels out to finish the century at levels similar to RCP2.6. Oil consumption remains high while biofuel and nuclear play a smaller role than in the other 3 scenarios. The cropping area continues on the current trend, while the grassland area is rapidly reduced. Natural vegetation is similar to RCP 4.5.

RCP 8.5

This is the nightmare scenario in which emissions continue to increase rapidly through the early and mid-parts of the century. By 2100 annual emissions have stabilized at just under 30 gigatonnes of carbon compared to around 8 gigatonnes in 2000. Concentrations of CO₂ in the atmosphere accelerate and reach 950 ppm by 2100 and continue increasing for another 100 years. Population growth is high, reaching 12 billion by centuries end. This is at the high end of the UN projections. Economic growth is similar to RCP 6 but assumes much lower incomes and per capita growth in developing countries. This scenario is highly energy-intensive with total consumption continuing to grow throughout the century reaching well over 3 times current levels. Oil use grows rapidly until 2070 after which it drops even more quickly. Coal provides the bulk of a large increase in energy consumption. Land use continues current trends with the crop with grass areas increasing and forest area decreasing.

The RCPs are an important development in climate research and provide a foundation for emissions mitigation and impact analysis. RCPs will facilitate the exchange of information among physical, biological, and social scientists. Researchers working on impacts, adaptation, and vulnerability will obtain model outputs sooner and have more time to complete their part of the AR5. Climate-model scenarios can also be developed without constraining future work on integrated assessments. As climate models improve, newer models can employ the same pathways, allowing modelers to isolate the effects of changes in the climate models themselves. The RCPs are supplemented with extensions (Extended Concentration Pathways, ECPs), which allow climate modeling experiments

through to the year 2300. Development of the RCPs also brings together a diverse range of research communities that will help create fully integrated Earth-system models that include representation of the global economy and society, impacts, and vulnerabilities.

Regional climate model data portal-CORDEX

The Coordinated Regional Downscaling Experiment (CORDEX) is a program sponsored by World Climate Research Program (WCRP) to develop an improved framework for generating regional-scale climate projections for impact assessment and adaptation studies worldwide within the IPCC AR5 timeline and beyond [46]. The program consists of several subcomponents: development of a framework for evaluating downscaling methodologies, develop improved downscaling techniques, both statistical and dynamical; and promote interactions among global climate modelers, downscaling modelers, and assessment community who assess the impact of climate change on specific sectors using the downscaled data.

Domains and resolution

Simulation output for 13 domains is in the preparation or already available, e.g. for the EUR domain (Europe). The number behind the domain abbreviation is the grid resolution in the native CORDEX simulation. Native EUR CORDEX simulations have a grid resolution of 0.44 or 0.11 degrees (EUR-44, EUR-11) and rotated poles. To facilitate the use of CORDEX data, also data on normal grids are available or will be calculated. The poles have been rotated back and the grid resolution has slightly been modified. Since these data have been calculated by interpolation, has been added to the domain name, e.g. EUR-44i. EUR-44i data have a grid resolution of 0.5 degrees, EUR-11i data a resolution of 0.125 degrees, latitude, and longitude. Interpolation will usually be done for monthly and semi-annual data only. Corresponding to the forcing data taken from CMIP5; CORDEX experiments have the same names as in the CMIP5 project. An exception is the evaluation experiment, which is forced by reanalysis data. CMIP5 calculations have been done for an ensemble of starting states. The names of the ensemble members in CORDEX are that of the CMIP5 data used for forcing.

Dataset and methods

The WCRP CORDEX fosters international partnerships to produce an ensemble of high-resolution past and future climate projections at a regional scale. This CORDEX dataset is comprised of downscaled climate scenarios for the South Asia region [22] that are derived from the Atmosphere-Ocean coupled General Circulation Model (AOGCM) runs conducted under the Coupled Model Intercomparison Project Phase 5 (CMIP5) and using three of the four greenhouse gas emissions scenarios known as Representative Concentration Pathways (RCPs) [24]. The CMIP5 AOGCM runs were developed in support of the Fifth Assessment Report of the Intergovernmental Panel on Climate Change (IPCC AR5). The coarser spatial resolution ranging from 1.0° to 3.8° , and systematic error (called bias) of these AOGCMs limits the examination of possible impacts of climate change and adaptation strategies on a smaller scale. The CORDEX South Asia dataset includes dynamically downscaled projections from the 10 models and scenarios for which daily scenarios were produced and distributed under CMIP5 [26]. The purpose of these datasets is to provide a set of high resolution (50 km) regional climate change projections that can be used to evaluate climate change impacts on processes that are sensitive to finer-scale climate gradients and the effects of local topography on climate conditions.

The dynamical downscaling method using high resolution limited area regional climate models (RCMs) utilizes the outputs provided by AOGCMs as lateral boundary condition to provide physically consistent spatiotemporal variations of climatic parameters at spatial scales much smaller than the AOGCMs' grid. The RCMs by resolving the topographical details, coastlines and land-surface heterogeneities allow the reproduction of small-scale processes and information that are most useful for impact assessment and in decision making for adaptation. An initial assessment of the ability of the CORDEX RCMs to simulate the general characteristics of the Indian climate indicated that the geographical distribution of surface air temperature and seasonal precipitation in the present climate for land areas in South Asia is strongly affected by the choice of the RCM and boundary conditions (i.e. driving AOGCMs) and the downscaled seasonal averages are not always improved [46].

3 METHODOLOGY

3.1 General

Hydrological modeling study which aims to derive scenarios of the future water situation in large river basins requires some basic data like digital elevation model, land use and soil information, weather data (precipitation, solar radiation, relative humidity, wind speed), and monitoring flow gauges. The model development includes numerous amount of preprocessing and post-processing that is quite challenging for the researchers. Assessment of the impact of future climate and upstream intervention on the inflow of any river basin using a hydrological model involves the following steps:

Step 1-Data Collection: This includes the digital elevation model (DEM), land use pattern, soil distribution, climate data, and flow time series.

Step 2- Model Setup: Model setup using SWAT which includes watershed delineation, processing of weather data, hydrologic response unit (HRU) definition, and selection of calculation methods.

Step 3-Model Development: Calibration and validation of the model, Sensitivity analysis of the model parameters, evaluation of the model performance.

Step 4-Selection of Scenarios: Selection of Regional Climate Models of RCP 4.5 and RCP 8.5 scenario for climate change impact assessment and different flow scenario selection for upstream intervention.

Step 5-Analysis of Scenarios: Model run using high resolution projected data and analyzing the impact due to different climatic and upstream intervention scenarios.

3.2 Data Collection

3.2.1 Digital elevation model, stream network, land use, and soil data

The Shuttle Radar Topography Mission (SRTM) is a collaborative effort from NASA (National Aeronautics and Space Administration) and NGA (National Geospatial-

Intelligence Agency) as well as DLR (Deutsches Zentrum für Luft-und Raumfahrt) and ASI (Agenzia Spaziale Italiana) [47] .

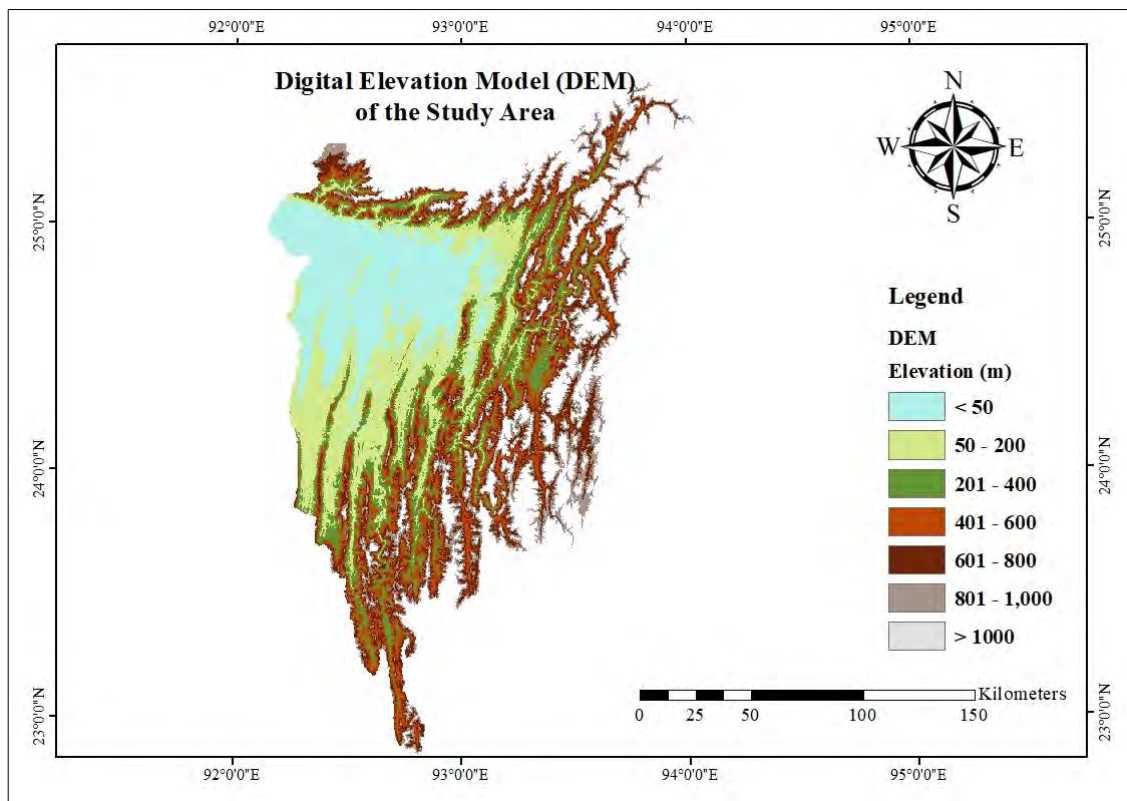


Figure 3.1 Digital Elevation Model (DEM) of the Meghna Basin

SRTM provides 90 m DEM's which have a resolution of 90 m (3 arc second) at the equator, and are provided in mosaicked 5 deg x 5 deg tiles. Digital elevation model (DEM) for the Meghna river basin of resolution 90 m (Figure 3.1) was collected from the NASA Shuttle Radar Topographic Mission (SRTM) website (<http://srtm.csi.cgiar.org>).

The River network for the basin area was collected from the USGS HydroSHEDS website (<https://hydrosheds.cr.usgs.gov/dataavail.php>). HydroSHEDS is a mapping product that provides hydrographic information for regional and global-scale applications in a consistent format. It offers a suite of geo-referenced data sets (vector & raster) at various scales, including river networks, watershed boundaries, drainage directions, and flow accumulations. Hydro SHEDS is based on high-resolution elevation data obtained during a Space Shuttle flight for NASA's Shuttle Radar Topography Mission (SRTM) [56]. The river network data is available at a resolution of 15 arc-second (500 m at the equator). But the data collected differs significantly from the real river network. So the river network

is edited based on the river maps of Bangladesh and India using GIS and google earth in the present study. The delineated stream network of the study area is shown in Figure 3.2.

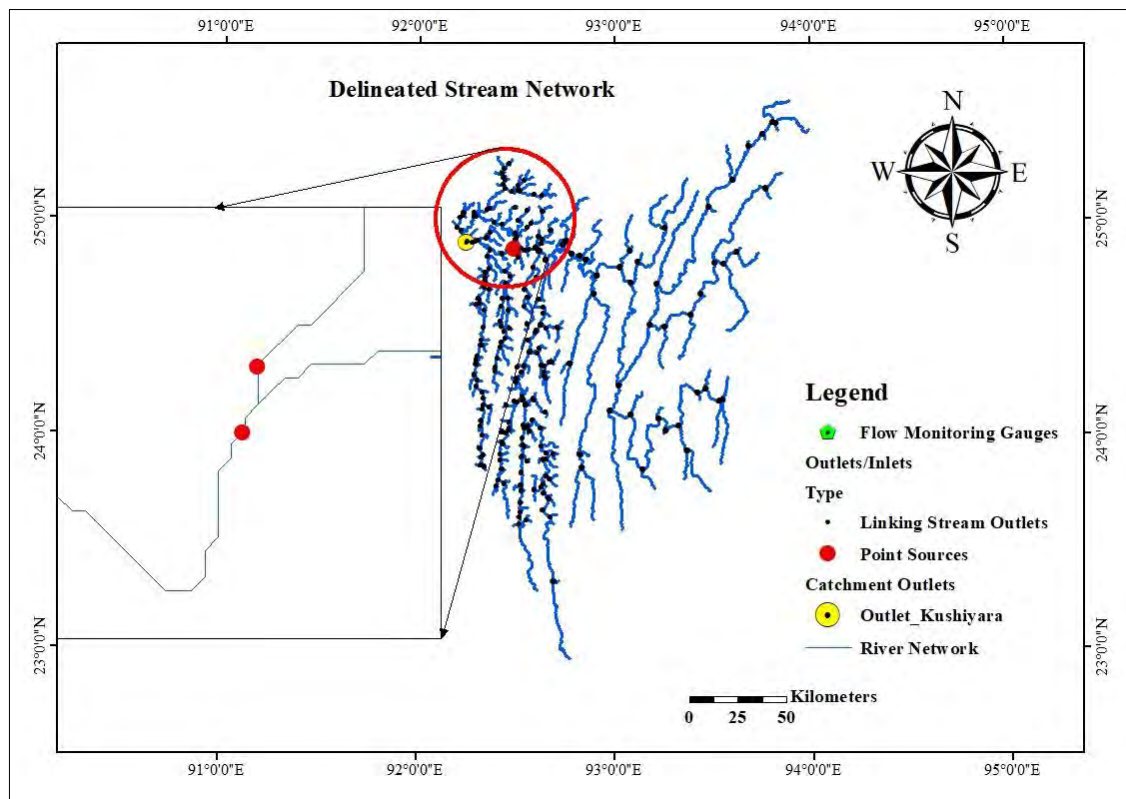


Figure 3.2 Stream network of the Meghna Basin

Land cover is one of the most important factors that affect surface erosion, runoff, and evapotranspiration in a watershed. GlobCover is an ESA initiative that began in 2005 in partnership with JRC, EEA, FAO, UNEP, GOFC-GOLD, and IGBP and provides global composites and land cover maps using as input observations from the 300m MERIS sensor onboard the ENVISAT satellite mission. Land cover data [23] for the study area were collected from the globe cover website (http://due.esrin.esa.int/page_globcover.php) and divided into 12 landuse classes according to SWAT land use database (Figure 3.3). Generic land cover types and their 4 letter codes that are included in the SWAT land use database has also been presented in Table 3.1.

A Soil Map of the world at 1:5 000 000 scale was downloaded from the FAO website (<http://www.fao.org/soils-portal/soil-survey/soil-maps-and-databases/harmonized-world-soil-database-v12/en/>). The Harmonized World Soil Database of FAO is a 30 arc-

second raster database with over 15 000 different soil mapping units that combine existing regional and national updates of soil information worldwide. The soil data was clipped for the study area and classified as per SWAT user soil data classification. Four prominent soil type has been found in the study area (Figure 3.4).

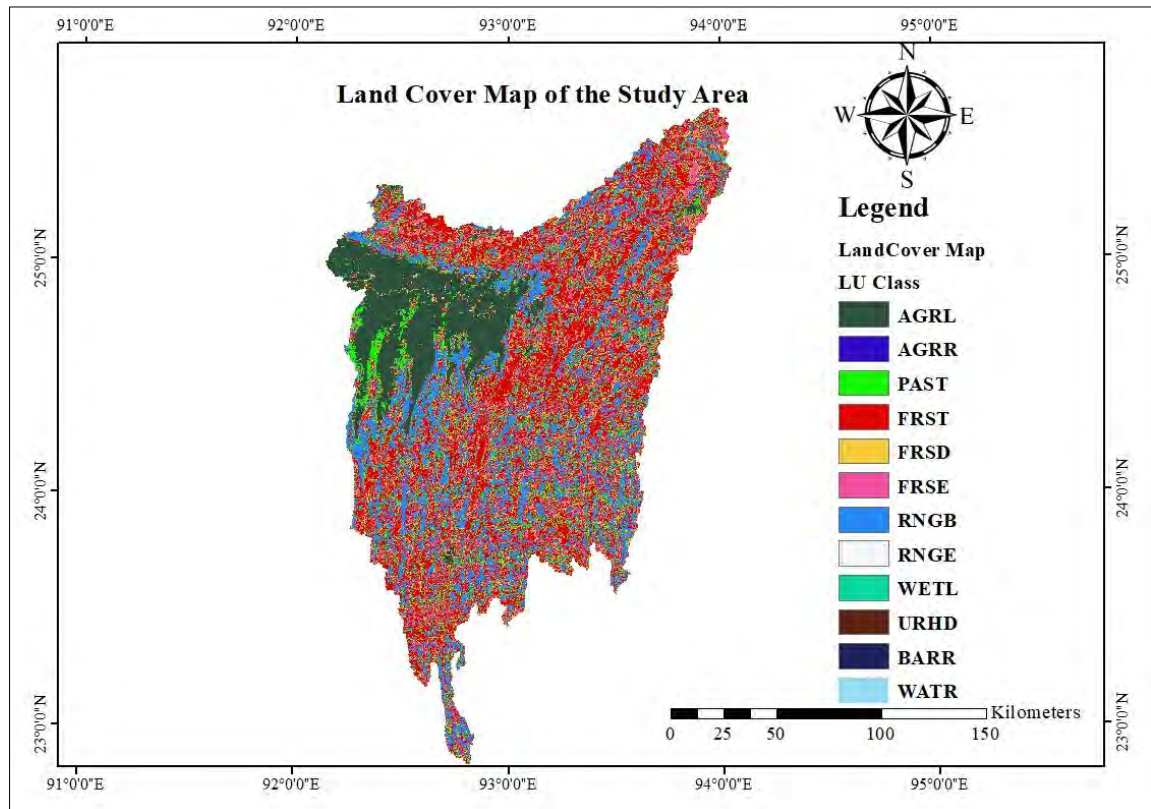


Figure 3.3 Land cover type and land use pattern map of Meghan river basin

Table 3.1 Generic Codes of Land Cover Types Used in SWAT

Land Cover Type	Code	Land Cover Type	Code
Agricultural Land-Generic	AGRL	Wetlands- nonforested	WETF
Agricultural Land-Row Crops	AGRR	Pasture	PAST
Agricultural Land-Close- grown	AGRC	Summer pasture	SPAS
Hay	HAY	Winter pasture	WPAS
Forest-mixed	FRST	Range-grasses	RNGE
Forest-deciduous	FRSD	Range-brush	RRGB

Land Cover Type	Code	Land Cover Type	Code
Forest-evergreen	FRSE	Range-southwestern US	SWRN
Wetlands	WETL	Water	WATR
Wetlands-forested	WETF		

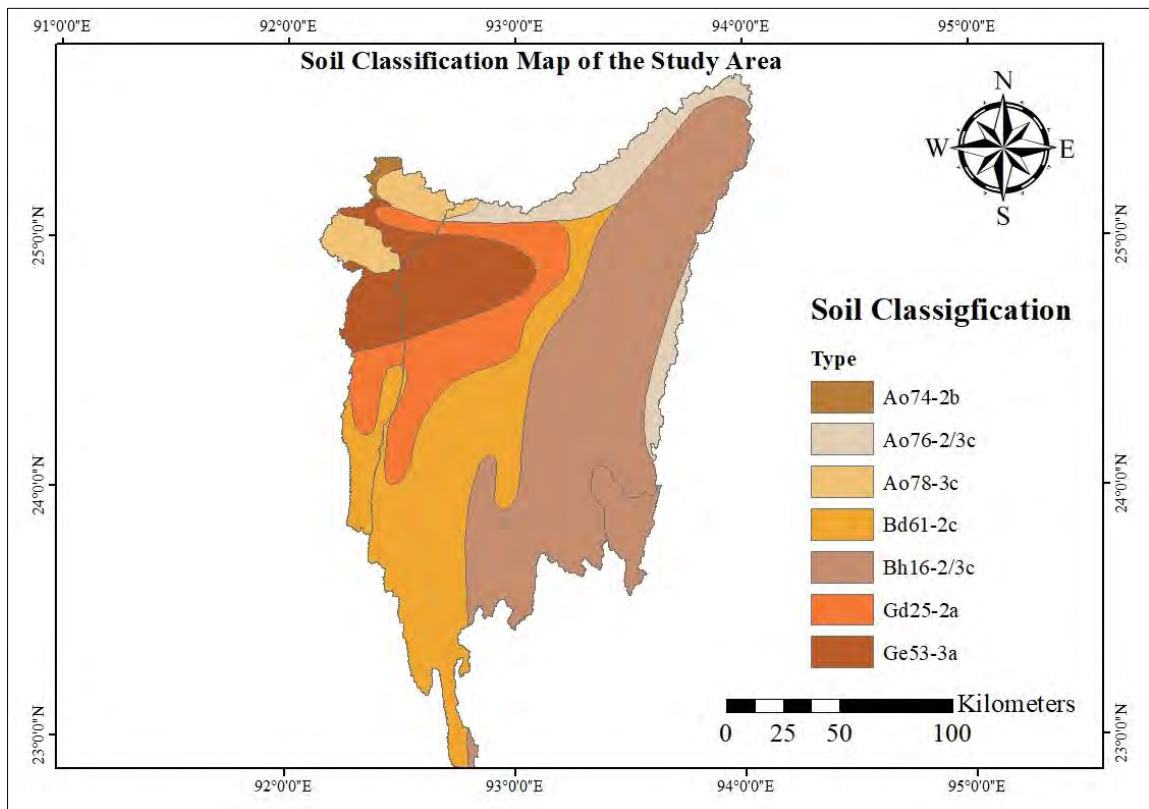


Figure 3.4 Soil Classification Map of Meghan River Basin

3.2.2 Weather, discharge, and water level data

SWAT requires daily precipitation, maximum/minimum air temperature, solar radiation, wind speed, relative humidity, etc. The values of all weather and climatic parameters have been collected from the satellite-derived data. Precipitation is a critical component of Earth’s hydrological cycle. Precipitation data on the daily basis has been collected from the Tropical Rainfall Measuring Mission (TRMM) from 1998 to 2018 (April). The NASA Tropical Rainfall Measuring Mission (TRMM) is the joint U.S. Japan satellite mission to provide the first detailed and comprehensive dataset of the four-dimensional distribution of rainfall and latent heating over vastly under sampled tropical and subtropical oceans

and continents (40°S–40°N) [51]. The daily product of 3B42RT is the derived daily precipitation totals derived from 3B42RT. The data is available on the daily basis from 1998-present. The present study used TRMM 3B42RT daily for 1998-2018 (April) from Mirador (<http://mirador.gsfc.nasa.gov/>). Mirador is designed to facilitate TRMM data searching, accessing, and downloading. The data portal consists of a search and access web interface developed in response to the search habits of data users.

Table 3.2 Collected input data for model setup and development

Type	Data Type	Resolution/ Location	Source	Time
Physical Data	Digital Elevation Model (DEM)	90 m	Shuttle Radar Topography Mission (SRTM)	2003
Physical Data	Land cover map	300 m	MERIS sensor, ENVISAT satellite mission	January - December 2009
Physical Data	Digital soil map	1:5,000,000	FAO	2007
Meteorological Data	Precipitation	Sylhet & Srimangal	Bangladesh Meteorological Department (BMD)	1954-2014
Meteorological Data	Precipitation	Meghna River Basin	Tropical Rainfall Measuring Mission (TRMM)	1998-2018 (April)
Meteorological Data	Maximum-minimum air temperature	Meghna River Basin	NASA-Prediction of Worldwide Energy Resource	1998-2018 (April)
Hydrological Data	Discharge and Water level	Sheola (SW 173) & Kanairghat (SW 266)	BWDB	1998-2018
Future Climate Data	Future precipitation and temperature data	RCP 4.5 & RCP 8.5	CORDEX	1970-2099
Data for Upstream Intervention Scenario	Reservoir Information and Operation Strategy	Secondary Data	Previous studies	April 2005

The calculation of potential evapotranspiration using the Hargreaves method in SWAT requires the input of maximum and minimum air temperature. The Prediction of

Worldwide Energy Resource (POWER) project of NASA provides climatic data from 1981 to the present. The system was initiated to improve upon the existing renewable energy data set and to create new data sets from new satellite systems. The POWER project targets three user communities: (1) Renewable Energy, (2) Sustainable Buildings, and (3) Agro climatology. The Renewable Energy Archive is designed to provide access to parameters specifically tailored to assist in the design of solar and wind-powered renewable energy systems. The Sustainable Buildings Archive is designed to provide industry-friendly parameters for the buildings community, to include parameters in multi-year monthly averages. The agro climatology Archive is designed to provide web-based access to industry-friendly parameters formatted for input to crop models contained within agricultural DSS. Daily maximum and minimum temperatures were collected from the NASA Power energy resources website (<https://power.larc.nasa.gov/data-access-viewer/>) from 1998 to 2018 (April). Table 3.2 summarizes basic data collected for the present study including data sources, resolution, and time.

One or more station discharge data is required to compare the developed hydrological model result and with which the model can be optimized. The discharge or runoff generated from the catchment area at the outlet due to precipitation needs to be checked against observed discharge data of the nearby station of the catchment outlet. In Bangladesh, discharge data is not collected daily. So the daily discharge values have to be generated by developing rating curves using the daily recorded water level. Bangladesh Water Development Board (BWDB) measures the actual river discharge and water level for several stations over the country. BWDB discharge and water level stations at Sheola (SW 173) were found along the river Kushiya. Discharge and water level data at station Sheola have been collected from 1998 through 2018. Rating curves have been plotted to get a daily discharge for each year.

CORDEX is a WCRP framework to evaluate regional climate model performance through a set of experiments aiming at producing regional climate projections. Therefore, future precipitation and maximum-minimum air temperature data considering RCP 4.5 and RCP 8.5 scenarios have been collected from the CORDEX website (<http://www.cordex.org/>).

3.3 Methodological Framework

The overall methodological framework of the study is presented in Figure 3.5. The framework represents the work procedure of the study. In summary, collected DEM and river networks were modified to represent the real scenario. Land use and soil map were prepared and classified, rainfall data were bias-corrected, rating curve was plotted to get daily discharge data. Calibrated and validated model performance will be evaluated, precipitation data from different RCM model output will be bias-corrected in the next chapters. Then the developed SWAT model for the Meghna River basin will be used to analyze climate change scenarios and the impact of reservoir operation.

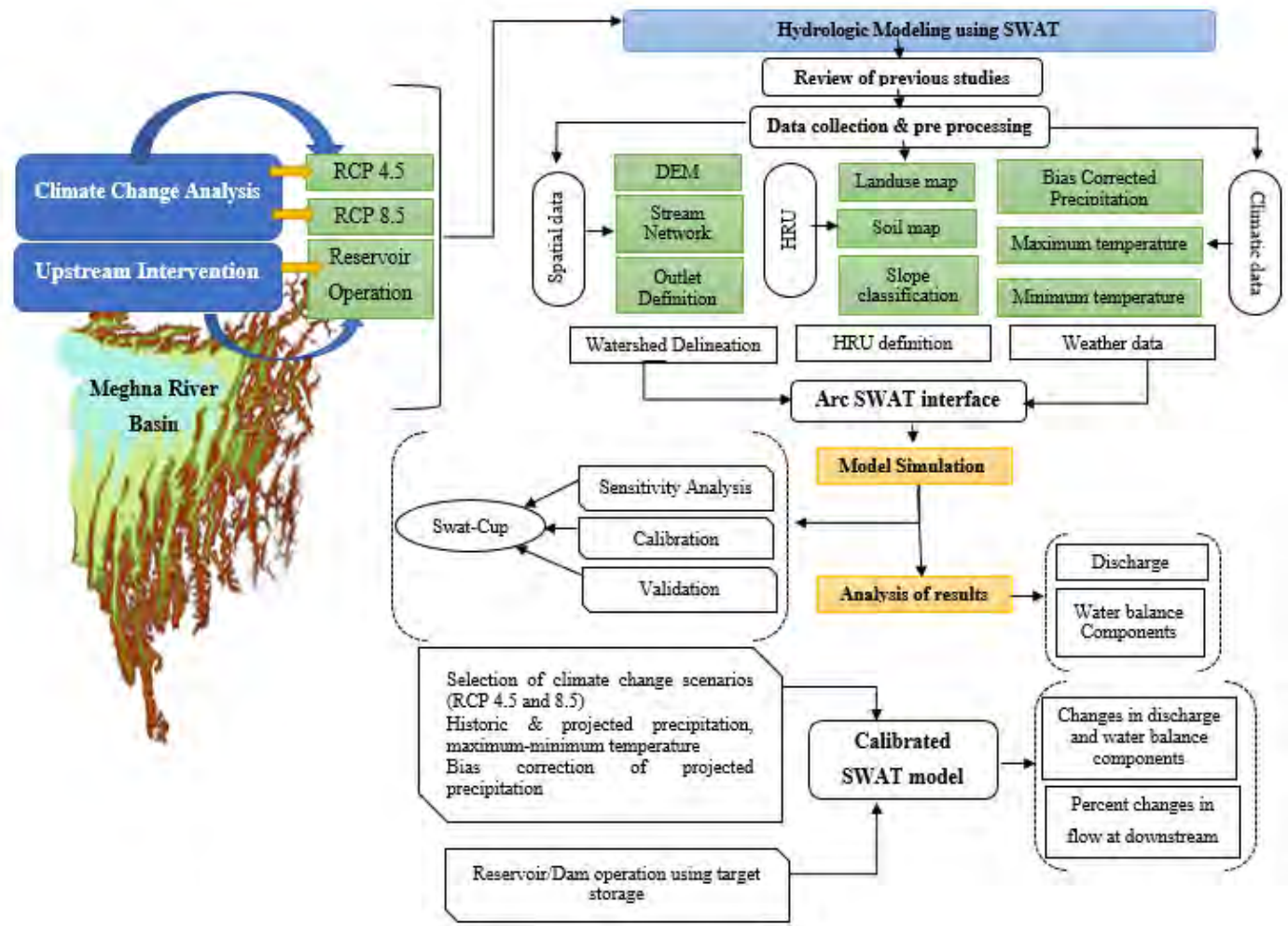


Figure 3.5 Schematic of SWAT model development and scenario analysis

4 MODEL SETUP AND SELECTION OF SCENARIOS

4.1 Model Setup

The surface runoff model setup in SWAT includes several steps which are discussed below-

4.1.1 Watershed configuration

Watershed delineation based on digital elevation models (DEM) is the prerequisite to set up the SWAT model for the Meghna river basin. The prevailing different topography and hydrologic processes of Bangladesh and India arise the following problems in watershed delineation (1) the reaches delineated from the DEM do not agree well with the realistic ones; (2) the braided streams cannot be identified by the SWAT model; (3) the bifurcation of Barak river into Surma and Kushiya river cannot be detected by SWAT model. Based on ArcGIS and ArcSWAT, an improved DEM-based method was applied in watershed delineation.

Traditional DEM-based watershed delineation methods have low precision in delineating stream network and the bifurcations. In this study, the “Burn-in” method cooperated with manual edit based on google earth was used to improve the streams and subbasin delineation in the basin area. Attributes such as location and hydrological connection can be edited in the GIS environment to make the extraction results agree with the realistic hydrological processes and meet the requirements of the model setup. First, the DEM grid of the study area was loaded into the SWAT model and then using the “Burn-in” function, digital stream network (polygon shapefile or feature class) was imported and superimposed onto the DEM to define the location of the stream network. Before that, the DEM was masked to clarify the extent of the study area which saves time in generating stream networks. In this study, two watersheds were delineated (1) for the Barak river basin with an outlet at Amalshid (2) for the Surma-Kushiya river basin with outlets near Sheola. The whole catchment area is about 32798.58 sq km which was subdivided into 498 subbasins (Figure 4.1). Two point sources were introduced to define the bifurcation of the Barak River and to define inlet points of upstream discharge.

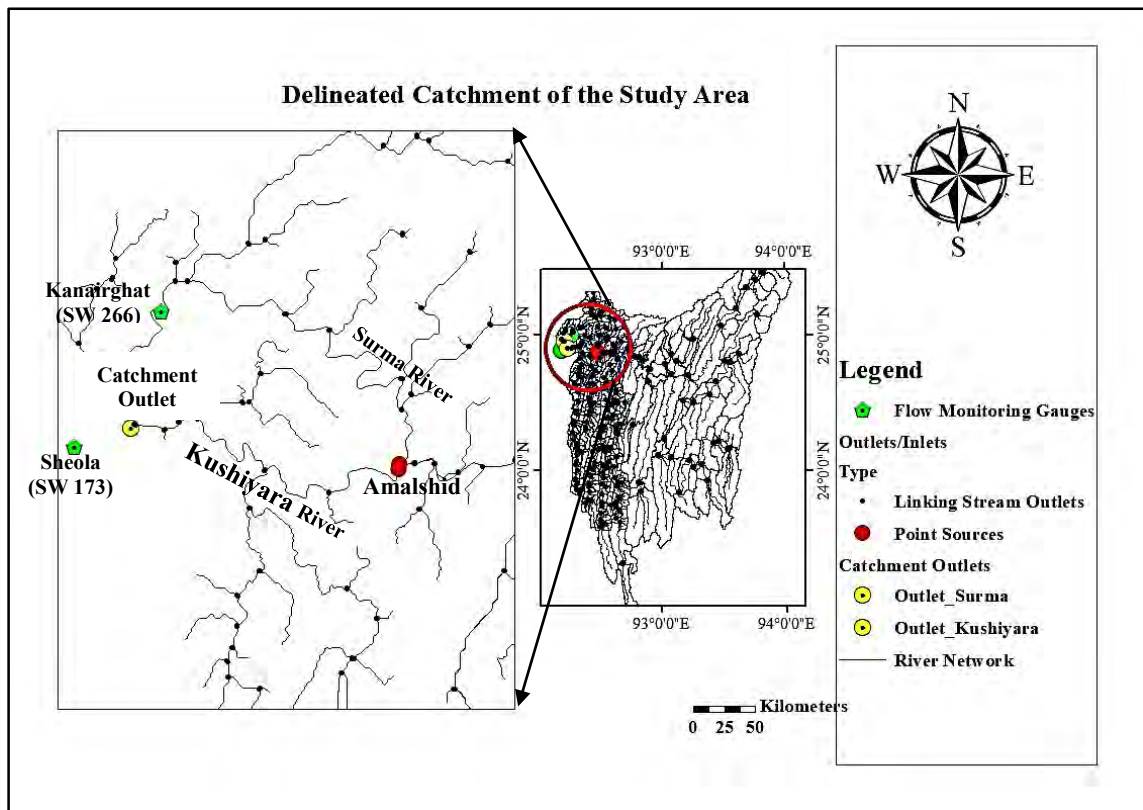


Figure 4.1 Delineated watershed of the Meghna river basin

4.1.2 HRU analysis

The Soil and Water Assessment Tool (SWAT) uses hydrologic response units (HRUs) as the basic unit of all model calculations. Hydrologic response units are portions of a subbasin that possesses unique land use/management/soil attributes. HRU definition in SWAT requires classified land use and soil maps as input so that it can capture the diversity of the land use and soils within the study area. Classified land use and soil map discussed in the previous section have been used as an input for land-use and soil definition. SWAT also requires classification of catchment land slope into multiple classes. The total catchment area was subdivided into three slope classes. Landuse, soil, and slope information are overlaid to divide the whole catchment area into a total of 2533 hydrologic response units (HRUs) (Figure 4.2). ArcSWAT, the ArcGIS interface for SWAT, allows users to specify thresholds of land cover, soil, and slope in defining HRUs to improve the computational efficiency of simulations while keeping key landscape features of a watershed in the hydrologic modeling. A threshold value of land use (10%), soil (20%), and slope (10%) were considered based on the previous studies of large basins.

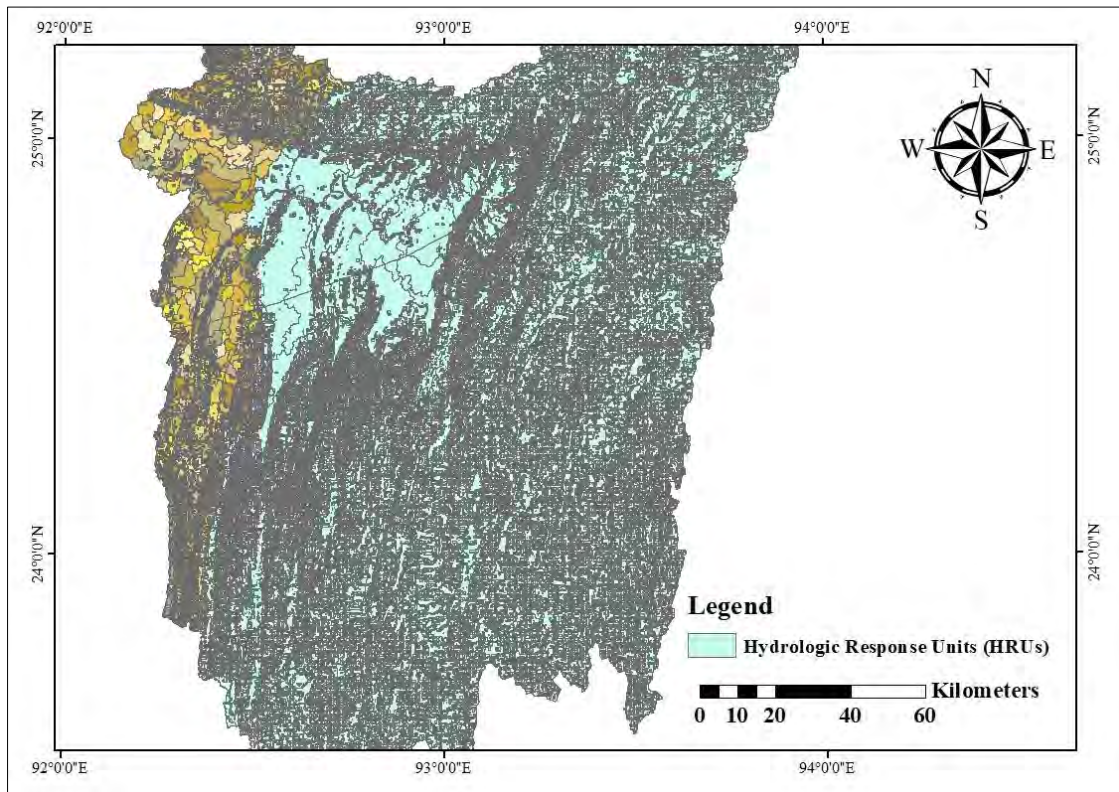


Figure 4.2 HRU definition within the study area

4.1.3 Bias correction of rainfall data

Satellite-derived climatic variables or that from climate model outputs can be used directly, but in climate change or impact studies, these outputs are often not useful because of significant biases [35]. To overcome these anomalies, rainfall data were bias-corrected basing on observed rainfall of the nearest rainfall stations using the linear scaling (LS) method of bias correction. It operates with monthly correction values based on the ratio of mean monthly observed and raw data. Precipitation is typically corrected with a multiplier. To bias correct, the satellite-derived rainfall data from TRMM, nearest rainfall stations of BMD (Sylhet and Srimangal) were collected. The correction factor was obtained from the ratio of mean monthly rainfall value of observed and raw data using the following equation 4.1. Then the average correction factor was applied to the all rainfall station. Bias corrected rainfall data are presented in the following figures (Figure 4.3 and Figure 4.4).

$$P_{\text{corrected}} = P_{\text{raw}} \times C.F \quad (4.1)$$

Where, Correction factor, C.F = $\frac{\mu(P_{\text{observed}})}{\mu(P_{\text{raw}})}$

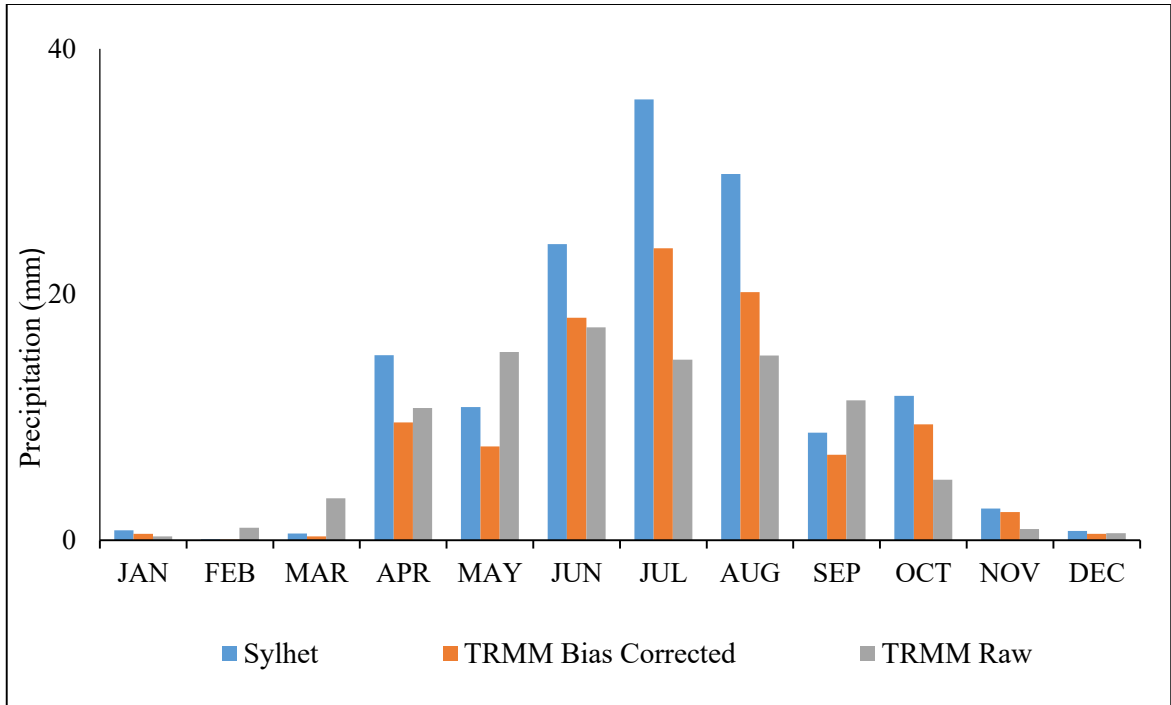


Figure 4.3 Bias correction at Sylhet

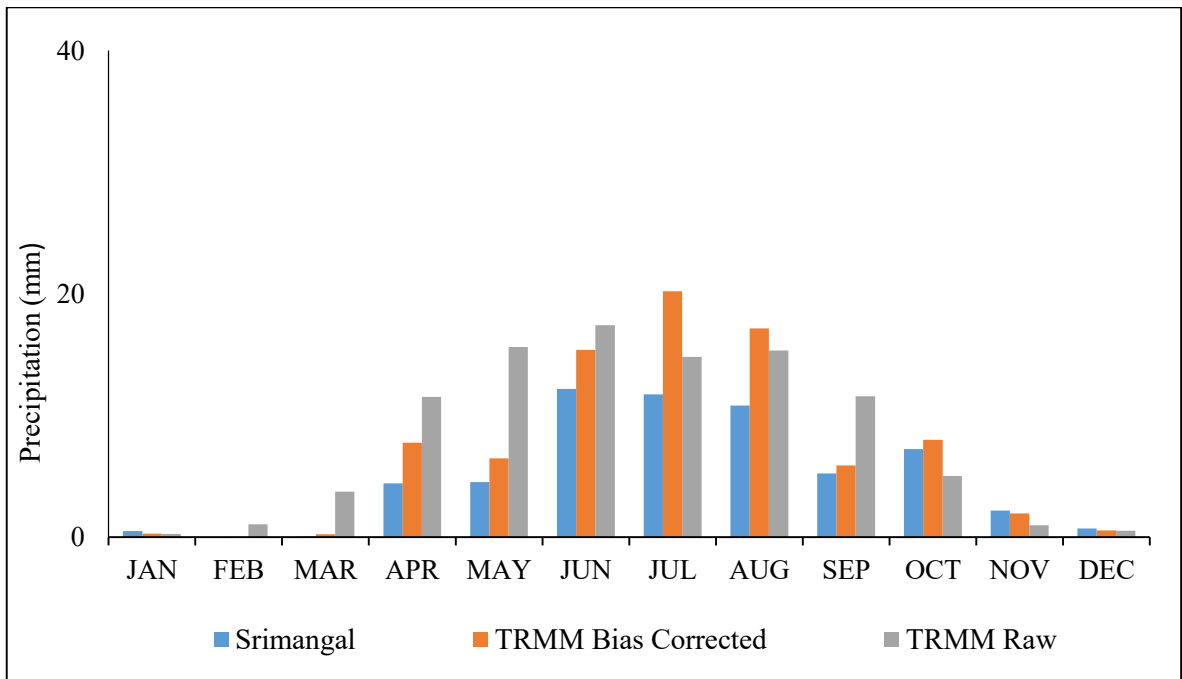


Figure 4.4 Bias correction at Srimangal

4.1.4 Weather data input

SWAT requires watershed level inputs that are used to model different processes throughout the watershed. SWAT model uses a master water balance approach to compute runoff volumes and peak flows (Arnold, Srinivasan, et al. 1998). The equation subtracts all forms of water loss on a day from precipitation on the day including surface runoff (Q_{surf}), evapotranspiration (E_a), loss to vadose zone (w_{seep}), and return flow (Q_{gw}) to calculate the final soil water content. So the model setup requires the input of user-defined daily precipitation over a longer period. The study used daily precipitation data for 118 rainfall stations for the period of 1998- April 2018 over the whole catchment area (Figure 4.5).

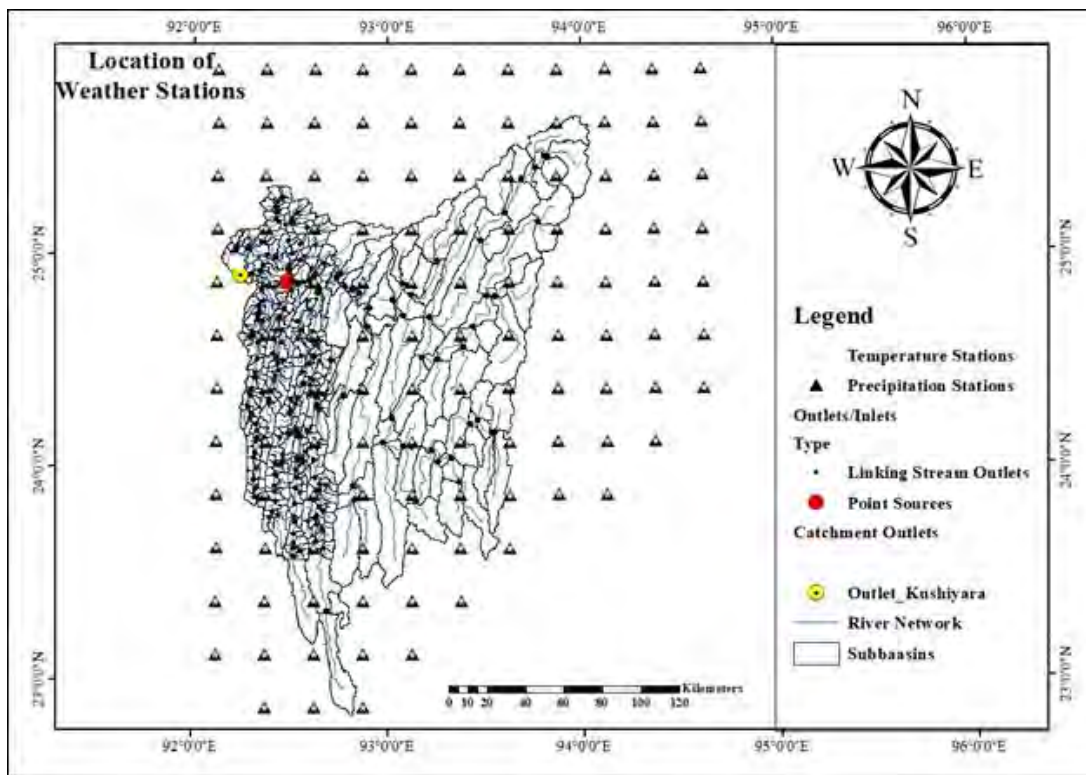


Figure 4.5 Location of satellite-derived weather data station

SWAT provides two methods for estimating surface runoff: the SCS curve number procedure (SCS, 1972) and the Green & Ampt infiltration method. The present study used the SCS curve number to calculate runoff volume. Three of PET calculation methods have been incorporated into SWAT: the Penman-Monteith method, the Priestley-Taylor method, and the Hargreaves method. From these three methods, researchers used the Hargreaves method which requires air temperature only. In the present study, the

maximum-minimum air temperature has also been input for 118 temperature gages (Figure 4.5) throughout 1998-2018 (April).

4.1.5 Point source discharge data input

SWAT directly simulates the loading of water, sediment, and other constituents of land areas in the watershed. To simulate the loading of water and pollutants from sources not associated with a land area (e.g. sewage treatment plants), SWAT allows point source information to be read in at any point along with the channel network. The point source loadings may be summarized on a daily, monthly, yearly, or average annual basis. The inflow coming from the upstream Barak river basin through Amalshid has been included in the Surma-Kushiyara river basin using point sources. The total discharge at Amalshid has been distributed between Surma (40%) and Kushiyara (60%) river and has been included in the model as two-point sources of water loadings. Point source discharges are provided daily in the subbasin 99 (for Surma river) and subbasin 106 (for Kushiyara river).

4.2 Model Simulation

DEM, Stream network layers, land use, and soil type have been used in the SWAT model as geospatial input. Weather variables like rainfall, maximum, and minimum temperature have been incorporated daily from 1998 to 2018. Water loading from upstream catchment has also been included using point source discharges. A warm-up period of two years (1998-1999) has been considered to allow "buckets" in the SWAT model (reservoirs, wetlands, soil moisture, aquifers) to fill up and reach stable values. Flows in the first two years have been underestimated because of this. After setting up the model, a daily time step SWAT model has been run through the ArcGIS environment for 2000-2018 excluding the warm-up period. The default output of SWAT is in the monthly time step; therefore, the output file type has been modified to include the daily output.

After model simulation with initial parameters, the simulated and observed variables have been plotted at the outlet stations for the entire period of record. The simulated discharge seems to have higher peak discharge values than the observed discharge at Sheola (SW 173) which depicts the need for adjusting peak discharges through model calibration. The

entire model period has been divided into calibration (2000-2009) and validation (2009-2018) periods while attempting to ensure that both periods have an almost similar number of wet and dry years and similar average water balance.

4.3 Model Calibration and Validation

Calibration and validation of process-based hydrological models are two major processes to simulate the hydrology and water balance of the catchment area. Through calibration, it is necessary to find a combination of the parameter values to calibrate the developed SWAT model. The desired parameter values will provide an acceptable match between the observed and simulated output data. Discharge and water level data of 19 years from 2000-2018 (April) were collected from BWDB. The daily discharge was generated using a rating curve from the collected daily water level and monthly discharge data. Then developed SWAT model was calibrated against observed streamflow from 2000 to 2008 near the outlets of the river basin. To assess whether the calibrated model can be considered valid for subsequent use, the model was evaluated (validated) from 2009 to 2018.

Calibration, validation, sensitivity analysis, and uncertainty analysis were done using SWAT-CUP which is an auto-calibration and uncertainty analysis module program based on the SWAT engine. SWAT-CUP is a relatively advanced optimization system that can deal with a range of input parameters. The intelligence of SWAT-CUP allows model parameters to be predefined and optimized throughout the auto-calibration process or manually adjusted iteratively between calibration batches. Using this SWAT-CUP interface, any calibration/uncertainty or sensitivity program can easily be linked to SWAT. A schematic of the linkage between SWAT and the five optimization programs used in SWAT-CUP is illustrated in Figure 4.6.

From the five optimization programs, Sequential Uncertainty Fitting version 2 (SUFI-2) was used in this study. In SUFI-2, uncertainty in parameters, expressed as ranges (uniform distributions), accounts for all sources of uncertainties such as uncertainty in driving variables (e.g., rainfall), conceptual model, parameters, and measured data. Propagation of the uncertainties in the parameters leads to uncertainties in the model output variables, which are expressed as the 95% probability distributions. These are calculated at the 2.5%

and 97.5% levels of the cumulative distribution of an output variable generated by the propagation of the parameter uncertainties using Latin hypercube sampling. This is referred to as the 95% prediction uncertainty, or 95PPU.

To quantify the fit between simulation result, expressed as 95PPU and observation expressed as a single signal (with some error associated with it) SWAT-CUP includes with two statistics: P-factor and R-factor. P-factor is the percentage of observed data enveloped the modeling result, the 95PPU. R-factor is the thickness of the 95PPU envelop.

4.3.1 Selection of calibration parameters

Numerous studies have reported input parameters used in SWAT model calibration including the detailed reporting of model parameterization, calibration procedures and parameter ranges, and/or final values [20]. Therefore, the most sensitive parameters for the observed values of interest were determined based on previous studies. Calibration parameters found from the previous studies have been listed in table 4.1 by the process.

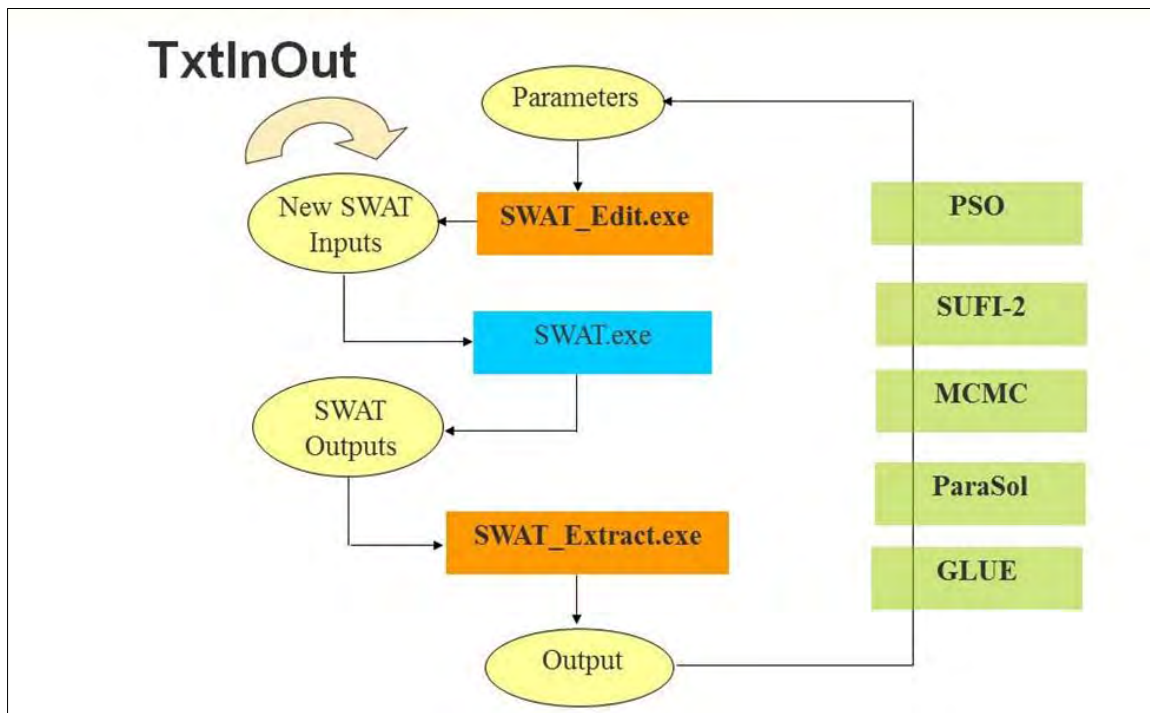


Figure 4.6 Linkage between SWAT and five optimization programs [67]

From the summary, it can be seen that CN directly impacts surface runoff; however, as surface runoff changes, all components of hydrology balance change. Soil erosion and

nutrient transport are also directly impacted by surface runoff, as are plant growth and nutrient cycling. It is also evident from table 4.1 that hydrology is calibrated in most studies, with CN2, AWC, ESCO, and SURLAG routinely. The baseflow process is also often calibrated with the baseflow recession parameters used in many studies. The general meaning of the parameters that are used often in SWAT model calibration is given below in table 4.2.

Table 4.1 Calibration parameters reported in various watershed studies [17]

Process	Input Parameters						
Surface runoff	CN2	AWC	ESCO	EPCO	SURLA G	OV_N	
Baseflow	GW_A LPHA	GW_R EVAP	GW_D ELAP	GW_ QWN	REVAP MN	RCHAR G_DP	
Snow	SFTM P	SMFM N	SMFM X	SMT MP	TIMP	SNO50C OV	SNOCOVMX
Sediment from channels	PRF	APM	SPEXP	SPCO N	CH_ERO D	CH_COV	
Sediment from landscape	USLE_ P	USLE_ C	USLE_ K	LAT_ SED	SLSOIL	SLOPE	
N from landscape	RCN	UBN	GWNO 3	EROR GN	NPERC O	ANION_ EXCL	
P from landscape	PSP	PHOSK D	UBP	PPER CO	WQMIN P	ERORGP	
Process	Input Parameters						
Pesticides	KOC	HL_SO IL	HL_FO L	WSO L	WOFFW		
Subsurface tile	TDRA IN	GDRA IN	DEP_I MP				
N and P from channels	BC1	BC2	BC3	BC4	RS4	RS5	
Plant growth	GSI	HI	BLAI	PHU	CN_YL D		
Bacteria	BACT RDQ	BACT MIX	BCNST	CFRT KG	WDPRC H	WDPQ	
Other	BIOMI X	SOL_R OCK	MSK_ COL	MSK_ CO2	CBNINT	SOL_BD	ALPHA_BNR EVRCH SOL_ALB LAT_TTIME

Table 4.2 Calibration parameters generally used for SWAT model [50]

Parameter	Details
CN2	Number of the initial curve for the moisture condition AMCII (dimensionless)
ALPHA_BF	Baseline flow recession constant (days)
GW_DELAY	Time interval for recharge of the aquifer (days)
GWQMN	Water limit level in the shallow aquifer for the occurrence of base flow (mm)
CH_K2	Effective hydraulic conductivity of the channel (mm h ⁻¹)
SURLAG	Delay time of direct surface runoff (days)
SOL_K	Saturated soil hydraulic conductivity (mm h ⁻¹)
CH_N2	Manning coefficient for the main channel (s m ^{-0.33})
ESCO	Soil water evaporation compensation factor (dimensionless)
SLSOIL	Slope length for lateral subsurface flow (m)
CANMX	Maximum amount of water intercepted by vegetation (mm)
SOL_AWC	Soil water storage (mm mm ⁻¹)
SOL_Z	Depth of soil layer (mm)
GW_REVAP	Coefficient of water rise to saturation zone (dimensionless)
BIOMIX	Efficiency of soil biological mix (dimensionless)
SOL_ALB	Soil Albedo (dimensionless)
REVAPMN	Water depth in the aquifer for the occurrence of water rise to the unsaturated zone (mm)
EPCO	The factor of compensation for water consumption by plants (dimensionless)
SLSUBBSN	Average slope length (m)

After observing the model performance, it was noticed that the peak flow was systematically overestimated and the base flow was underestimated by the model at the outlet of the basin. At first, 11 parameters have been chosen as initial calibration parameters. But it has been found from the sensitivity analysis that few of these parameters have no significant effect on the model result. Finally, nine parameters have been determined to be the most sensitive parameters for streamflow calibration and validation.

Table 4.3 shows the initial ranges of the calibration parameters. Where V_ means the existing parameters have to be replaced by a given value, A_ means a given value is added to the existing parameter and R_ means an existing parameter value is multiplied by (1 + a given value). An initial uncertainty range of 30% (typical range is 20%-30%) has been assigned to each parameter globally to scale the parameters identically for each HRU. The final fitted values were derived from several iterations until the objective function was reached [17]. The objective function was defined by the Nash-Suttcliffe efficiency coefficient using a minimum value of objective function threshold 0.5 for the behavioral solutions to seek good performance.

Table 4.3 Initial range of the calibration parameters

Parameters	Initial Range	Parameters	Initial Range
V__ESCO.hru	0.4 -1	V__GW_REVAP.gw	0.02-0.1
A__RCHRG_DP.gw	-0.05 - 0.05	A__GWQMN.gw	-1000-1000
R__CN2.mgt	-0.1-0.1	V__ALPHA_BF.gw	0-1
R__SOL_AWC.sol	-0.05 - 0.05	A__GW_DELAY.gw	-30-90
A__REVAPMN.gw	-750-750		

4.4 Sensitivity Analysis

Nine different parameters were examined in the sensitivity analysis using a global sensitivity analysis of SWAT_CUP to identify the most influential parameters on the flow components to optimize the objective function. From the definition of the parameters to be calibrated and the subsequent calibration, SWAT-CUP defines the parameters most sensitive to calibration using the Latin Hypercube (LH) and one-factor-a-time (OAT) methods, using this information for the next iteration.

The ranking of the parameters based on the “t-stat” and “p-value” indices, is presented in table 4.4 and figure 4.7. The t-stat provides a measure of sensitivity (a larger absolute value is more sensitive) and the p-value determines the significance of the sensitivity (a value close to zero has more significance). The finally adjusted parameters are then used to calibrate and validate the SWAT model. The calibration output has been shown using flow vs time graph (Figure 4.6). Graphical techniques like hydrograph or time series plot

of simulated and measured flow throughout the calibration and validation periods help to identify model bias and can identify differences in timing and magnitude of peak flows.

Table 4.4 Ranking of sensitive parameter based on t-stat and p-value

Parameters	t-stat	p-value	Ranking
R_SOL_AWC.sol	0.178515793	0.861882657	9
A_GWQMN.gw	0.198914446	0.846315740	8
V_ESCO.hru	-0.202846142	0.843323055	7
A_REVAPMN.gw	0.299141295	0.770956823	6
R_CN2.mgt	0.312296647	0.761229828	5
V_GW_REVAP.gw	-0.871197709	0.404076282	4
A_GW_DELAY.gw	1.274963393	0.231147533	3
A_RCHRG_DP.gw	-1.345290312	0.208242892	2
V_ALPHA_BF.gw	-1.543126246	0.153829904	1

The most sensitive parameters were CN2, ESCO, SOL_AWC, REVAPMN, GW_REVAP, GWQMN, GW_DELAY, RCHRG_DP, and ALPHA_BF, ranked according to the highest sensitivity tested at a significance level of 5% (Table 4.4 and Figure 4.5). The parameters with the maximum t-stat value (large absolute) are the most sensitive parameters and vice versa. The model parameter with the highest t-stat value is the most sensitive parameter that is ranked 1 and the parameter with the lowest t-stat values is the least sensitive parameter and ranked 9.

These sensitive model parameters are related to the peak flow in the channel (CN2), water in the soil (SOL_AWC, REVAPMN, GW_REVAP, GWQMN, GW_DELAY, RCHRG_DP, ALPHA_BF), and the water evaporation compensation factor (ESCO). It is interesting to note that the CN2 parameter did not show the expected sensitivity, since it is related to direct surface flow, however; it was shown to be one of the less sensitive parameters. The most sensitive parameter is ALPHA_BF, the baseflow alpha-factor

(1/days), Value of which varies from 0.1-0.3 for land with slow response to recharge to 0.9-1.0 for land with a rapid

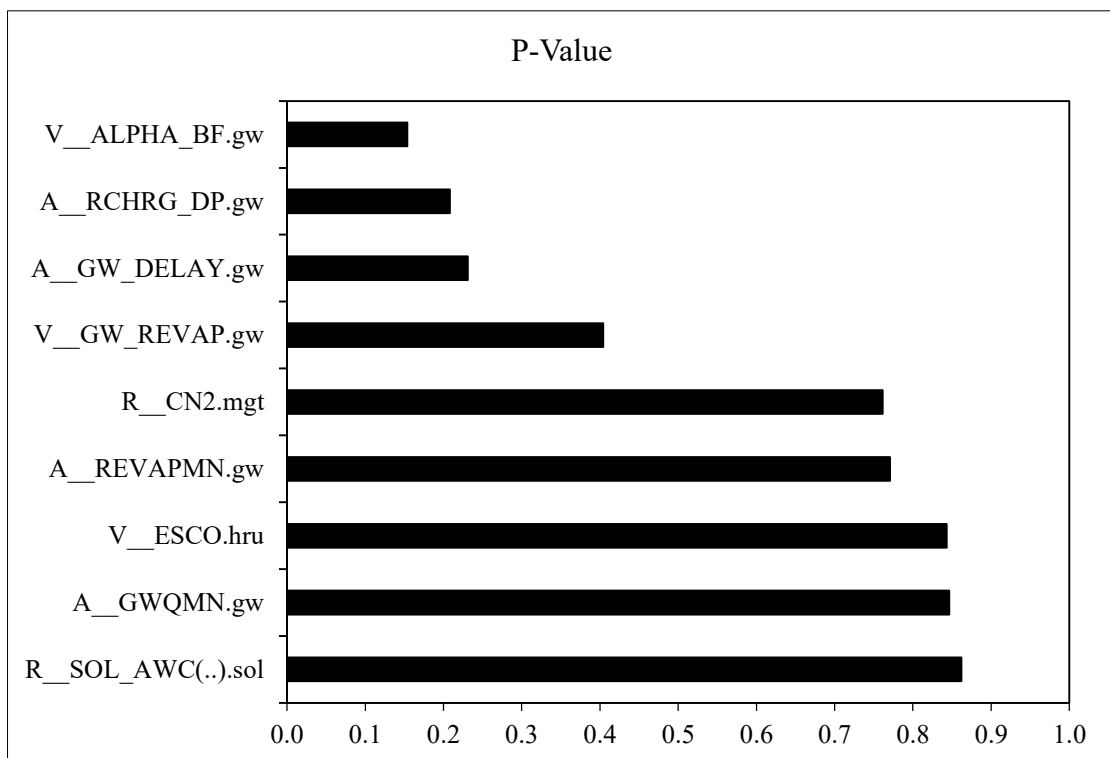
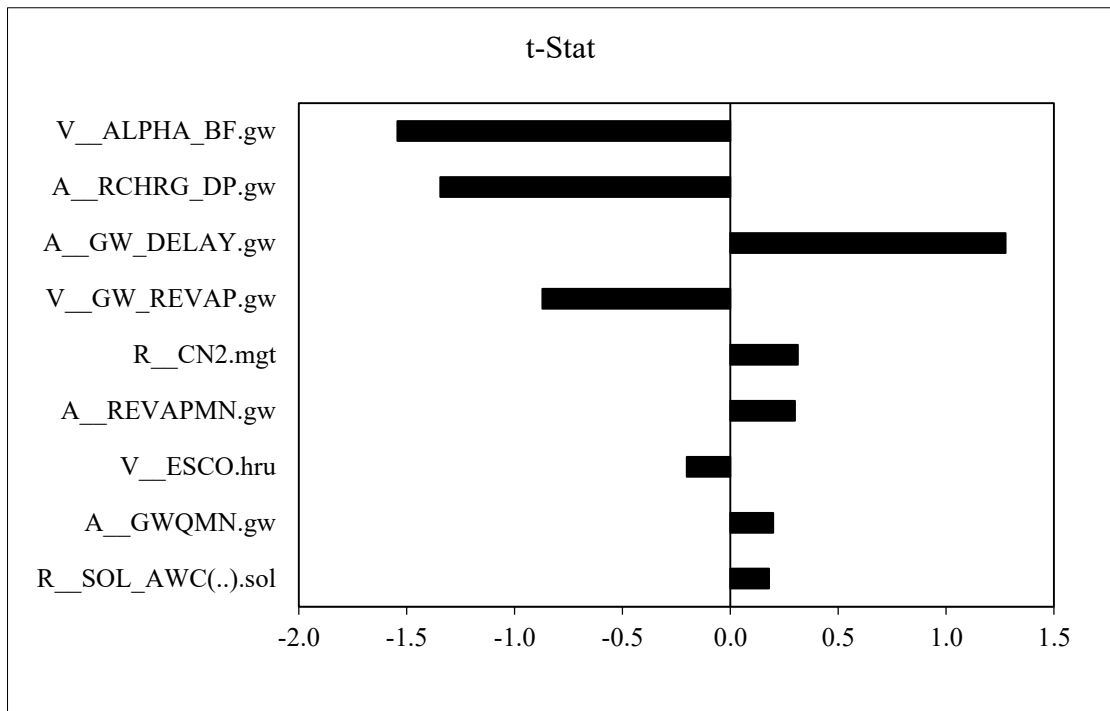


Figure 4.7 Graph of statistical index values: “t-stat”; and “p-value” vs calibrated parameters

response. The second most sensitive parameter is deep aquifer percolation fraction RCHRG_DP value of which varies in between 0 to 1. The high sensitivity of these groundwater parameters implies that if the watershed properties associated with these parameters are disturbed, the corresponding changes in watershed hydrology can be substantial.

4.5 Calibration Outputs

After each simulation the SWAT-CUP suggests new values of intervals, always aiming at the statistical optimization of precision. Although SWAT-CUP provides the best parameter set as a fitted value, it is suggested by [17] is to use the parameter ranges to fit the SWAT simulated results. Due to this characteristic, the calibrated value for each parameter can appear outside the initial intervals. The fitted values (Table 4.5) were then used to re-write the SWAT model inputs and simulate the land cover and climate change scenarios. Graphical results during calibration and validation (Figure 4.9) indicates adequate calibration and validation over the range of streamflow.

Table 4.5 Final adjusted intervals and calibrated value for each parameter

Parameters	Fitted Value	Parameters	Fitted Value
V__ESCO.hru	0.94	V__GW_REVAP.gw	0.072932
A__RCHRG_DP.gw	0.0131317	A__GWQMN.gw	-925.101990
R__CN2.mgt	0.060349	V__ALPHA_BF.gw	0.0277719
R__SOL_AWC.sol	-0.024574	A__GW_DELAY.gw	2.299479
A__REVAPMN.gw	-417.5451412		

4.6 Evaluation of Model Performance

4.6.1 Model evaluation statistics

4.6.1.1 Pearson's correlation coefficient (r) and coefficient of determination (R²)

Pearson's correlation coefficient (r) and coefficient of determination (R²) describe the degree of co-linearity between simulated and measured data. The correlation coefficient,

which ranges from -1 to 1 , is an index of the degree of the linear relationship between observed and simulated data. If $r = 0$, no linear relationship exists. If $r = 1$ or -1 , a perfect positive or negative linear relationship exists. Similarly, R^2 describes the proportion of the variance in measured data explained by the model. R^2 ranges from 0 to 1 , with higher values indicating less error variance, and typically values greater than 0.5 are considered acceptable [42]. Although r and R^2 have been widely used for model evaluation, these statistics are oversensitive to high extreme values (outliers) and insensitive to additive and proportional differences between model predictions and measured data.

4.6.1.2 Nash-Sutcliffe efficiency (NSE)

The Nash-Sutcliffe efficiency (NSE) is a normalized statistic that determines the relative magnitude of the residual variance (“noise”) compared to the measured data variance (“information”) (Nash and Sutcliffe, 1970). NSE indicates how well the plot of observed versus simulated data fits the 1:1 line. NSE is computed as shown in equation 4.2:

$$NSE = 1 - \left[\frac{\sum_{i=1}^n (Y_i^{obs} - Y_i^{sim})^2}{\sum_{i=1}^n (Y_i^{obs} - Y^{mean})^2} \right] \quad (4.2)$$

where, Y_i^{obs} is the i th observation for the constituent being evaluated, Y_i^{sim} is the i th simulated value for the constituent being evaluated, Y_{mean} is the mean of observed data for the constituent being evaluated and n is the total number of observations. NSE ranges between $-\infty$ and 1.0 (1 inclusive), with $NSE = 1$ being the optimal value. Values between 0.0 and 1.0 are generally viewed as acceptable levels of performance [42].

4.6.1.3 Percent bias (PBIAS)

Percent bias (PBIAS) measures the average tendency of the simulated data to be larger or smaller than their observed counterparts [42]. The optimal value of PBIAS is 0.0 , with low-magnitude values indicating accurate model simulation. Positive values indicate model underestimation bias and negative values indicate model overestimation bias. PBIAS is calculated with equation 4.3-

$$PBIAS = \left[\frac{\sum_{i=1}^n (Y_i^{obs} - Y_i^{sim}) * (100)}{\sum_{i=1}^n (Y_i^{obs})} \right] \quad (4.3)$$

Where, PBIAS is the deviation of data being evaluated, expressed as a percentage.

4.6.1.4 RMSE-observations standard deviation ratio (RSR)

RMSE-observations standard deviation ratio (RSR), was developed. RSR standardizes RMSE using the observations standard deviation, and it combines both an error index and the additional information. RSR is calculated as the ratio of the RMSE and standard deviation of measured data, as shown in equation 4.4-

$$RSR = \frac{RMSE}{STDEV_{obs}} = \frac{\left[\sqrt{\sum_{i=1}^n (Y_i^{obs} - Y_i^{sim})^2} \right]}{\left[\sqrt{\sum_{i=1}^n (Y_i^{obs} - Y^{mean})^2} \right]} \quad (4.4)$$

RSR varies from the optimal value of 0, which indicates zero RMSE or residual variation and therefore perfect model simulation to a large positive value. The lower RSR, the lower the RMSE and the better the model simulation performance [42].

Table 4.6 Classification of statistical indices

NSE	PBIAS	RSR	Classification
$0.75 < NSE \leq 1.00$	$PBIAS \leq \pm 10$	$0.0 < RSR \leq 0.50$	Very good
$0.65 < NSE \leq 0.75$	$\pm 10 < PBIAS \leq \pm 15$	$0.50 < RSR \leq 0.60$	Good
$0.50 < NSE \leq 0.65$	$\pm 15 < PBIAS \leq \pm 25$	$0.60 < RSR \leq 0.70$	Satisfactory
$NSE \leq 0.50$	$PBIAS \geq \pm 25$	$RSR > 0.70$	Unsatisfactory

After the calibration of the sensitive parameters, different model performance statistics were applied to the SWAT 2012 model for the Meghna river basin, the following (Table 4.7) results were obtained. It has been observed that NSE values for the daily streamflow calibration and validation ranges from 0.60 to 0.64.

Table 4.7 Model performance evaluation

Evaluation Statistic					
		NSE	PBIAS	RSR	R ²
Subbasin 86	Calibration	0.60 (satisfactory)	23.55 (satisfactory)	0.39 (very good)	0.71 (Good)
	Validation	0.64 (Good)	19.19 (satisfactory)	0.36 (very good)	0.68 (Good)

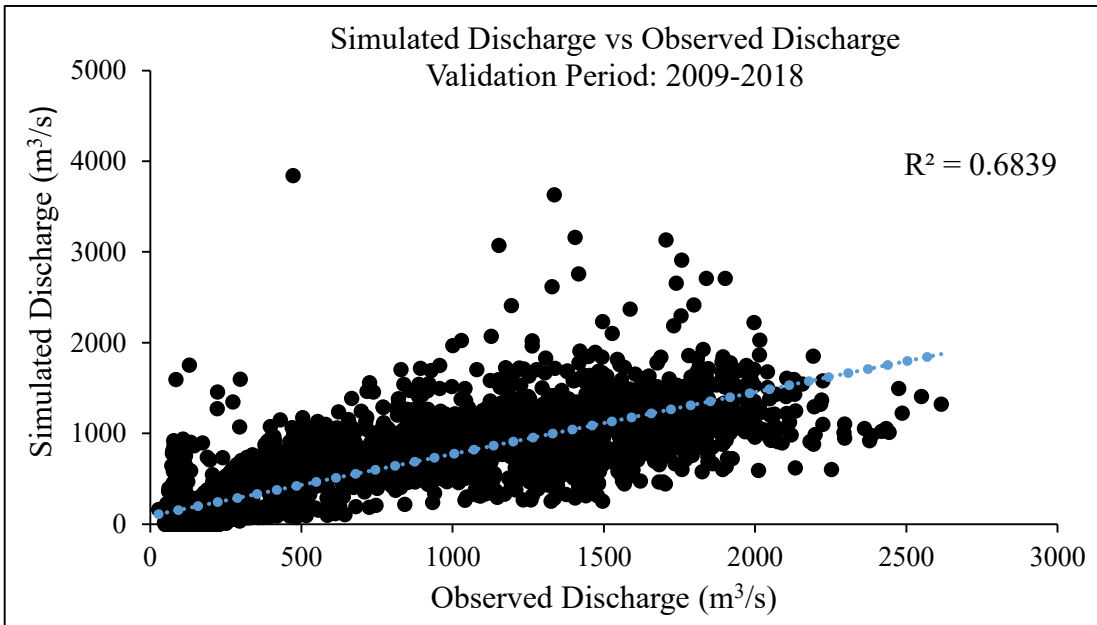
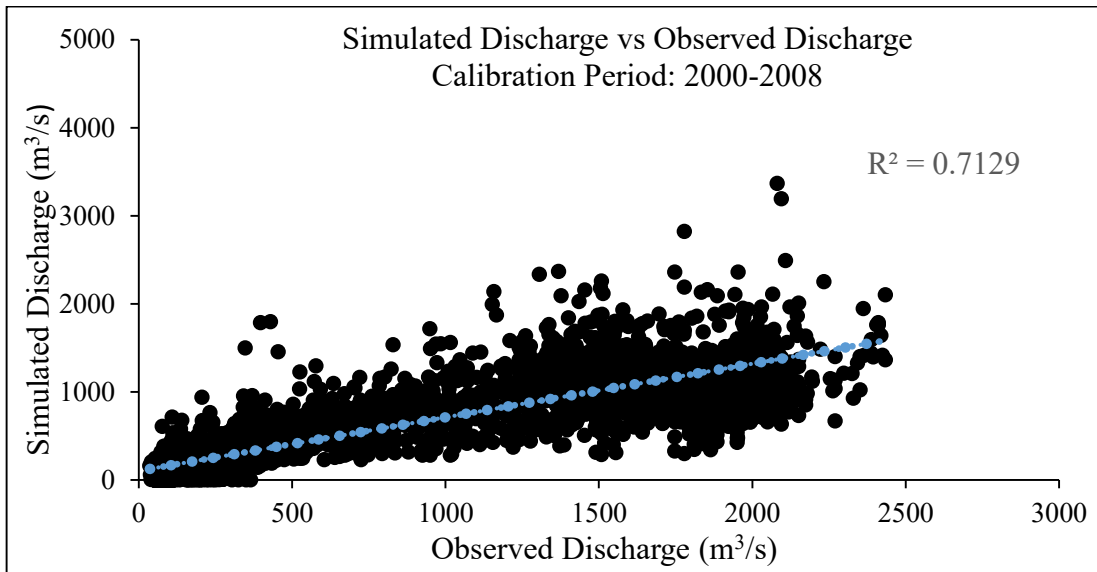


Figure 4.8 Scatter plot of simulated vs observed discharge at Sheola for the calibration and validation period of the model

According to the model evaluation guidelines, SWAT2012 simulated the streamflow trends quite well, as shown by the statistical results, which are also in agreement with the graphical results. The RSR values ranged from 0.36 to 0.39 during both calibration and validation. These values indicate that the model performance for streamflow residual variation is satisfactory. The PBIAS values varied from 19.19% to 23.55% indicating that the average magnitude of simulated daily streamflow values is within satisfactory range ($PBIAS < \pm 25$) for the subbasin during calibration (Table 4.7).

To understand the correlation between the simulated and observed discharge scatter plot (Figure 4.8) of these two values has been used. For both calibration and validation, the value of R^2 is quite good. Simulated flow values depicted a good correlation (0.68-0.71) with the observed flow values in calibration and validation for subbasin 86. Thus SWAT2012 simulation of streamflow was satisfactory in terms of trends (NSE), residual variation (RSR), average magnitude (PBIAS), and R^2 .

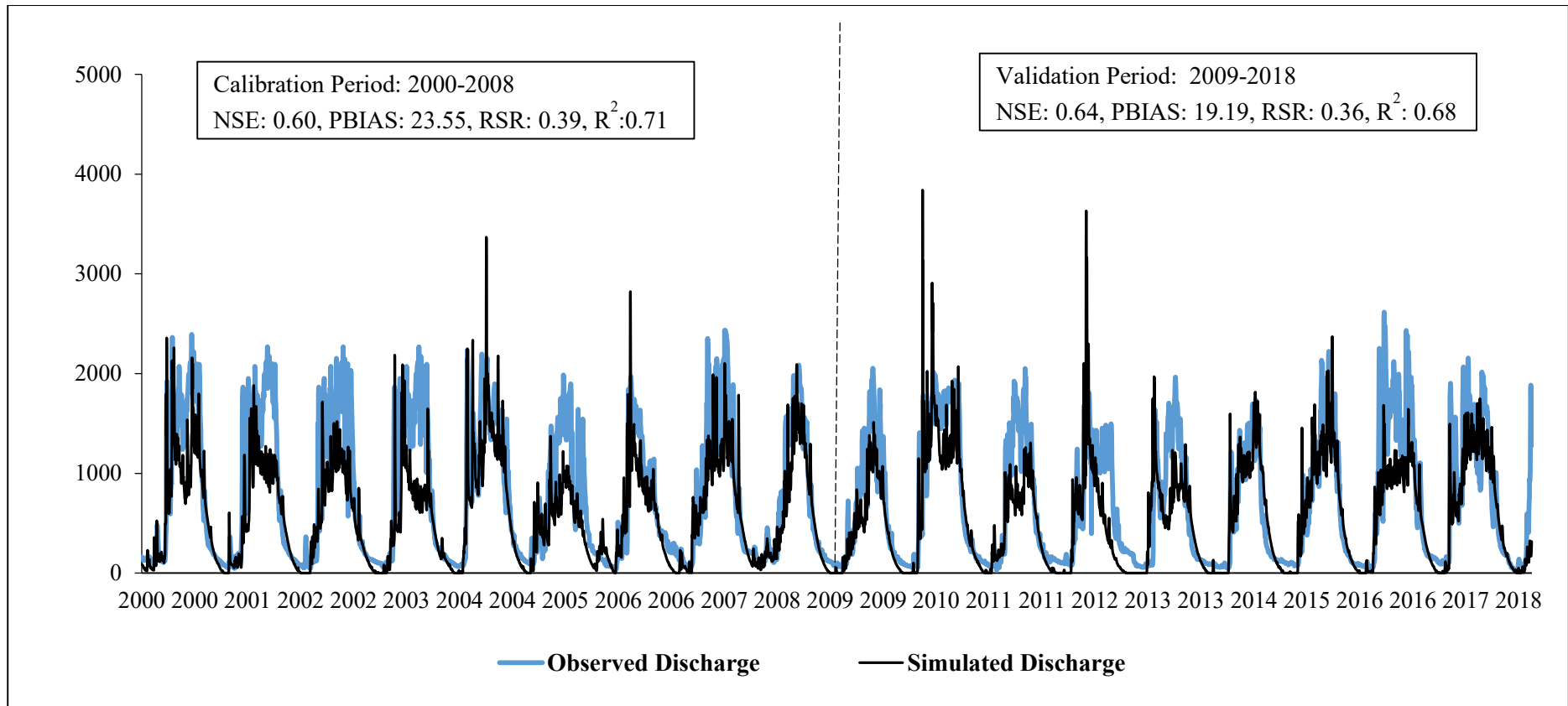


Figure 4.9 Daily observed discharge (at Sheola) and simulated discharge (at Sheola) hydrograph for calibration and validation of the model

4.7 Selection of Climate Change Scenario

Four representative concentration pathways (RCPs) are normally used as a basis for future climate modeling according to the IPCC 5th assessment report. One is a very high baseline emission scenario (RCP8.5), two medium stabilization scenarios (RCP4.5 and RCP6) and one is a mitigated scenario (RCP 2.6). The present study intended to include emission scenarios, covering an extreme and moderate range of radiative forcing and future temperature. Therefore, out of the four options, RCP 2.6 was not considered in the current selection as it seemed to be the least likely. From the remaining three RCPs, the extreme baseline emission scenario (RCP 8.5) and one moderate scenario (RCP4.5) were selected for the current study. RCP 8.5 scenario was included because it covers the higher end of radiative forcing. For the moderate stabilization scenarios (RCP 4.5 and RCP 6), due to time constraints and because RCP 4.5 shows a better match (1.5%) of the trends of the average annual CO₂ emission growth rates than RCP 6 (1.0%), RCP 4.5 has been selected. Also, the available model runs for the ensemble member *r1plil* are included and evaluated for RCP 4.5 and RCP 8.5.

4.7.1 Shortlisting of GCMs/RCMs

The full spectrum of Global Climate Models (GCMs) projections is wide, with large uncertainties and the available future projections differ vastly from each other and may range from very wet to drier or very warm to colder future climates. RCMs are being used not only to dynamically downscale GCM climate change simulations, but also seasonal climate predictions with similar goals of obtaining useful regional climate information. The present study includes the four CORDEX-SA experiments for future climate scenario analysis. CORDEX is a WCRP-sponsored program to organize an international coordinated framework to produce an improved generation of regional climate change projections worldwide for input into impact and adaptation studies within the AR5 timeline. GCMs have been dynamically downscaled by CORDEX, using different RCMs. Their RCM outputs are at a considerably finer scale (0.44°).

Initially, four RCM models derived outputs have been selected and analyzed using three climatic variables daily maximum near-surface air temperature, daily minimum near-surface air temperature, and precipitation to identify the future wet, dry, cold, and warm scenarios. The choice of these RCM models has been based on the previous climate change studies using the RCM model ([18], [32], [63]). These GCMs are downscaled by CORDEX using two different RCMs: RCA4 and RegCM4 and derived precipitation data have been bias-corrected by the researcher of the present study using observed rainfall. The four CORDEX-SA experiments that have been used for future temperature and precipitation changes in this study are listed in the following table 4.8. The current study adopted a way suggested in [30] to shortlist the climate models mentioned above based on the projected changes in the mean value of the climatic variables (temperature and precipitation). At first, the four model runs (ensemble member *r1p1i1*) for RCP 4.5 and RCP 8.5, have been evaluated in terms of the mean annual precipitation sum (ΔP) and the mean air temperature (ΔT), averaged across the Meghna river basin between the simulated reference period historical data (1970–1999) and the end of 21st-century in the 2080s (2070–2099).

Table 4.8 List of experiments by CORDEX-SA initially considered for climate change analysis

Domain	Driving Models	RCP Scenario
WAS-44i	MPI-M-MPI-ESM-LR	4.5 and 8.5
WAS-44i	NorESM1-M	4.5 and 8.5
WAS-44i	ACCESS1-0_CSIRO_CCAM_1391M	4.5 and 8.5
WAS-44i	CCCma-CanESM2	4.5 and 8.5

For this purpose, 10th, 50th, and 90th percentile values of average precipitation and average temperature for the entire ensemble considered for each RCP, to explore the extent of the full spectrum of the projected changes in temperature and precipitation under that RCP. This was followed by determining the closest projections to each of the corners. The four corners are defined as per the procedure stated in the study in [30].

(a). The Dry-Cold corner (lower left) is represented by the 10th percentile of ΔP and ΔT ;

- (b). The Dry-Warm corner (upper left) is represented by the 10th percentile ΔP but the 90th percentile value of ΔT ;
- (c). The Wet-Cold corner (lower right) is represented by the 90th percentile ΔP and the 10th percentile value of ΔT ;
- (d). The Wet-Warm corner (upper right), represented by the 90th percentile values for both ΔP as well as ΔT ; and
- (e). The median projected future climate, represented by the 50th percentile values of both ΔP and ΔT .

It has been seen that the projection range of ΔP and ΔT is much larger for RCP 8.5 than RCP 4.5. In the case of the extreme scenario (RCP 8.5) precipitation ranges from -10.76% to 26.16% with a temperature increase of 4.00 °C to 4.54 °C (Figure 4.8). Whereas, for RCP 4.5 ΔP varies in between -14.59% to 15.56%, and ΔT ranges between 2.20 °C to 2.59 °C (Figure 4.10 and Figure 4.11).

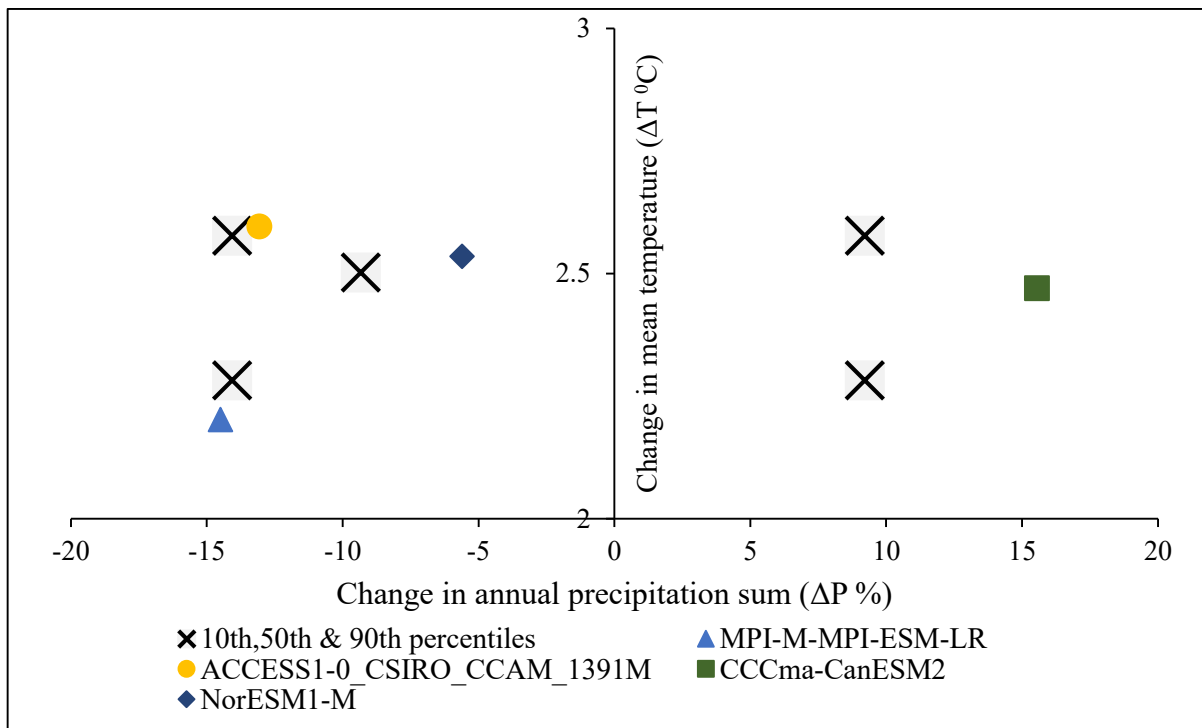


Figure 4.10 Projected changes in mean air temperature (ΔT) and annual precipitation sum (ΔP) between the historic period and 2080s for four RCP 4.5 RCMs

The inspection of the closest model runs to any corner point from the change mean temperature (ΔT) vs change in mean precipitation (ΔP) plot reveals that three RCMs fall closer to the three different corners with one RCM ranges close to the median for RCP 4.5. For the latter case, two RCMs were found to be closest to the two different corners and the other two remain closer to the median. It should be noted that the 10th and 90th percentiles were selected as the central points of the corners, rather than the maximum or minimum values, to avoid selection of any outlier projections. Finally, the models are classified basing on their difference with the 10th, 50th, and 90th percentile values of ΔT and ΔP (Table 4.9). The model runs that best represent the corners of the full spectrum are MPI-M-MPI-ESM-LR (Dry-Cold corner) and CCCma-CanESM2 (Wet-Warm corner) which will be further used for climate change impact analysis in this study. The selected two (CORDEX-SA) RCM outputs have been bias-corrected using the linear scaling method for RCP 4.5 and RCP 8.5 for three sets of durations, i.e., the 2020s (2010–2039), 2050s (2040-2069), and 2080s (2070–2099).

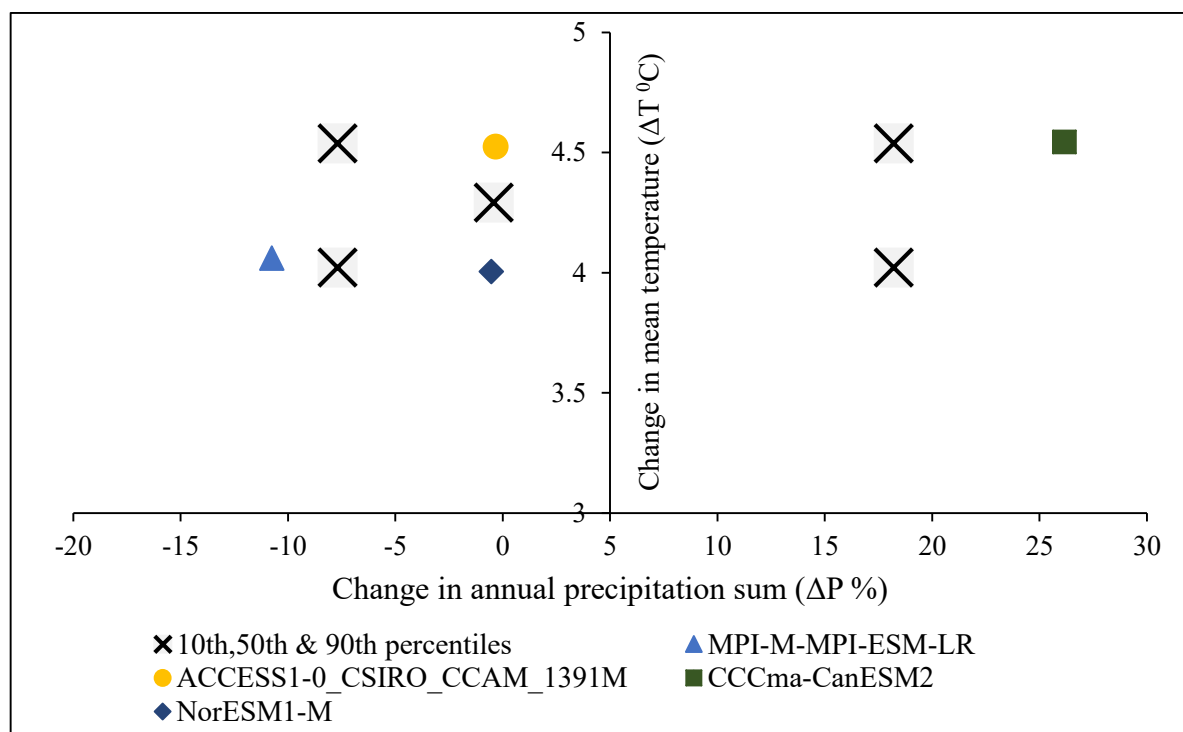


Figure 4.11 Projected changes in mean air temperature (ΔT) and annual precipitation sum (ΔP) between the historic period and 2080s for four RCP 8.5 RCMs

Table 4.9 List of RCM models classified based on projection scenario

Scenario	Experiment	RCP	RCM
Wet-Warm	CCCma-CanESM2	4.5 and 8.5	RegCM4
Wet-Cold	-	-	-
Mean	NorESM1-M	4.5	RCA4
	ACCESS1-0_CSIRO_CCAM_1391M	8.5	
Dry-Warm	ACCESS1-0_CSIRO_CCAM_1391M	4.5	RCA4
Dry-Cold	MPI-M-MPI-ESM-LR	4.5 and 8.5	RCA4

4.8 Selection of Upstream Intervention Scenario

The rate of reservoir construction has been competitively increased after 1950. Every year about 600 reservoir or dams is being constructed all over the world now. The environmental impacts of such projects are recognized in comparatively recent reports and documents. The report of the World Commission on Dams of 2000 noted that large dams and diversion projects can be led to the loss of forests and wildlife habitat, aquatic biodiversity and can affect downstream floodplains, wetlands, estuarine and adjacent marine ecosystem. Any dam or reservoir in the upstream of the Meghna river basin can significantly alter the hydrology of the Surma and Khushiyara River. Therefore, in this study, a reservoir or dam has been considered on the Barak River upstream of Amalshid in Manipur state India. Secondary data collected from “Hydrological Impact Study of Tipaimukh Dam of India on Bangladesh” by [58] and other resources considered to remain the same for the present study with necessary modification.

4.8.1 Secondary data and information collected from the previous study

The Detailed Project Report on Tipaimukh Hydro Electric (Multipurpose) Project, published by North Eastern Electric Power Corporation Ltd. (NEEPCO) 2000 has been collected from a previous study for the present study [59]. Lots of information is presented in that report related to a dam project.

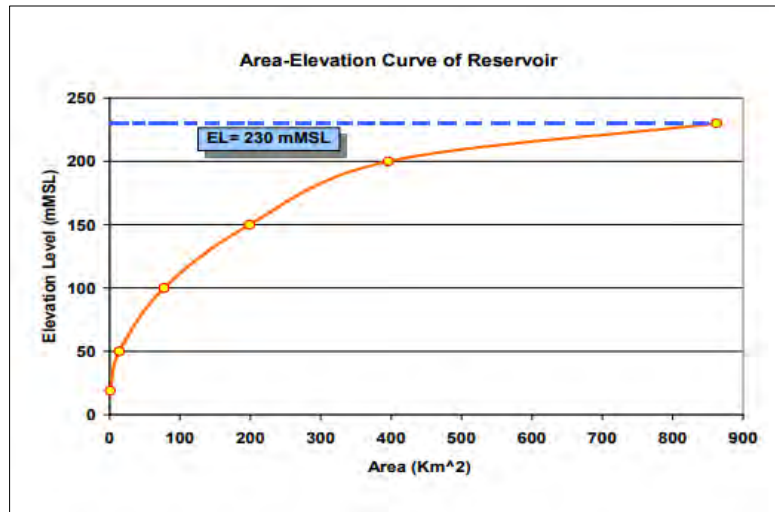


Figure 4.12 Area-Elevation curve collected for Dam Reservoir [59]

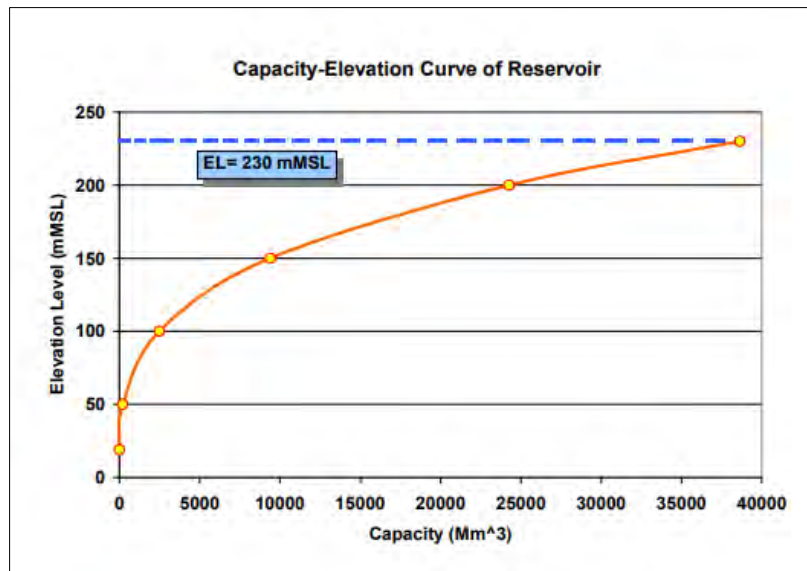


Figure 4.13 Capacity-Elevation curve collected for Dam Reservoir [59]

The data and information, which are found useful for the present study from that report, have been presented below:

Dam Height: 162.8 m high rock-filled earthen dam

Design head: 125 m.

Full Reservoir Level (FRL): 174 m MSL

Minimum Draw Down Level (MDDL): 136.1 m MSL

Full Supply Level (FSL): 172.5 m MSL

Flood moderation: Reservoir storage from FSL 172.5 m to FRL 174.0 m

Head loss due to friction: 3% of the design head

Collected reservoir data area-elevation curve and capacity-elevation curve of the reservoir is graphically presented in Figure 4.12 and 4.13.

As daily discharge data is not available for Amalshid point collected by BWDB secondary discharge data collected from a previous study was used as a reference flow data. Also, the suggested reservoir rule curve was collected (Figure 4.15).

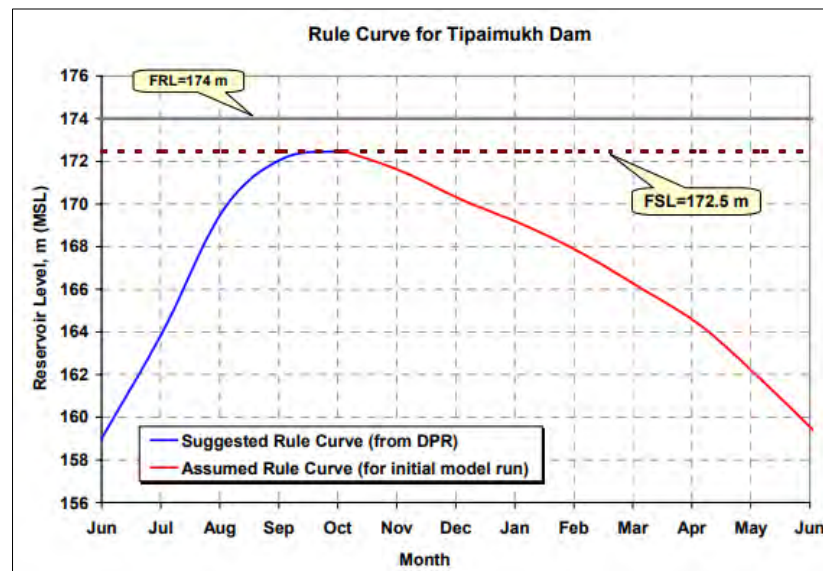


Figure 4.14 DPR suggested or desired rule curve (for June to October) and assumed rule curve for the rest of the period [59]

In [58] researchers described that the initial proposal of developing the Cachar Irrigation Project was by constructing a barrage at Fulertal in the Cachar plain of India, some 95 km. downstream of the Tipaimukh Dam and 100 km. upstream from Amalshid point of Bangladesh. The extra water for this irrigation project was supposed to be met from the possible augmented flow of the Barak River during the dry period for the post-dam condition. Thus the possible monthly withdrawal from the Barak River should be considered. Figure

4.16 depicts the amount of monthly water withdrawal from the Barak River for the irrigation project as provided in the DPR on Tipaimukh Project.

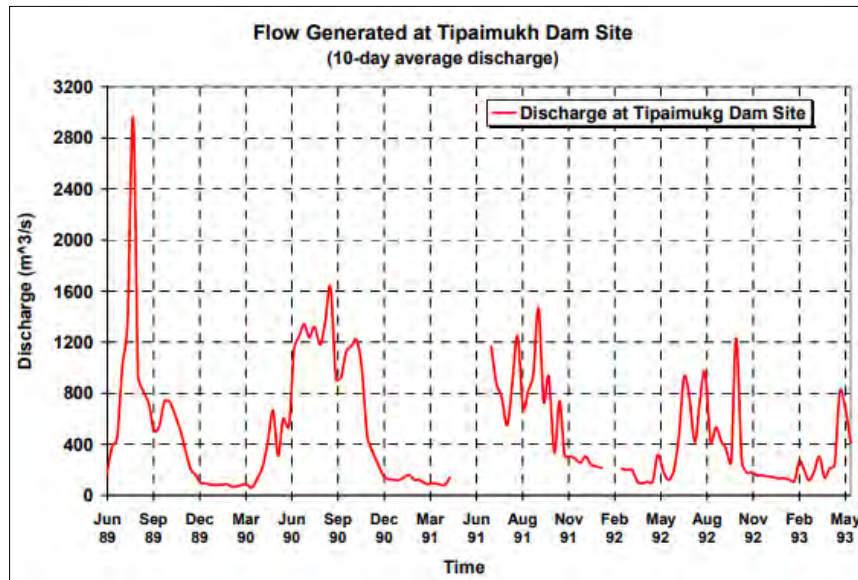


Figure 4.15 Day average discharge at dam site on the Barak River [59]

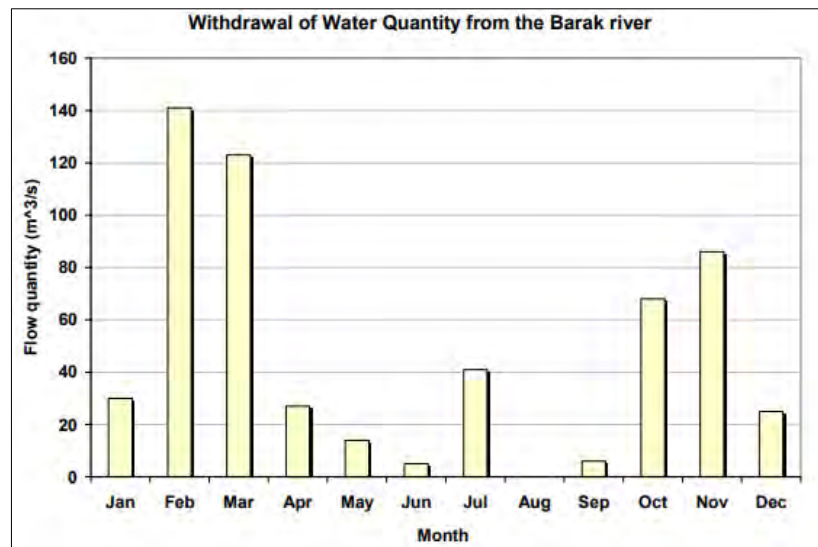


Figure 4.16 Possible withdrawal of water from the Barak River for an irrigation project [59]

The present study will use these secondary data to create a hypothetical scenario of reservoir (storage) operation at the upstream of Bangladesh on the Barak river at Manipur. As the

observed discharge is not available at Amalshid and reservoir location, flow calibration at these points is not possible. The study will set the target storage volume of the reservoir as per the DPR rule curve and use SWAT to simulate the monthly release.

5 ANALYSIS AND RESULTS

The developed model of the Meghna river basin was calibrated by changing parameters for runoff, groundwater, evapotranspiration, soil, and shows good results in terms of simulated discharge. Calibrated and validated models were then further used for its output analysis (discharge and water balance components) and climate change and upstream intervention scenario analysis. In this chapter model outputs will be discussed, secondary data will be processed (if necessary) and different scenarios will be analyzed.

5.1 Model Outputs

5.1.1 Daily and monthly discharge

The model of the Meghna river basin was simulated for January 2000 –2018 with a warm period of two years. Though the calibrated and validated model have a few larger peak flow values than the observed one, the overall average flow values are a little bit lower than the observed flow values. The average daily discharge for calibration and validation were found to be 567.68 m³/s and 599.29 m³/s concerning the observed mean daily discharge of 707.89 m³/s and 815.93 m³/s for the same period respectively (Table 5.1). The average mean monthly discharge was also plotted (Figure 5.1) to understand the monthly variation of the model results.

Table 5.1 Monthly observed and simulated discharge at the catchment outlet station near Sheola (SW 173)

Mean Monthly Discharge (m ³ /s)			Total Discharge in Different Season (m ³ /s)			
	Calibration Period	Validation Period	Dry	Pre- monsoon	Monsoon	Post- monsoon
Observed	707.89	815.93	216.57	559.35	1311.07	2212.33
Simulated	567.68	599.29	109.27	475.38	1128.69	1800.10

Flow values were also summarized for different seasons. It shows that simulated mean monthly discharge gradually increases from April and reaches in peak in August (1110.23 m³/s) as similar to the observed one (1577.27 m³/s). Both the simulated and observed

data show a large volume of flow during post-monsoon (1800.10 m³/s and 2212.33 m³/s respectively) with the least volume of flow during the dry season (Table 5.1).

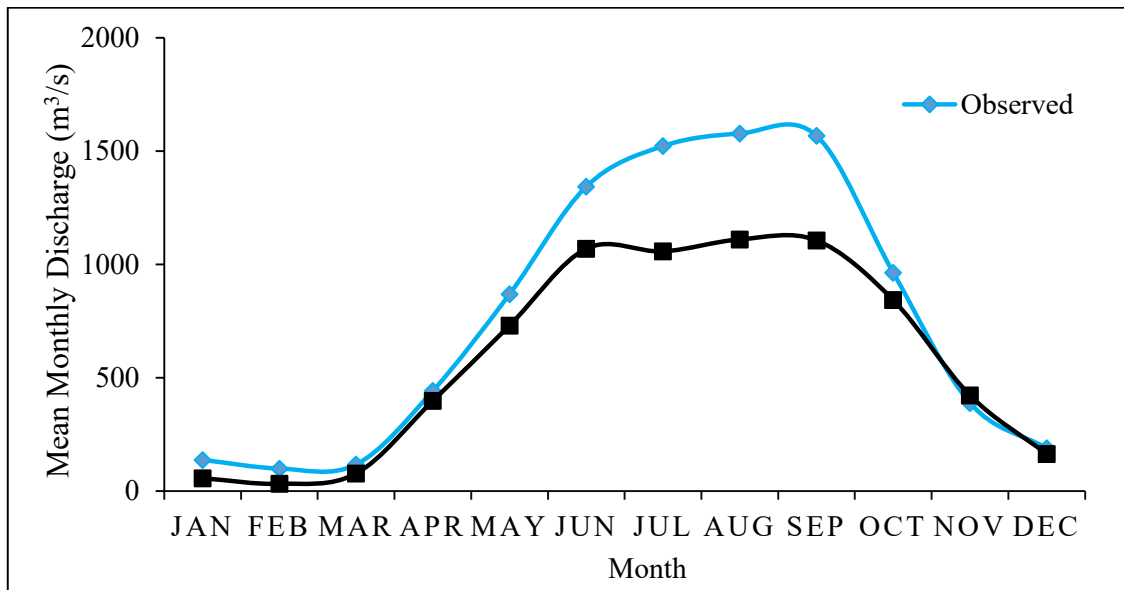


Figure 5.1 Observed and simulated mean monthly discharge at the catchment outlet station near Sheola (SW 173) for 2000-2018

5.1.2 Water balance components

Quantification of the water balance components in a large basin area is of great importance in assessing the changes in hydrological components. These water balance components contribute to the discharge of the river and the overall hydrological cycle of the basin. All the hydrological parameters such as runoff and evapotranspiration were computed in the SWAT model. The study does not have the observed data of the different water balance components for the basin so the outputs from the calibrated and validated model cannot be compared with the observed values. The spatial variation of water balance components is shown in Figure 5.3 to understand the changing pattern of these parameters over the simulation period. The overall average annual precipitation ranges between 3000 mm to more than 3500 mm with maximum rainfall values in the year 2004, 2007, 2010, and 2017.

Water yield which refers to the net amount of water contributed by the sub-basins and HRUs to the stream flow seems to have a similar pattern as the precipitation on annual basis with a maximum average value of 3302 mm. Annual average evapotranspiration ranges from 103 mm to 502 mm. The average yearly runoff depth before transmission,

pothole, wetland, and pond losses is a maximum of 207 mm. Higher temperatures and precipitation tend to increase the evapotranspiration and total rainfall amount of the basin. Thus potential evapotranspiration remains higher over the model simulation period (above 1000 mm) annually. Groundwater contribution to the stream has a maximum value of 3123 mm. Percolation loss ranges between 103 mm to 3151 mm yearly. Lateral flow contribution to the stream has a maximum value of 2126 mm.

Mean monthly values (in mm) of these components are represented using a bar diagram to show the monthly variation of each component over the model simulation period (Figure 5.2).

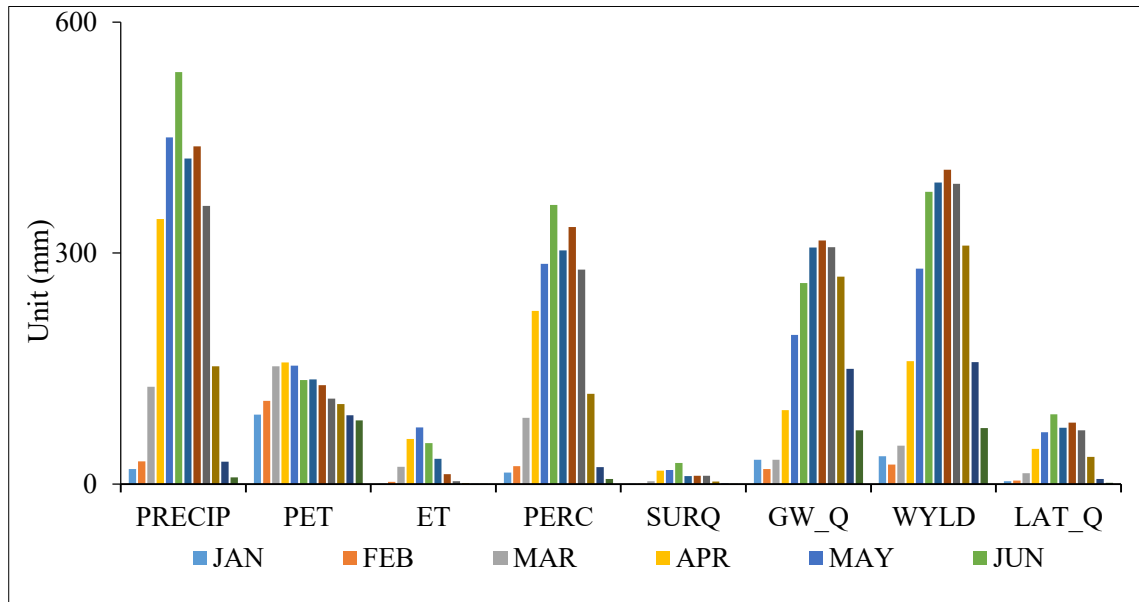


Figure 5.2 Mean monthly water balance components of the basin (2000- 2018)

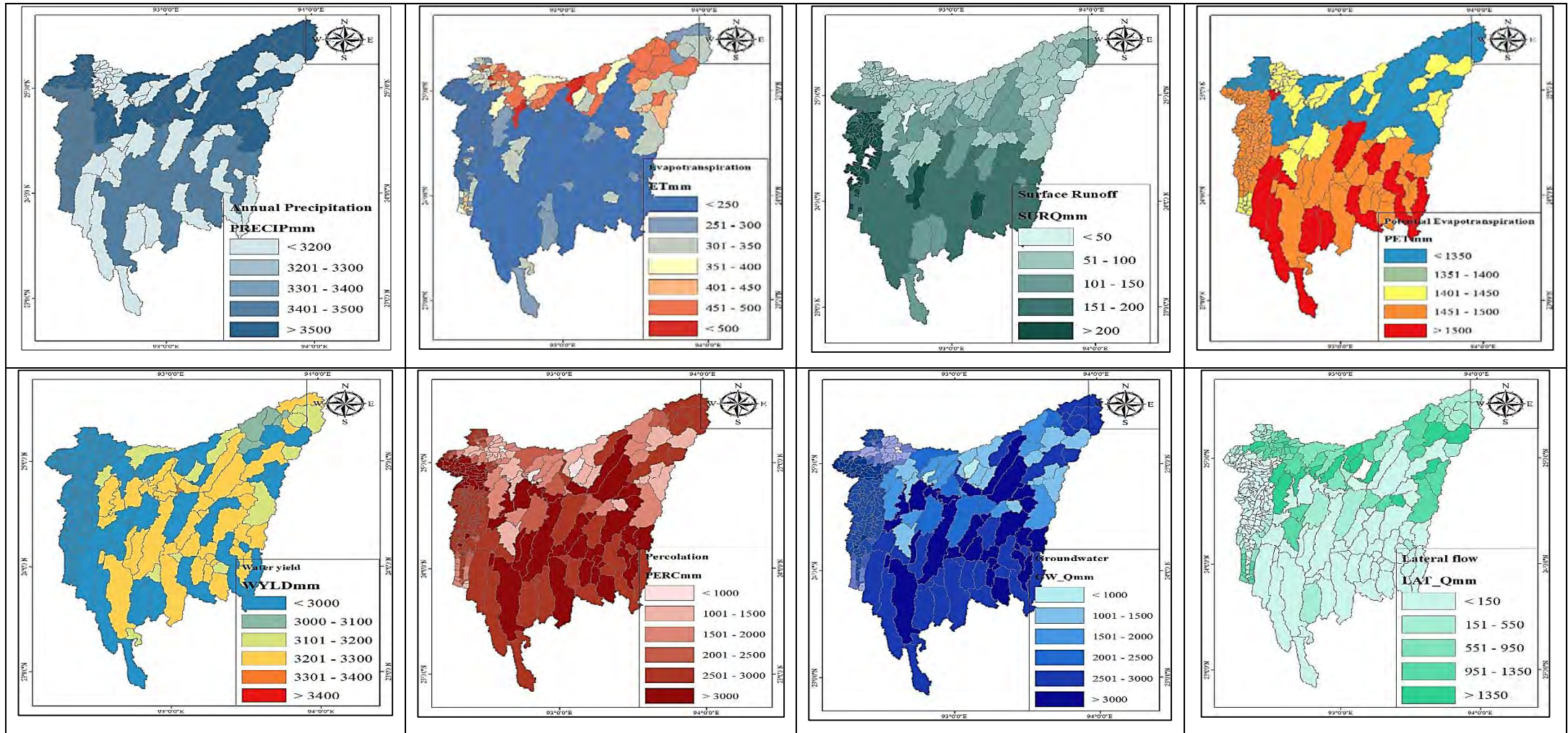


Figure 5.3 Spatial distribution of average annual rainfall, evapotranspiration, surface runoff, potential evapotranspiration, water yield, percolation, groundwater in the basin area

5.2 Climate Change Analysis

Two CORDEX-SA RCM outputs were selected for climate change analysis for three different periods 2020s, 2050s, and 2080s to the reference period of 1970-1999. Each of these climate periods is of 30-year duration: 2020s (2010-2039), 2050s (2040-2069), and 2080s (2070-2099). Climatic variables projected by MPI-M-MPI-ESM-LR (Dry-Cold scenario) and CCCma-CanESM2 (Wet-Warm scenario) were analyzed and used as model input to predict future changes in the basin.

5.2.1 Projected precipitation

Precipitation data from CORDEX were used to analyze the projected precipitation for the wet-warm and dry-cold scenario. These data were bias-corrected using observed rainfall data. The dry-cold projection by the MPI-M-MPI-ESM-LR model shows a decreased precipitation trend for both RCP 4.5 and RCP 8.5 scenarios for all periods on annual basis. RCP 8.5 shows less change in annual precipitation. The least decrease in precipitation projected was about 6.97% (during the 2020s) and 10.72% (during 2050s) in RCP 4.5 and RCP 8.5 scenarios respectively (Figure 5.4). In contrast, under wet-warm projection, an increase in annual precipitation was observed.

Table 5.2 Percent changes in annual precipitation sum

		2020s	2050s	2080s
RCP 4.5	MPI-M-MPI-ESM-LR	-12.27	-10.72	-14.49
	CCCma-CanESM2	21.69	-3.06	15.56
RCP 8.5	MPI-M-MPI-ESM-LR	-6.97	-16.88	-10.76
	CCCma-CanESM2	2.39	13.77	26.16

There is a maximum increase of up to 26.16% during the 2080s compared to the baseline average annual precipitation. The wet-warm projection shows a decrease in midcentury (the 2050s) of about -3.06% under RCP 4.5 (Table 5.2). The overall trend of the projected precipitation under RCP 4.5 shows that the percent changes in rainfall decrease over the three climate period. Further projection of RCP 8.5 shows that annual average

precipitation tends to increase by 2.39 %, 13.77 %, and 26.16 % in the 2020s, 2050s, and 2080s respectively.

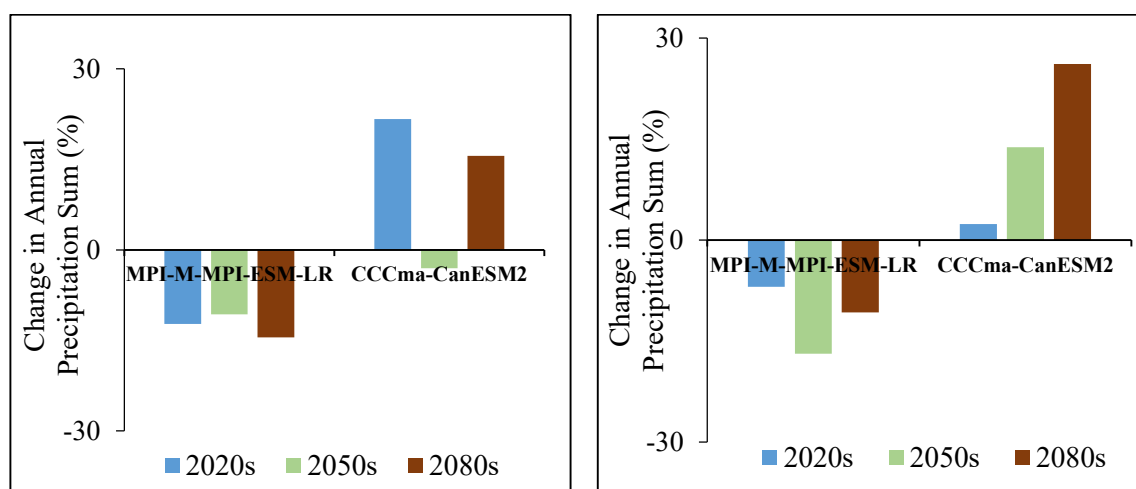


Figure 5.4 Changes in annual precipitation under RCP 4.5 and RCP 8.5

5.2.2 Projected temperature

Another crucial parameter for climate change analysis is temperature. The projected average annual temperature seems to increase over the three climatic periods (Figure 5.5). The increase in temperature appears progressive for all model outputs on a temporal basis, unlike precipitation that showed no particular trend of increase or decrease across time. The maximum temperature change (4.54⁰C) is observed in the 2080s under RCP 8.5 whereas the least (0.74⁰C) is during the 2020s under RCP 4.5.

Table 5.3 Percent changes in average annual temperature

		2020s	2050s	2080s
RCP 4.5	MPI-M-MPI-ESM-LR	0.74	1.41	2.20
	CCCma-CanESM2	1.36	2.0	2.24
RCP 8.5	MPI-M-MPI-ESM-LR	1.33	2.44	4.29
	CCCma-CanESM2	1.58	2.95	4.54

By the end of the century, all model outputs projected temperature increase is at least 2⁰ C under RCP 8.5. It was also observed that there is no sign of a decrease in annual

temperature (Table 5.3). Higher temperatures will increase evapotranspiration and melting of snow and ice within the region.

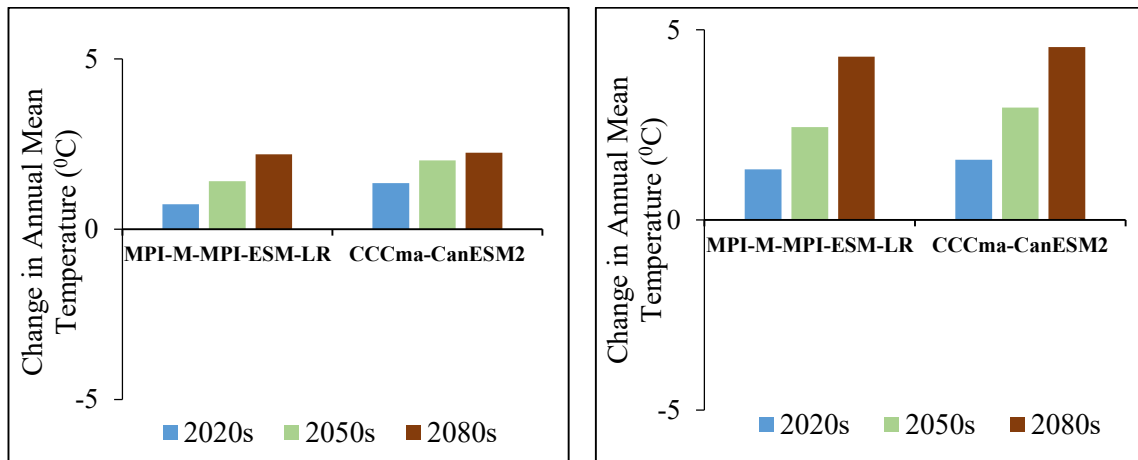


Figure 5.5 Changes in average annual temperature under RCP 4.5 and RCP 8.5

5.2.3 Impact on discharge

Discharge can be affected by various water balance components. The discharge at the outlet station of the Kushiyara River is expected to change significantly under both scenarios. The changes in discharge are analyzed separately for the wet-warm scenario and dry-cold scenario in this section. Under wet-warm projection, precipitation and temperature seem to increase according to the projection of the wet-warm scenario which will eventually increase the discharge over the three climatic periods in 2080s. The general trend may not be the same for RCP 4.5 and RCP 8.5 but the monthly peak flow volume will increase compared to the reference period (1259.45 m³/s). On the other hand, according to dry-cold scenario, precipitation and temperature seem to increase according to the projection of the wet-warm scenario which will eventually increase the discharge over the three climatic periods. The general trend may not be the same for RCP 4.5 and RCP 8.5 but the monthly peak flow volume will increase compared to the reference period (1259.45 m³/s).

Changes in mean monthly discharge

RCP 4.5

Wet-Warm scenario

Overall mean monthly flow volume is higher than the reference period for each climatic period (Figure 5.6). The highest mean monthly flow value is observed in the 2020s (2065.57 m³/s). As projected precipitation decreases after the 2020s with increasing temperature, peak discharge also gradually decreases in 2050s (1548.09 m³/s) and 2080s (1477.96 m³/s) than 2020s. During the 2020s and 2050s peak value occurs in July whereas in the 2080s the flow volume reaches its peak in August. Mean monthly flow values less than the reference period are mostly observed in April, May, and November during the 2020s and 2050s. In the 2080s, the average discharge is lower than the historic period in November.

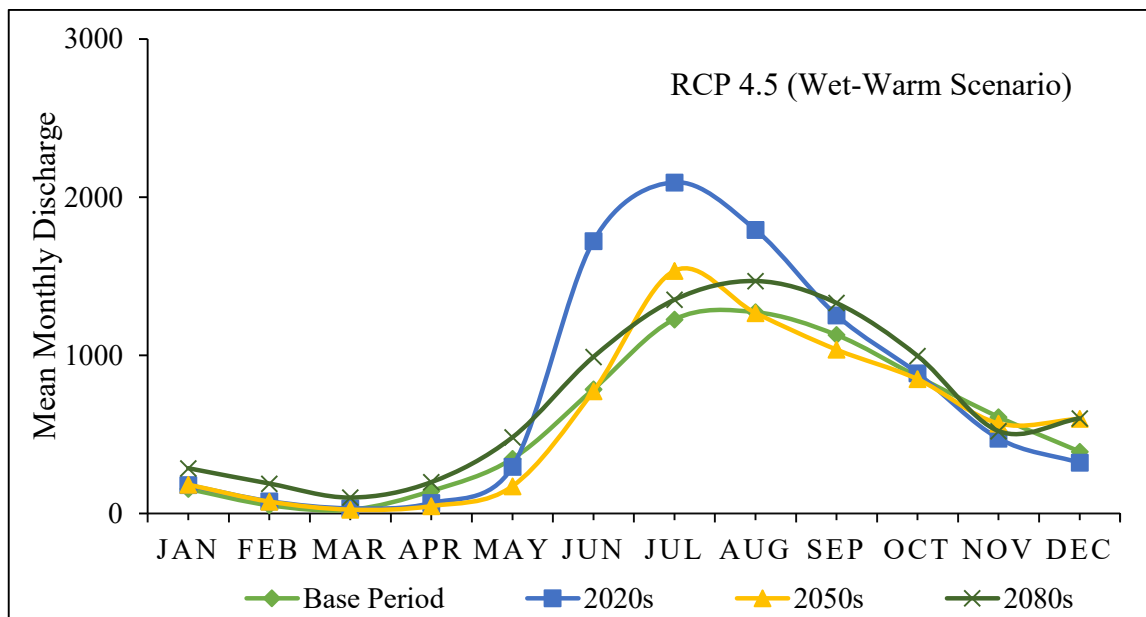


Figure 5.6 Mean monthly discharge under RCP 4.5 (wet-warm scenario)

The percent change in monthly discharge for each climatic period is presented using box plots in Figure 5.7- Figure 5.9 which depicts the uncertainty range in the changes in flow volume for every month and each year over a climatic period.

In the 2020s, uncertainty is observed in the percent increase of the monthly discharge with a predicted maximum increase in June (about 120%). In the 2050s, though the flow value may increase in the rainy season a sudden rise may be observed in December. The predicted flow volume seems to increase more than 50% (on average) of the reference value in this month. Overall maximum uncertainty is observed in June in the 2080s with the increase of flow about 200%. It has been also observed that discharge may vary from -200% to 200% with respect to the baseline period for each of the three climatic periods under wet-warm scenario.

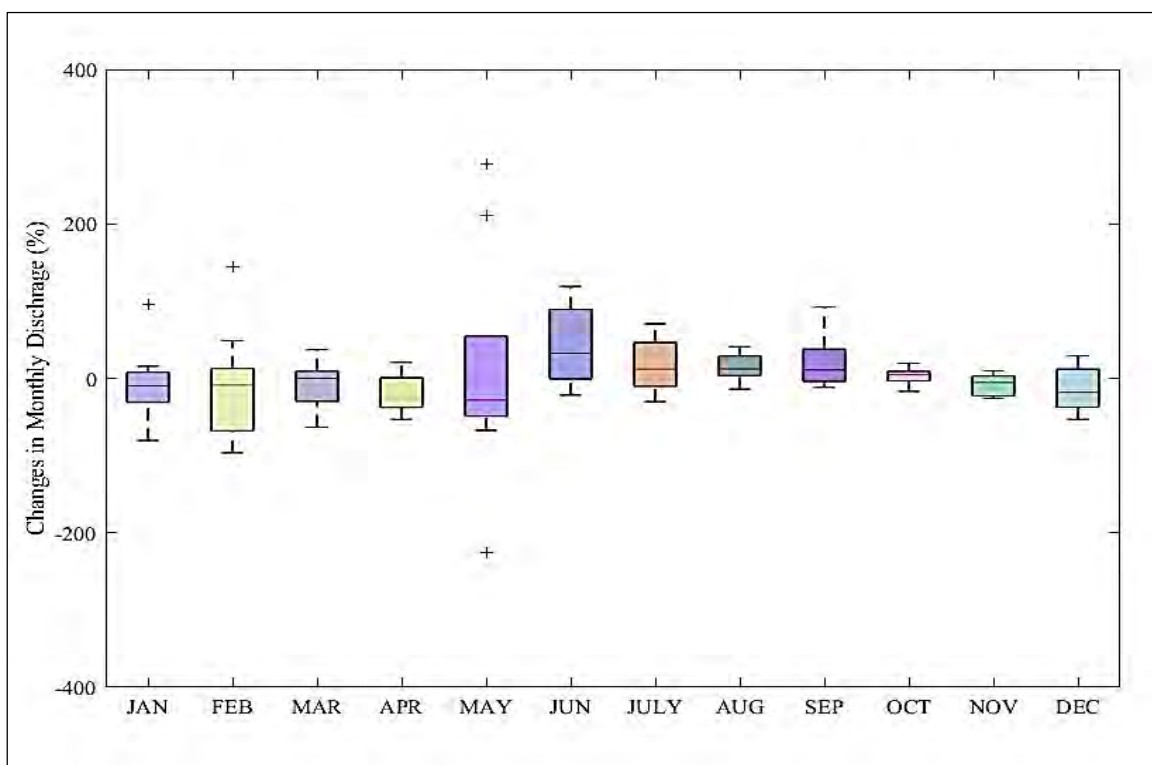


Figure 5.7 Changes in monthly discharge in the 2020 under RCP 4.5 (wet-warm scenario)

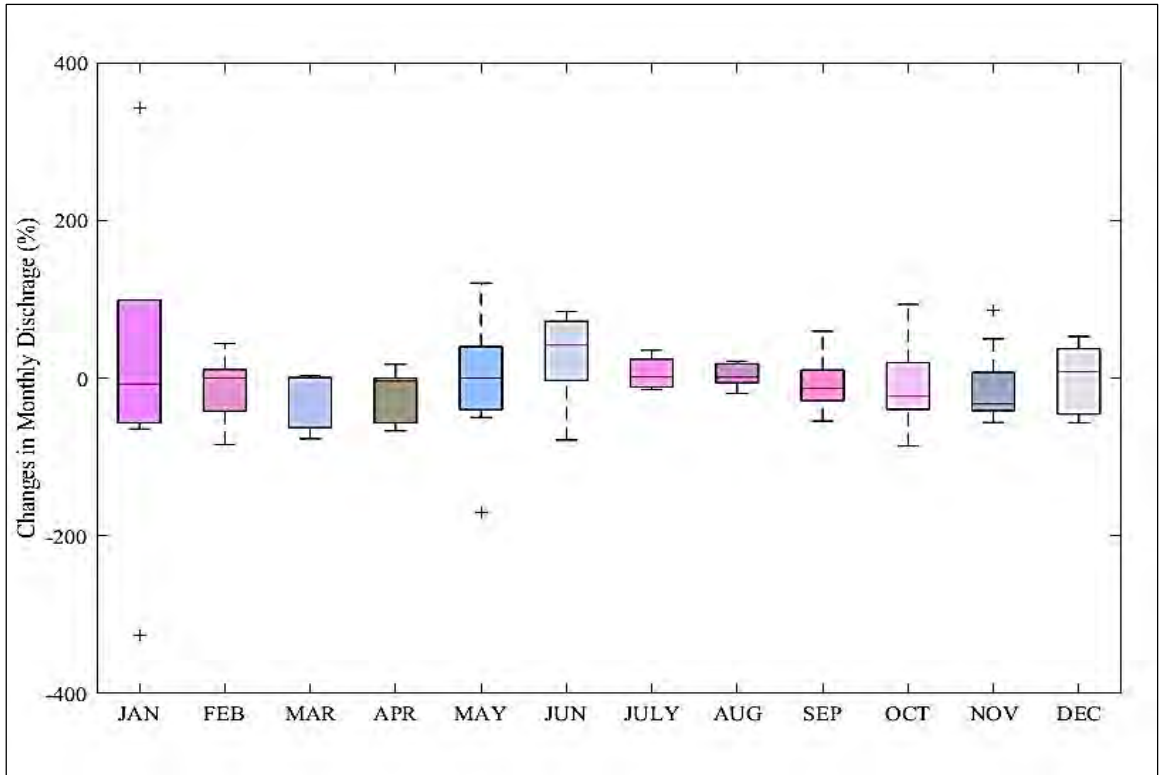


Figure 5.8 Changes in monthly discharge in the 2050s under RCP 4.5 (wet-warm scenario)

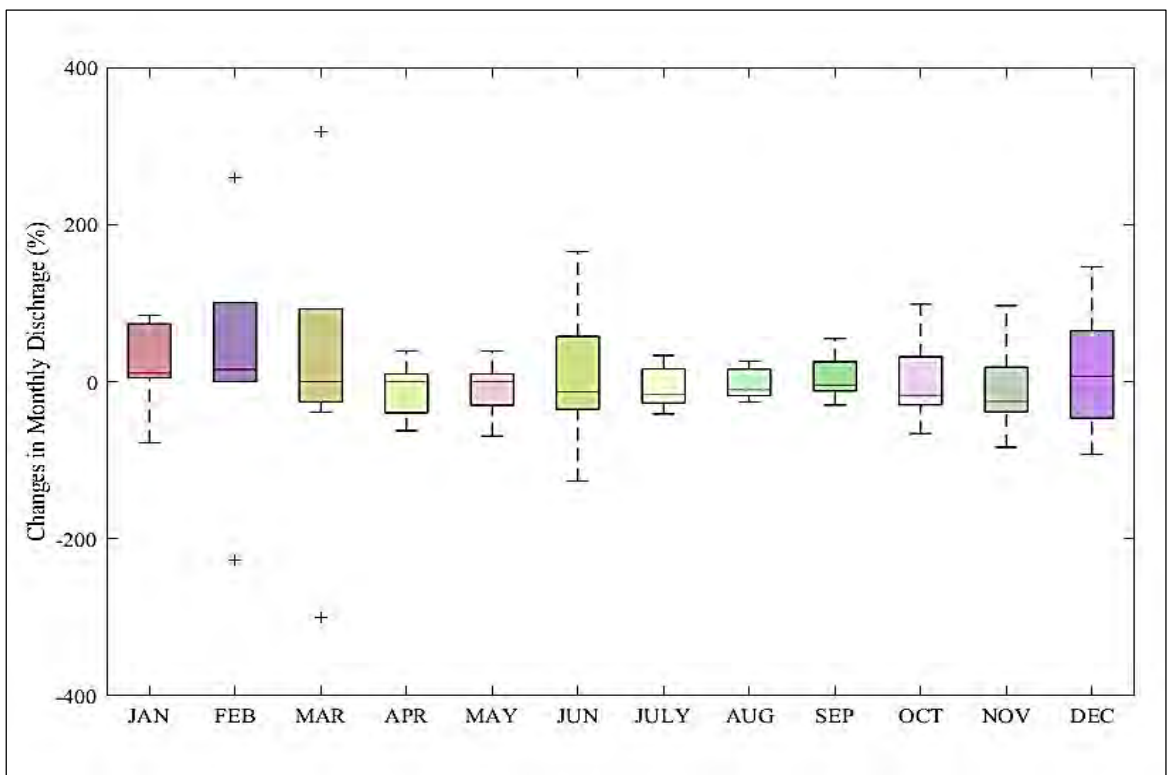


Figure 5.9 Changes in monthly discharge in the 2080s under RCP 4.5 (wet-warm scenario)

Dry-Cold scenario

With the increase in temperature projected precipitation of dry-cold scenario decreases significantly under RCP 4.5. As a result flow volume is quite closer to the historic period with a slight increase in peak value over the climatic period (Figure 5.10). Observed maximum discharge occurs in July for the 2020s and 2050s and in August for the 2080s. During the 2020s, a 5.5% increase in the average mean monthly discharge leads to the peak flow of 1377.73 m³/s to the reference period (1305.34 m³/s). After that in midcentury peak flow reduces by almost 9% and peak discharge reaches a value of 1193.51 m³/s. At the end of the century, the maximum flow value increases to 1318.345 m³/s. Other than the wettest months, flow values reduce significantly in each climatic period.

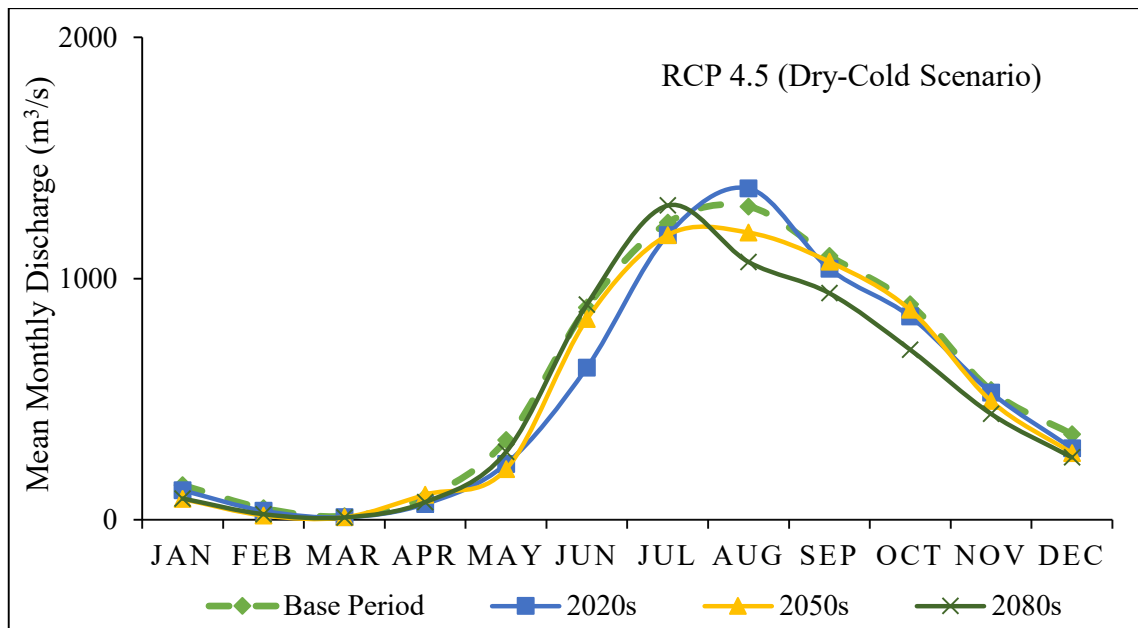


Figure 5.10 Mean monthly discharge under RCP 4.5 (dry-cold scenario)

A significant reduction in discharge is observed in March and April in the 2020s which is about 33%. In the 2080s, flow decreases by more than 50% in February. At the end of the century, the maximum flow value increases to 1318.345 m³/s. Other than the wettest months, flow values reduce significantly in each climatic period. Mean monthly changes in discharge are shown using box plots in Figure 5.11-Figure 5.13.

A significant reduction in discharge is observed in March and April in the 2020s which is about 33%. In the 2080s, flow decreases by more than 50% in February. On the other hand, 70% of the mean monthly discharge is reduced in March during the 2050s. Least flow reduction of about 3% is observed during the 2020s and 2050s. The maximum uncertainty range is observed during June, July, and August over each climatic period.

Although the changes in average discharge value for three climatic periods seem quite less the uncertainty range is quite higher when changes are calculated for each of every year of a climatic period. The basin area may experience a change that ranges between -100% to slightly more than 100% in monthly discharge each year over a particular climatic period. Changes in monthly discharge are shown using box plots in Figure 5.10-Figure 5.13.

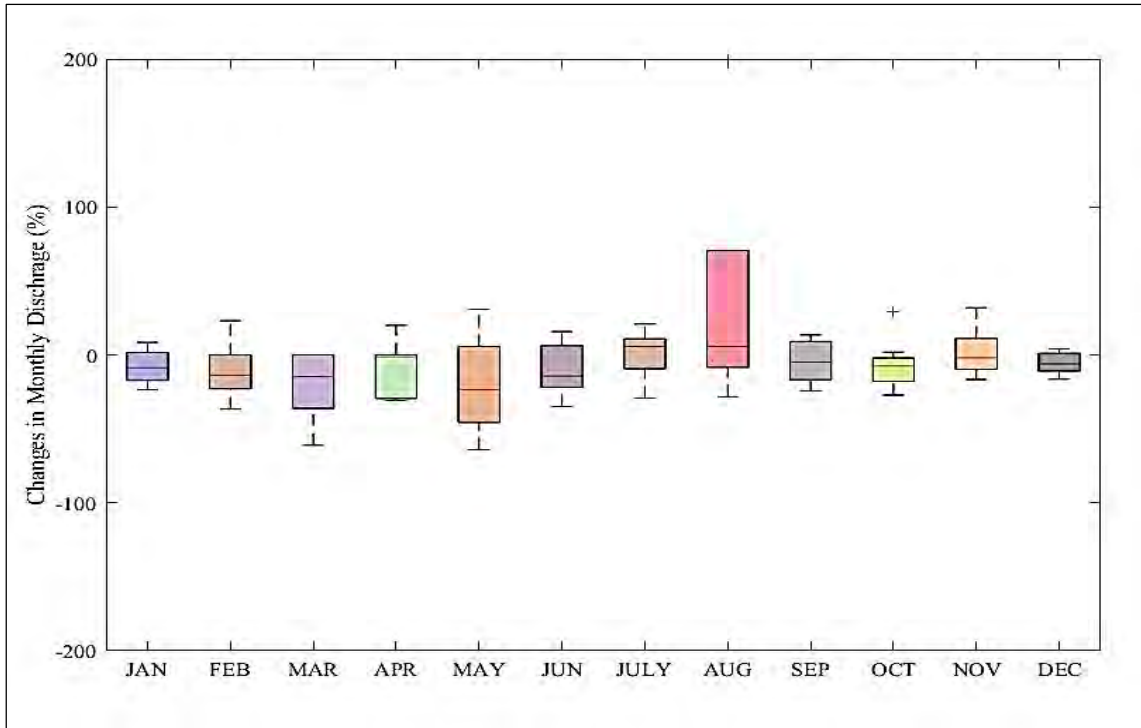


Figure 5.11 Changes in monthly discharge in the 2020s under RCP 4.5 (dry-cold scenario)

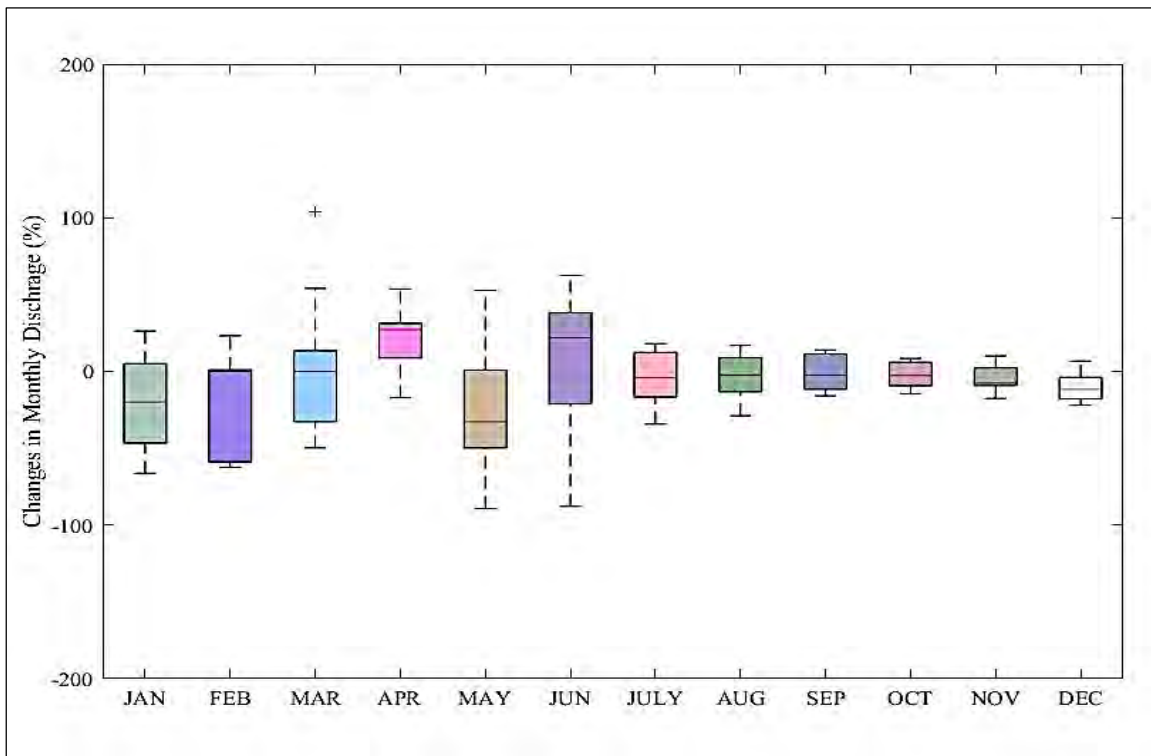


Figure 5.12 Changes in monthly discharge in the 2050s under RCP 4.5 (dry-cold scenario)

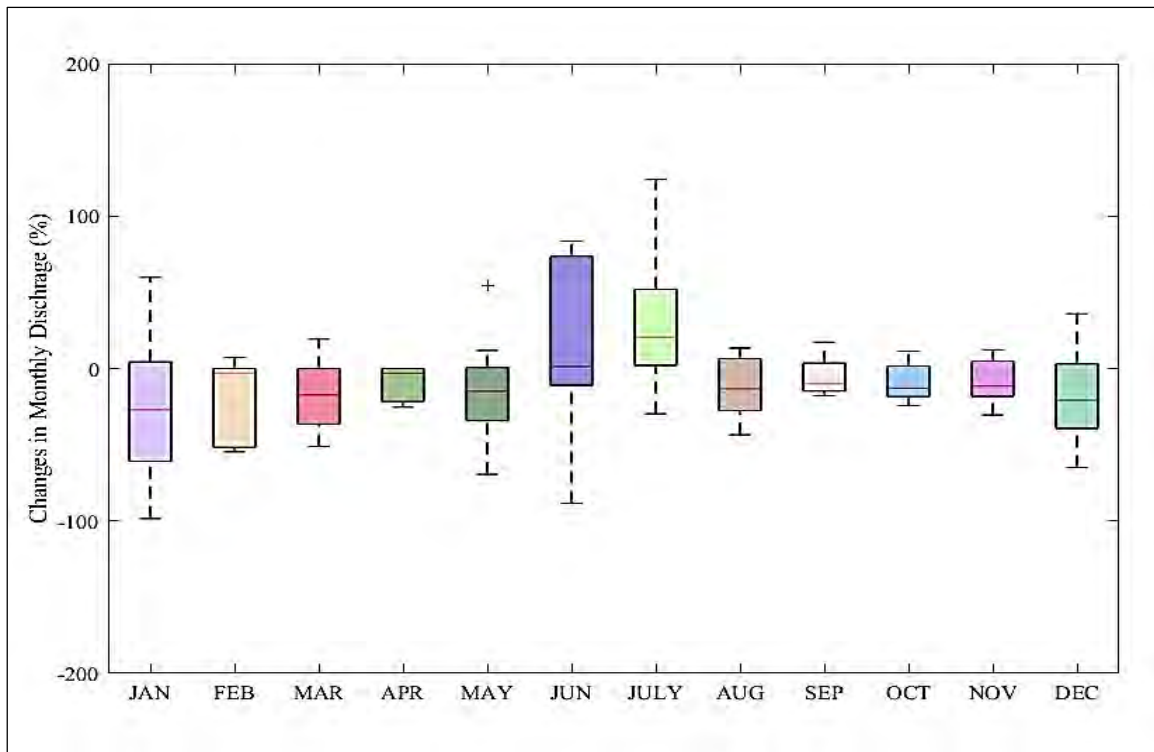


Figure 5.13 Changes in monthly discharge in the 2080s under RCP 4.5 (dry-cold scenario)

RCP 8.5

Wet-Warm scenario

Projected precipitation and temperature tend to follow an increasing trend under RCP 8.5 in the wet-warm scenario which may lead to large changes in monthly flow volume. Flow volume increases gradually during the 2020s, 2050s, and 2080s. Mean monthly discharge reaches its peak in July in the 2020s and in August during the 2050s and 2080s (Figure 5.14). The expected largest flow volume is observed at the end of the century which is about 4547.12 m³/s. Maximum discharge is around 1500 m³/s and 3000 m³/s during the 2020s and 2050s respectively. Flow values less than the reference period are mostly observed from January to May. As the peak is highest in August during the 2080s, it shows the overall maximum change of more than 400% to the reference period. In the 2050s, the maximum changes in discharge are more than 100%. Changes in the flow volume of each month of 2020s are slightly lower compared to other climatic periods. Maximum flow values may increase by up to 200%. Changes in mean monthly flow volume are presented in Figure 5.15-Figure 5.17.

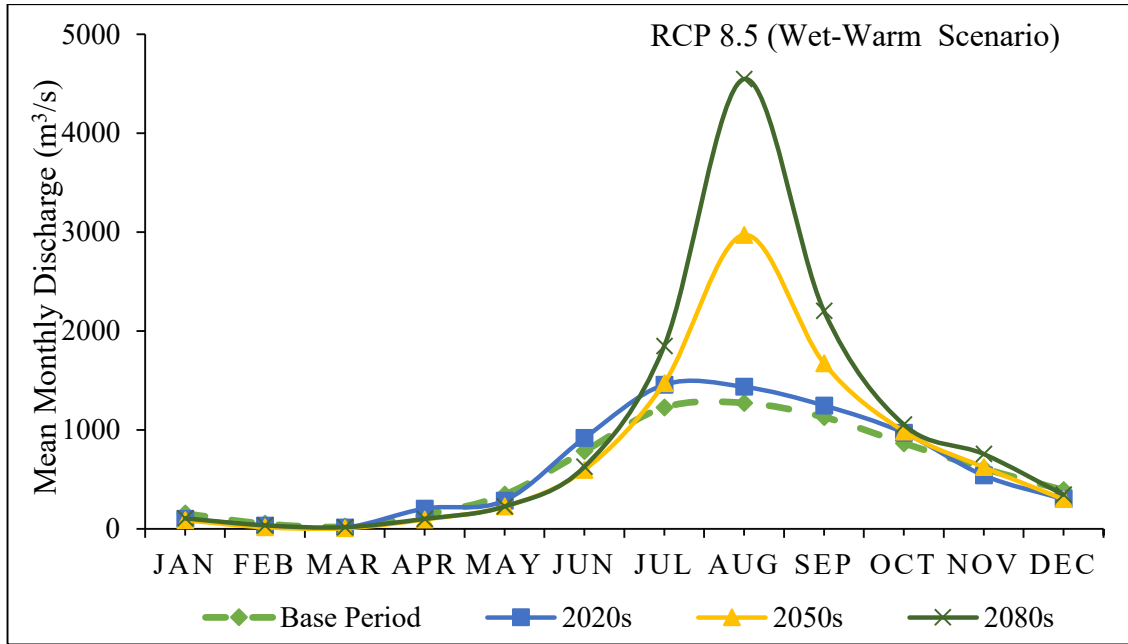


Figure 5.14 Mean monthly discharge under RCP 8.5 (wet-warm scenario)

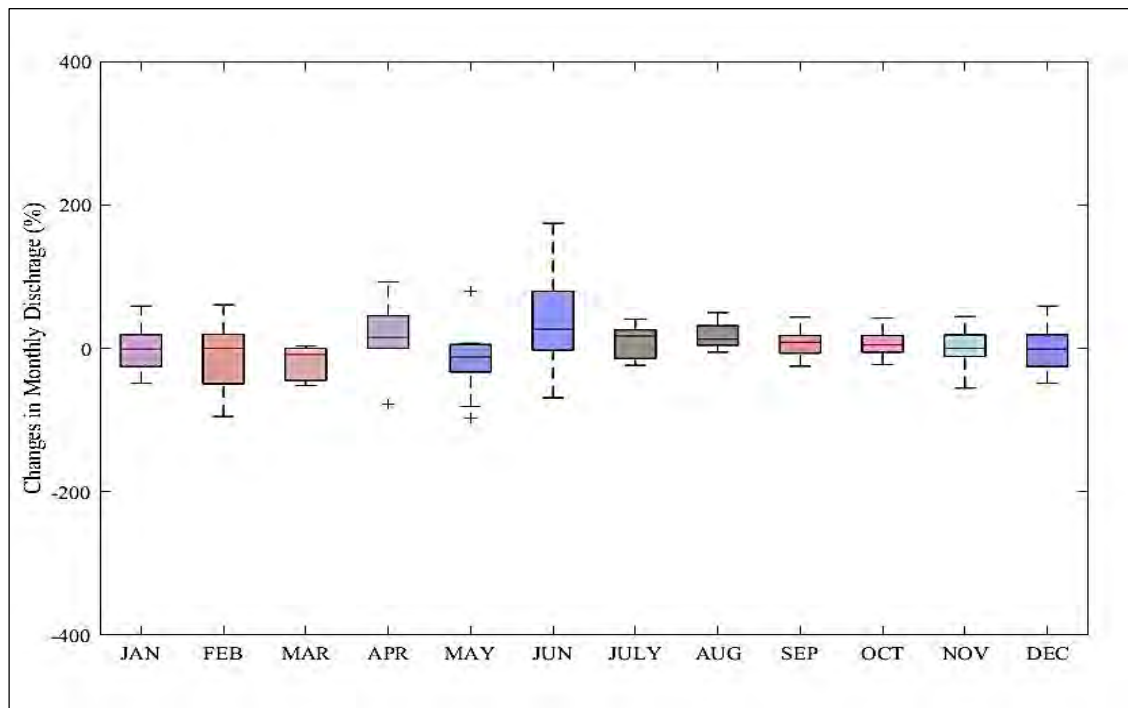


Figure 5.15 Changes in monthly discharge in the 2020s under RCP 8.5 (wet-warm scenario)

Changes in the discharge amount do not flow any general trend. While there is a mild change in flow values (in the 2050s) there is also much higher uncertainty in changes

(June-December, 2080s) due to an increase in precipitation. Flow value may decrease and increase within range of -200% to 500%.

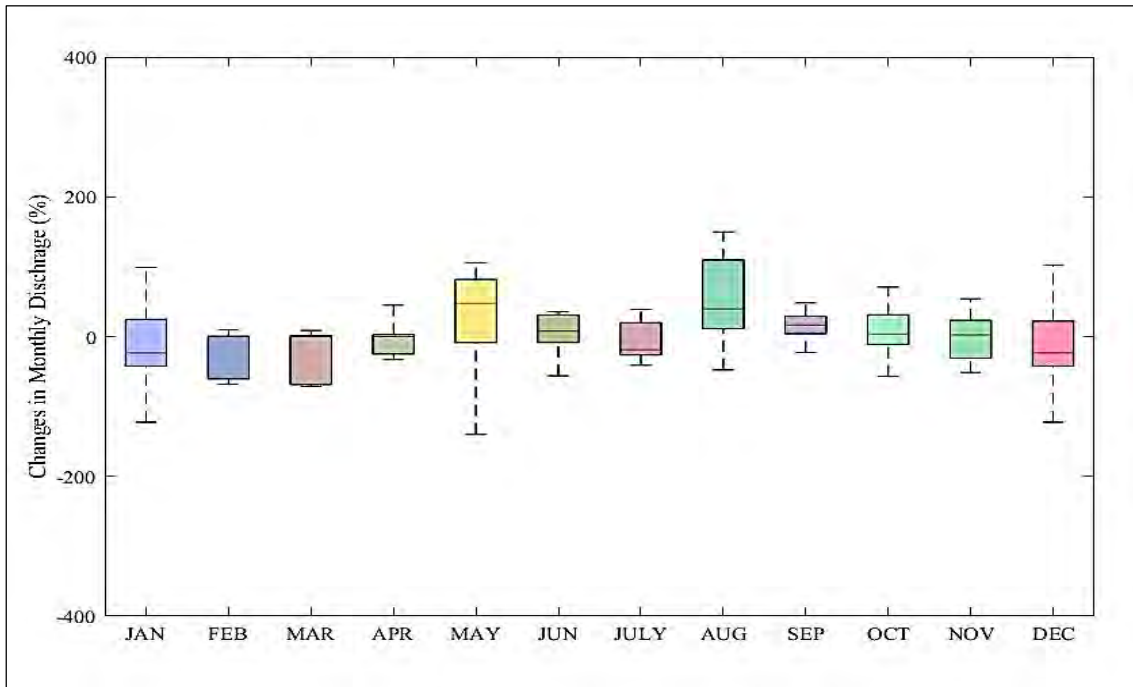


Figure 5.16 Changes in monthly discharge in the 2050s under RCP 8.5 (wet-warm scenario)

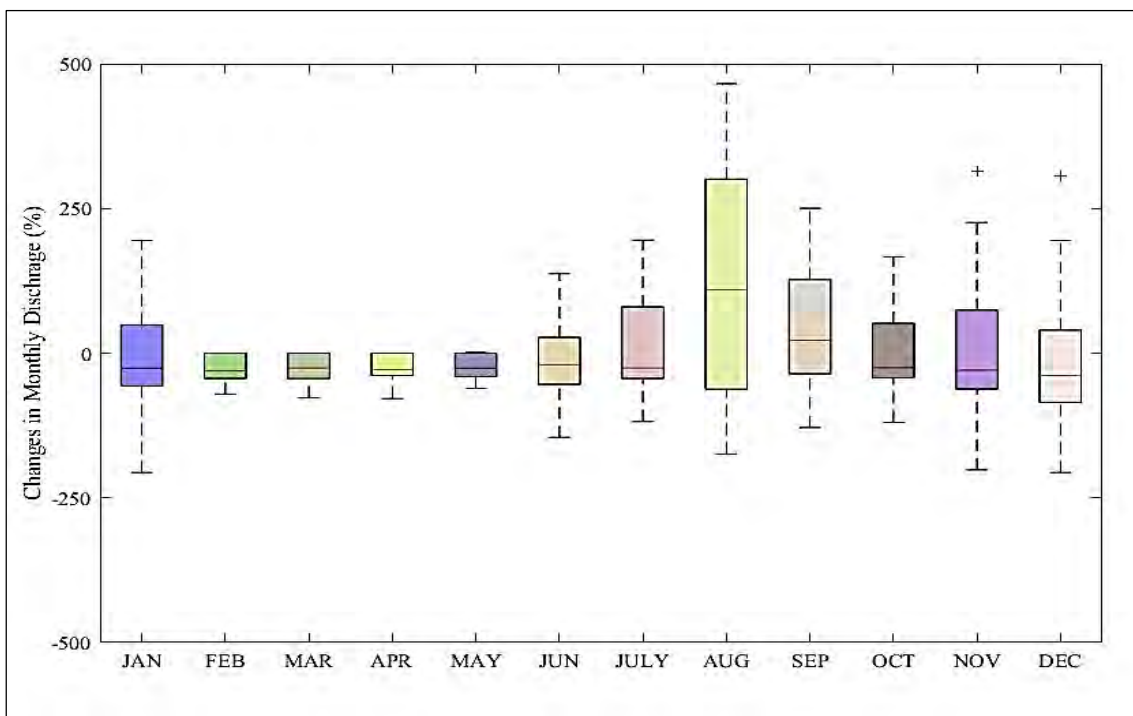


Figure 5.17 Changes in monthly discharge in the 2080s under RCP 8.5 (wet-warm scenario)

Dry-Cold scenario

Projected precipitation and temperature by dry-cold scenario under RCP 8.5 shows less precipitation to higher temperature changes. This may lead to significant changes in monthly flow volume. As similar to RCP 4.5, peak flow volume increases during the 2020s and 2080s and decreases in 2050s (Figure 5.18). Mean monthly discharge reaches its peak in July in the 2020s and 2080s whereas in August during 2050s.

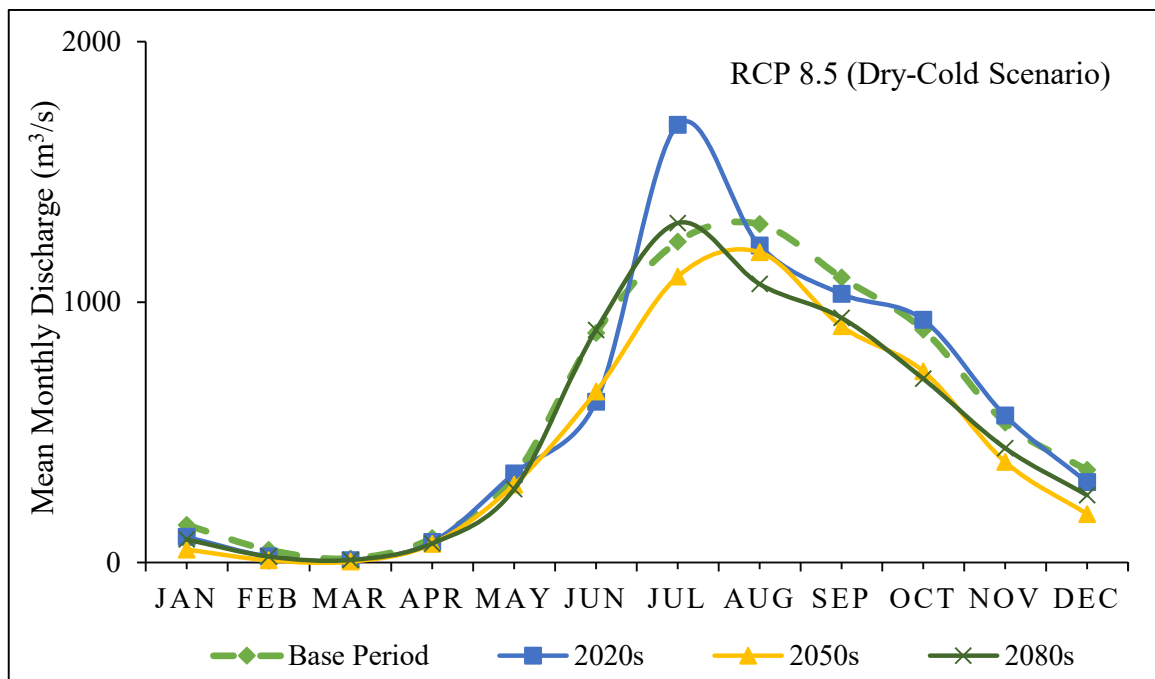


Figure 5.17 Mean monthly discharge under RCP 8.5 (dry-cold scenario)

The maximum increase in the flow volume is observed during the 2020s which is about 1693.71 m³/s. Maximum discharge is around 1181.48 m³/s and 1318.35 m³/s during the 2050s and 2080s respectively. Flow value less than the reference period is observed in most of the month except in July for all cases. As the peak is highest in July during the 2020s it shows the overall maximum change of 5.5 % with a maximum flow reduction of more than 50%. In the 2050s, the maximum decrease in discharge is about 80% in the month of less rainfall, February.

Changes in monthly flow volume are presented in Figure 5.19-Figure 5.21 where the uncertainty ranges between -100% to more than 100% in monthly discharge each year over a particular climatic period.

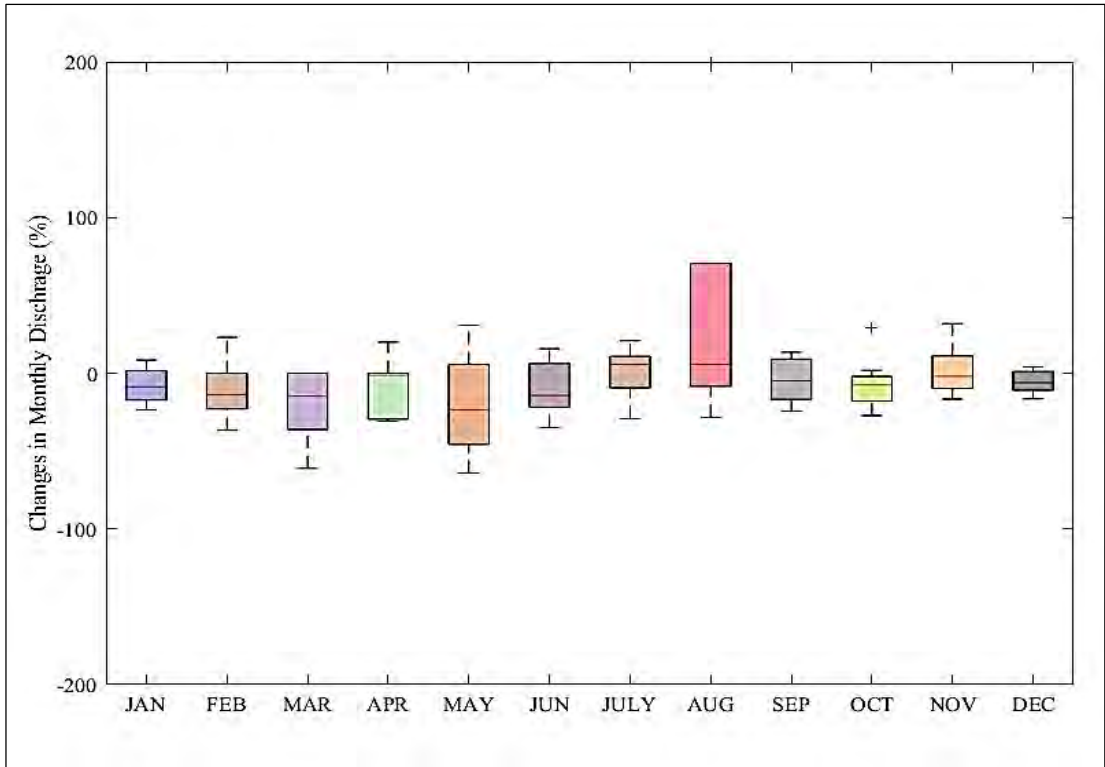


Figure 5.18 Changes in mean monthly discharge in the 2020s under RCP 8.5 (dry-cold scenario)

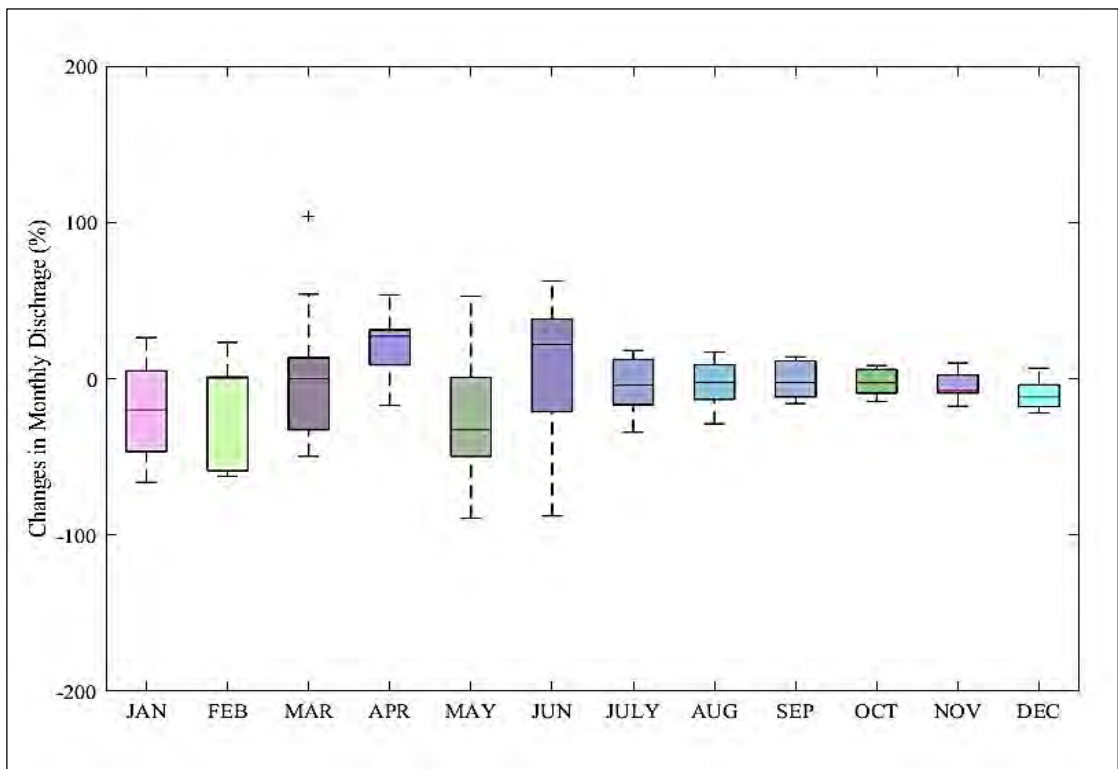


Figure 5.19 Changes in mean monthly discharge in the 2050s under RCP 8.5 (dry-cold scenario)

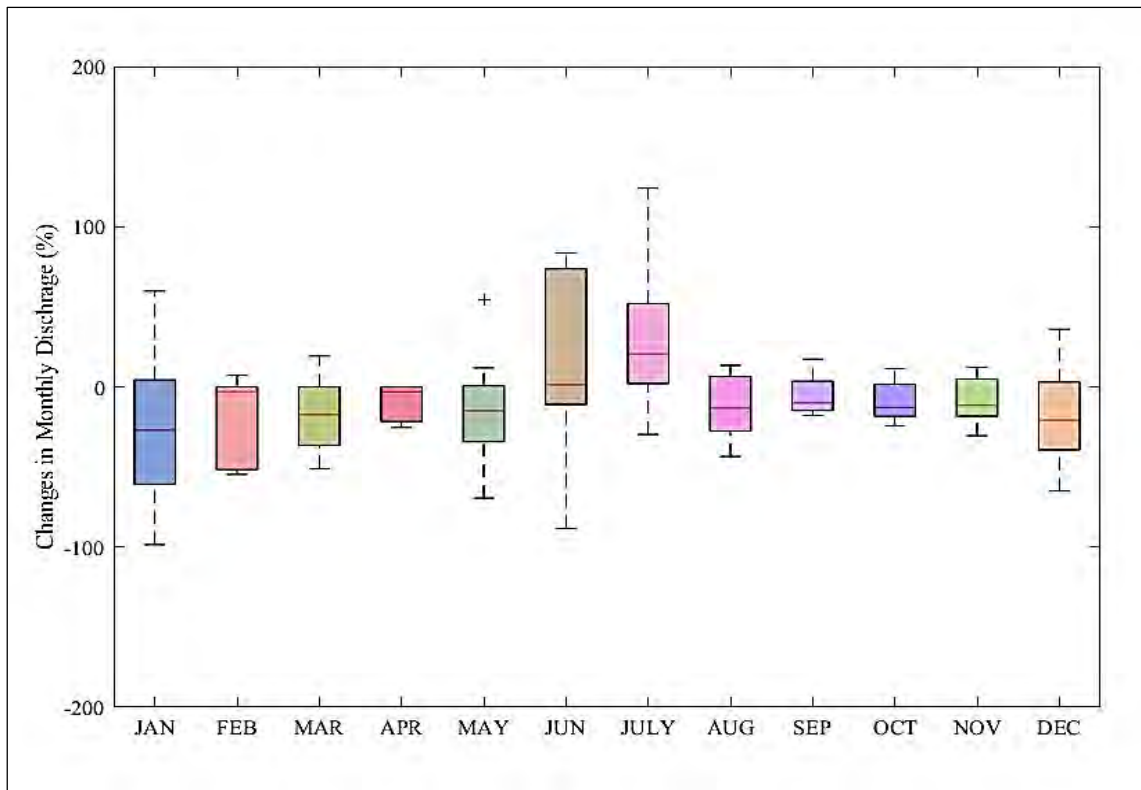


Figure 5.20 Changes in mean monthly discharge in the 2080s under RCP 8.5 (dry-cold scenario)

Changes in seasonal flow

From the meteorological viewpoint, the climate is divided into the following seasons. Winter: December, January, and February, Pre-monsoon: March, April, and May. Monsoon: June, July, August, and September, Post Monsoon: October and November. Changes in flow at the outlet station for the different seasons over each climatic period are analyzed in this section.

RCP 4.5

Wet-Warm scenario

The seasonal variation of discharge is presented in Figure 5.21 for RCP scenario 4.5. The driest season of a year receives the least rainfall and the generated flow volume is usually low. It is observed that the dry season flow volume is about 2% less than the reference period during the 2020s under RCP 4.5. But the flow volume tends to increase for the later periods by 45% and 80% approximately. Pre-monsoon is generally the hottest season of the year and receives the least volume of flow according to the wet-warm scenario

Under RCP 4.5. Maximum flow reduction is more than 50% in this season during the 2050s. Discharge changes about 22% in the 2020s and about 1% in the 2080s. Monsoon season includes the wettest months. Flow increases more than 50% seasonally in the 2020s. About 7% and 30% value increases during the monsoon period of the 2050s and 2080s. The changes in discharge are much lesser over the three climatic periods and the maximum reduction inflow is about 8% in the 2020s. In midcentury, discharge decrease rate almost half that is observed in the 2020s and at the end of the century flow volume slightly increases by 2.4%.

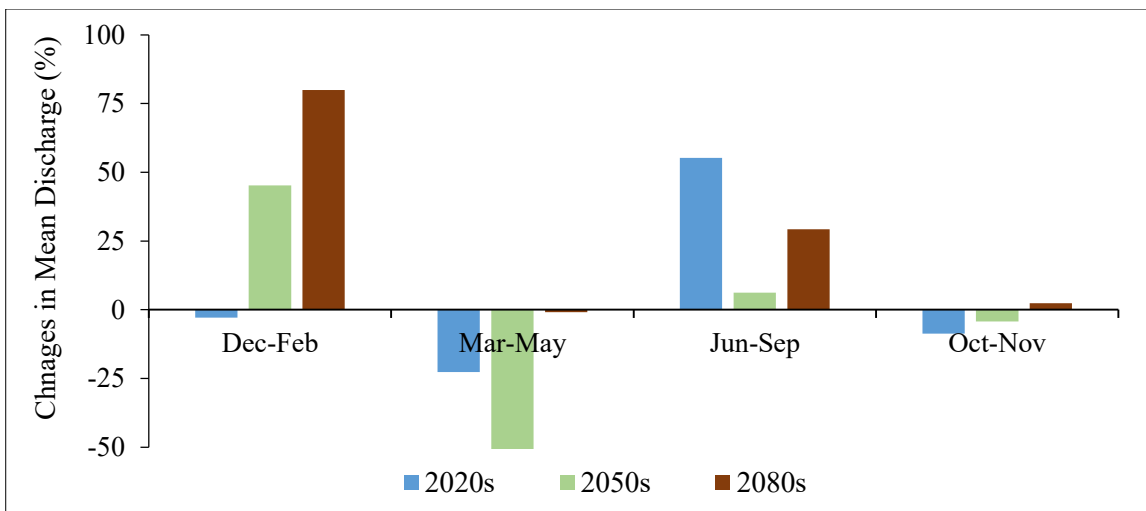


Figure 5.21 Changes in seasonal flow under RCP 4.5 (wet-warm scenario)

Dry-Cold scenario

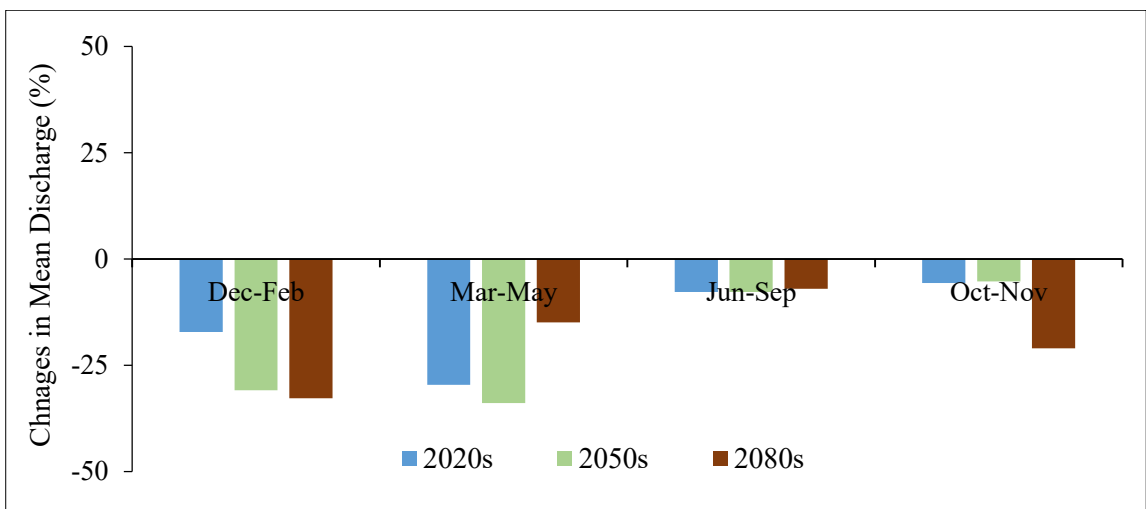


Figure 5.22 Changes in seasonal flow under RCP 4.5 (dry-cold scenario)

Predicted changes in the flow volume indicate that discharge will be less in every season over the three climatic periods. The Driest months (dry season) and the hottest months (pre-monsoon) of the year will receive the least amount of flow. The maximum reduction in flow is around 30% for both cases in these two seasons. In the rainy season, 7% of the total discharge will be reduced. At the end of the century, post-monsoon will have a maximum reduction of about 20% (Figure 5.22).

RCP 8.5

Wet-Warm scenario

Percent changes in seasonal discharge are presented in Figure 5.23 for RCP scenario 8.5. Dry season flow volume is found to be decreasing over each climate period. The maximum decrease in the flow volume was observed in the 2050s which is more than 30%. In the 2020s and 2080s, discharge is about 28% and 19% less than the reference period. Flow reduction is more than 65% in the pre-monsoon season at the end of the century. Similarly, in midcentury the flow seems to reduce more than 30%. Pre-monsoon flow increased by approximately 2% during the 2020s. Monsoon discharge changes about 16% in the 2020s, more than 50% in 2050s, and increases more than 100% in the 2080s. Post-monsoon flow increases up to 21% at the end of the century.

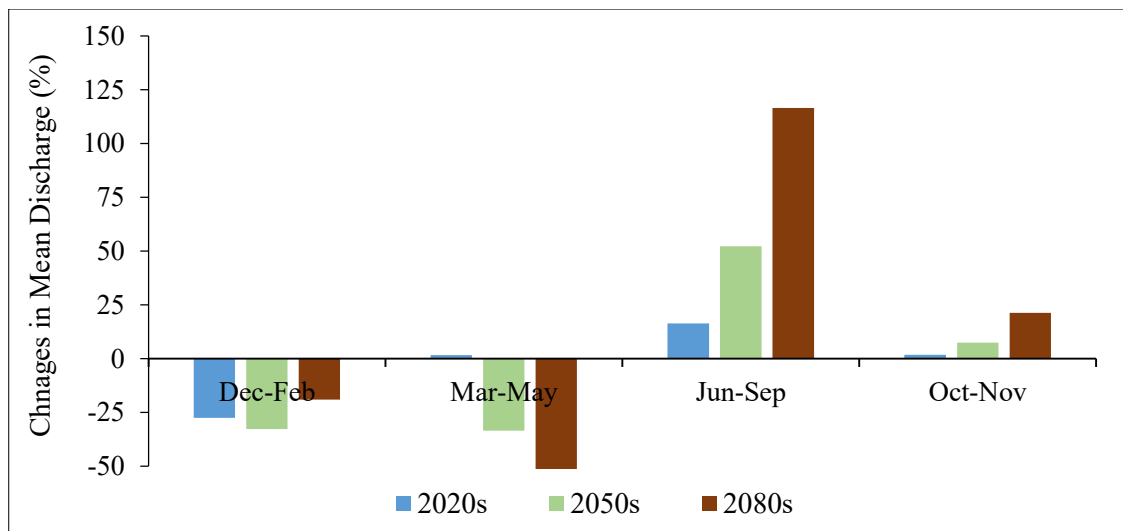


Figure 5.23 Changes in seasonal flow under RCP 8.5 (wet-warm scenario)

Dry-Cold scenario

As similar to RCP 4.5, dry and pre-monsoon period experiences a maximum decrease in discharge which exceeds 50% of the total volume. A slight increase in discharge is observed in the monsoon and post-monsoon period which is very less (less than 3%) in the 2020s. For the monsoon period, the maximum decrease is observed in the 2050s which is about 15%. On the other hand, post-monsoon will have the least amount of flow in the 2050s which is more than 20% (Figure 5.25).

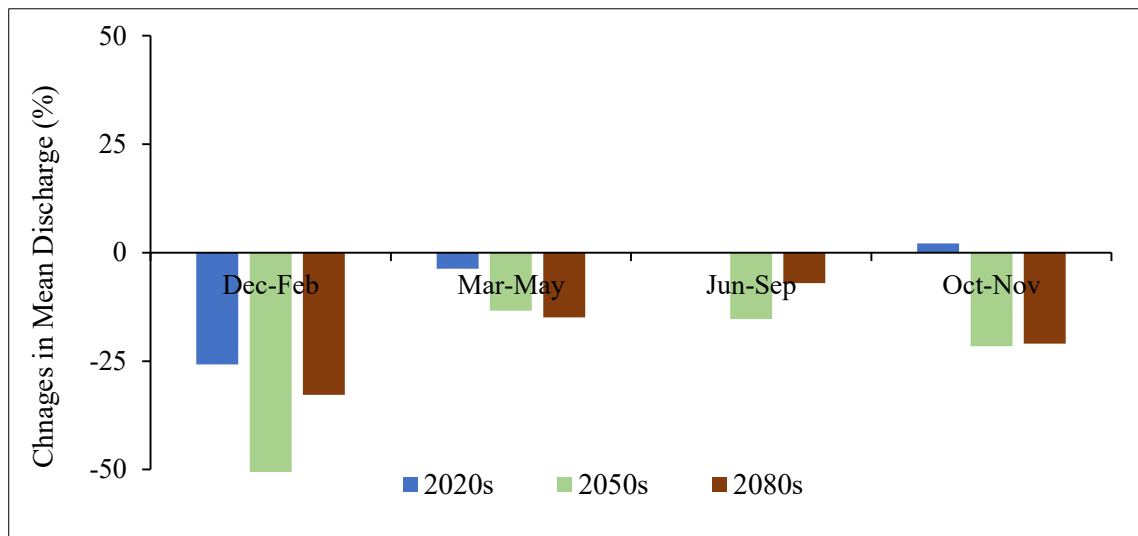


Figure 5.24 Changes in seasonal flow under RCP 8.5 (dry-cold scenario)

5.2.4 Impact on water balance components

The water balance components in this research for the future period were compared to the reference simulated water balance components (from 2000 to April 2018) obtained from the SWAT model, after the calibration and validation of the model with the observed data. As changes in precipitation and discharge were discussed earlier this section will cover other changes in the other water balance components.

Impact on evapotranspiration

RCP 4.5

Wet-Warm scenario

The increase in the rate of evapotranspiration is progressive in the dry and post-monsoon period, as it is crucially affected by the increase in temperature in the basin. Combining

the effect of a change in precipitation with the increase in temperature will significantly influence the evapotranspiration of the basin. A mild increase was observed during the monsoon period, ranging from 2-8% in the 2020s and 2080s with a drop in 2050s. A moderate increase (almost 70%) is projected during the dry period (Figure 5.26). Maximum evapotranspiration is projected in the post-monsoon (the 2020s, 2050s, and 2080s) up to 108%. This might be the influence of a projected increase in minimum and maximum temperatures, which causes a shortening of the lesser rain in this season.

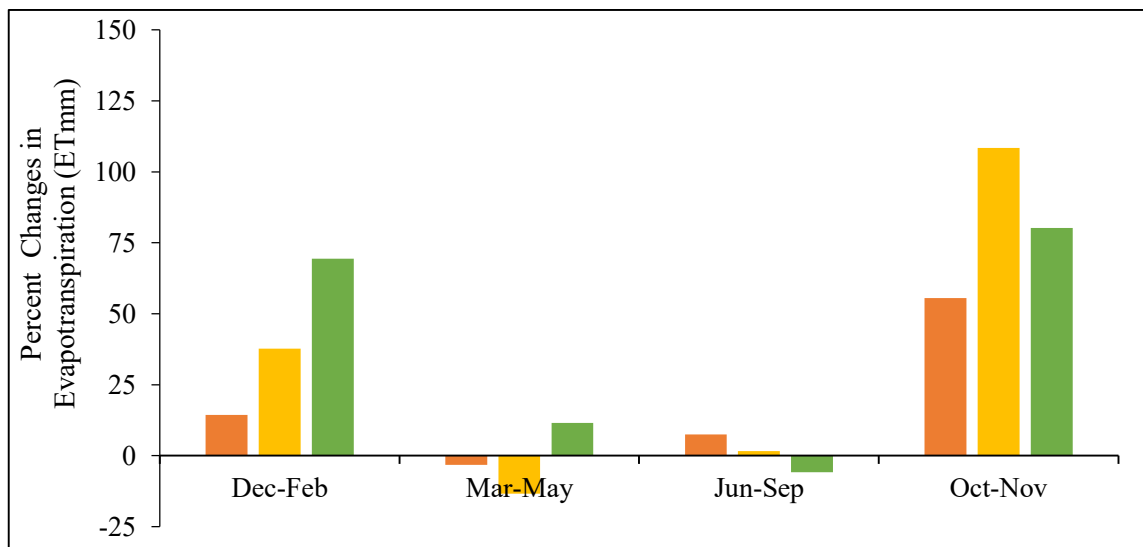


Figure 5.25 Percent changes in evapotranspiration (ET mm) under RCP 4.5 (wet-warm scenario)

Dry-Cold scenario

The evapotranspiration rate seems to decrease in pre-monsoon and monsoon periods whereas, the value increases in the post-monsoon period of the year. The dry season has an increasing value of ET in the 2080s which is about 25%. The maximum decrease in ET value is observed in the Monsoon period of the 2080s which is about 34%. During post-monsoon, progressive ET values decrease from 85% to 35% over the three climatic periods (Figure 5.26).

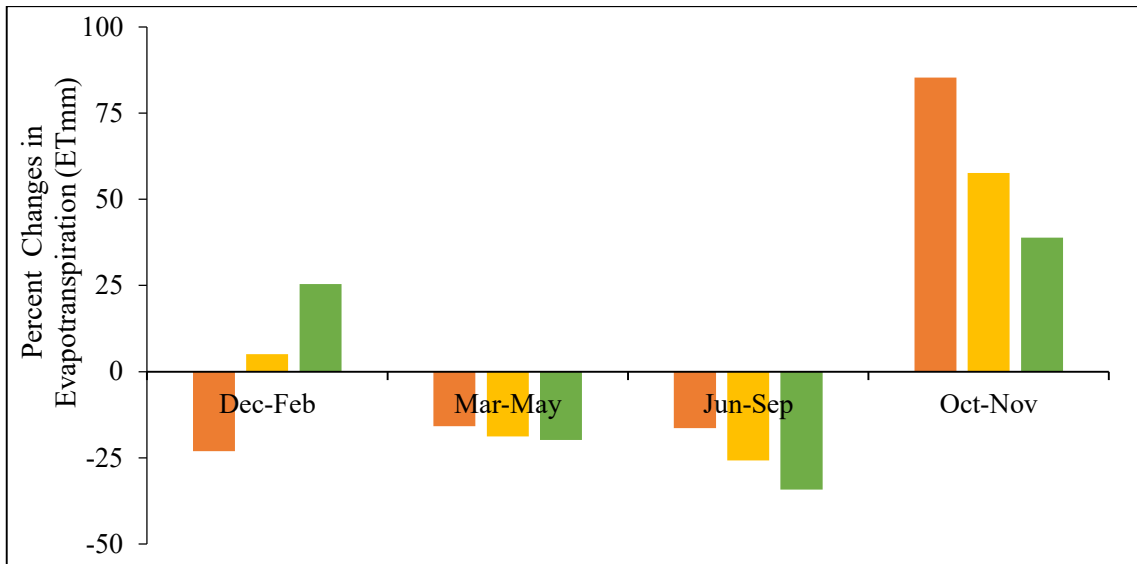


Figure 5.26 Percent changes in evapotranspiration (ET mm) under under RCP 4.5 (dry-cold scenario)

RCP 8.5

Wet-Warm scenario

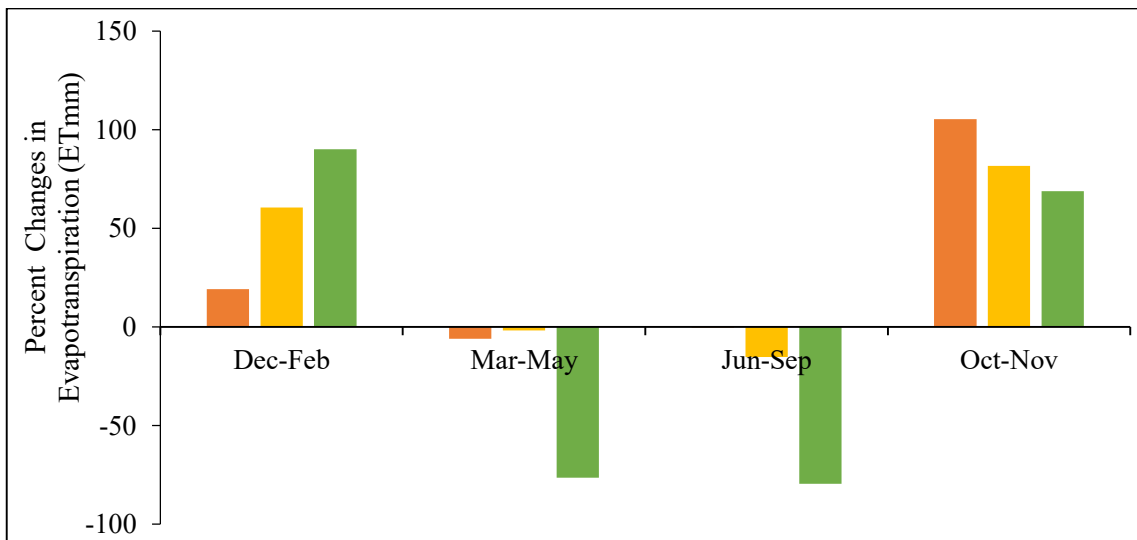


Figure 5.27 Percent changes in evapotranspiration (ET mm) under RCP 8.5 (wet-warm scenario)

During the monsoon period, evapotranspiration decreases ranging from 0.35-80% due to the projected increase in precipitation (Figure 5.27). Maximum evapotranspiration is projected in the dry and post-monsoon season with a maximum increase of more than 100%.

Dry-Cold scenario

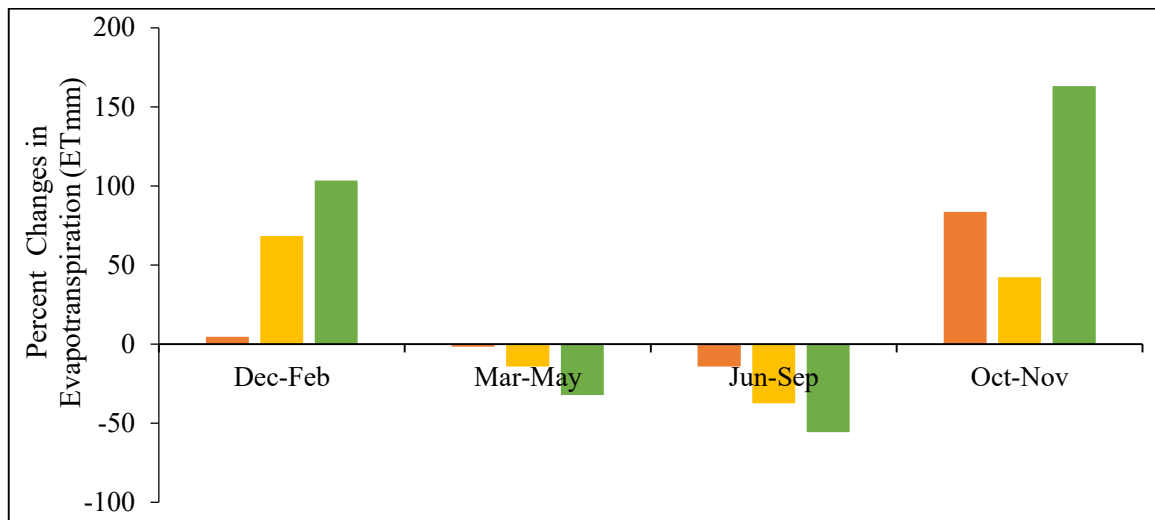


Figure 5.28 Percent changes in evapotranspiration (ET mm) RCP 8.5 (dry-cold scenario)

Evapotranspiration increases in dry and post-monsoon periods whereas the value decreases in the pre-monsoon and monsoon period of the year. ET value increases in the dry season from 5% to more than 100%. The maximum decrease in ET value is observed in the pre-monsoon period of the 2020s which is about 32%. During post-monsoon, progressive ET values increase from 84% to 163% in the 2020s and 2080s with a value drop in 2050s (Figure 5.28).

Impact on water yield

Water yield takes into account the surface runoff, lateral flow, groundwater flow, transmission losses, and pond abstraction. The increase in water yield is relatively higher in the dry and pre-monsoon period to the simulation period.

RCP 4.5

Wet-Warm scenario

Water yield (mm) is maximum in the monsoon period. Projected water yield values remain quite closer to the reference values therefore the change is less. But due to higher precipitation concerning the change in temperature, water yield increases in the driest

period of the year with a maximum increase of more than 200%. In the hottest months of the year (pre-monsoon) water yield decreases by more than 60% (Figure 5.29). During both monsoon and post-monsoon, the projected water yield values remain closer to the reference period.

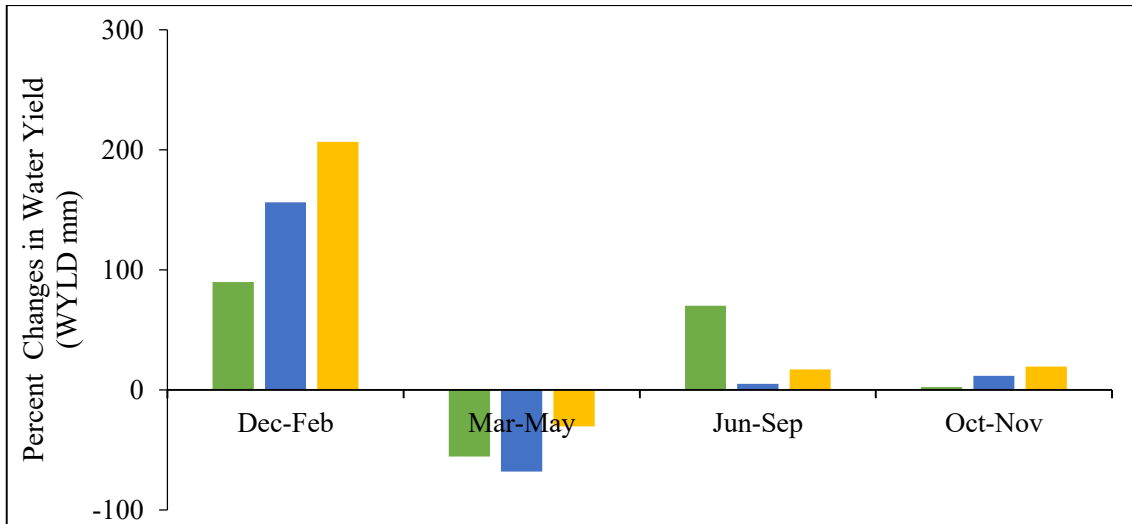


Figure 5.29 Percent changes in water yield (WYLDmm) under RCP 4.5 (wet-warm scenario)

Dry-Cold scenario

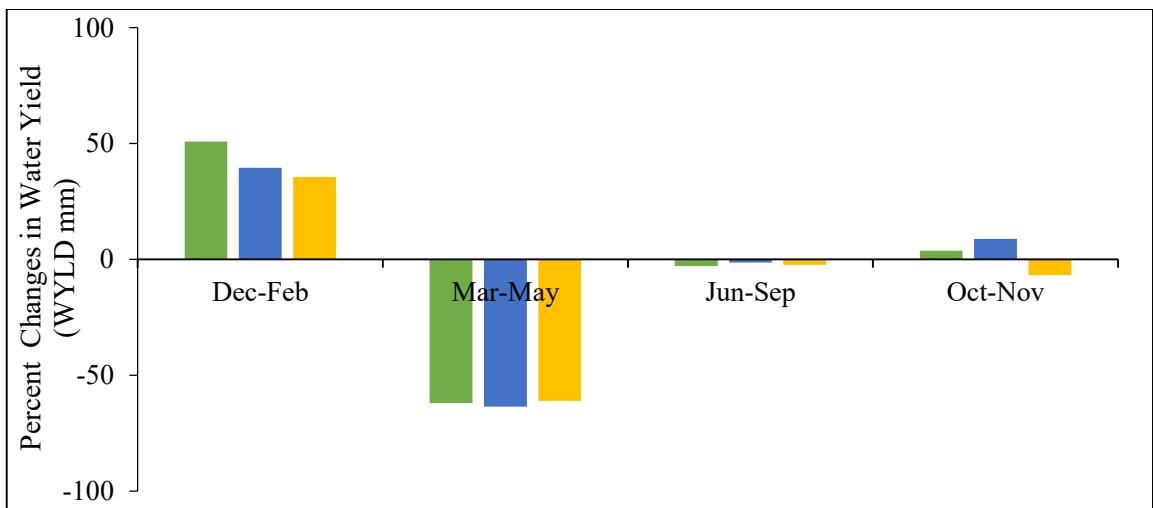


Figure 5.30 Percent changes in water yield (WYLDmm) under RCP 4.5 (dry-cold scenario)

Water yield (mm) is maximum in the monsoon period. Projected water yield values slightly decrease from the reference values, therefore the change is very mild (2%-8%).

Water yield increases in the driest period of the year with a maximum increase of more than 60%. In the hottest months of the year (pre-monsoon) water yield decreases by more than 60% (Figure 5.30). During post-monsoon, the projected water yield values remain closer to the reference period.

RCP 8.5

Wet-Warm scenario

Due to higher rainfall under RCP 8.5, projected water yield values increase more than the reference values therefore the change is highest. But in the driest period of the year, there is a maximum increase of more than 50%. In the hottest months of the year (pre-monsoon) water yield decreases by almost 70% (Figure 5.31). Moderate changes were observed during post-monsoon which ranges between 22% to 37%.

Dry-Cold scenario

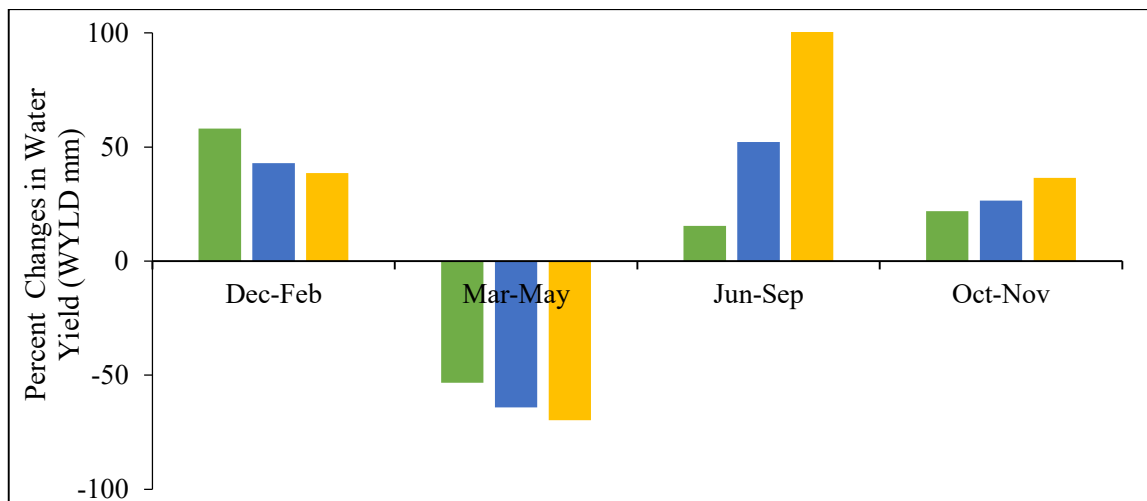


Figure 5.31 Percent changes in water yield (WYLDmm) under RCP 8.5 (wet-warm scenario)

Projected water yield values increase in the 2020s and 2080s but decrease in 2050s from the reference values. The change is very mild (-9% to 30%). In the driest period of the year with the basin will experience a maximum increase of more than 60%. In the hottest months of the year (pre-monsoon), water yield decreases more than 65% (Figure 5.32). During post-monsoon, the projected water yield values remain closer to the reference period but increase by almost 67% in the 2020s.

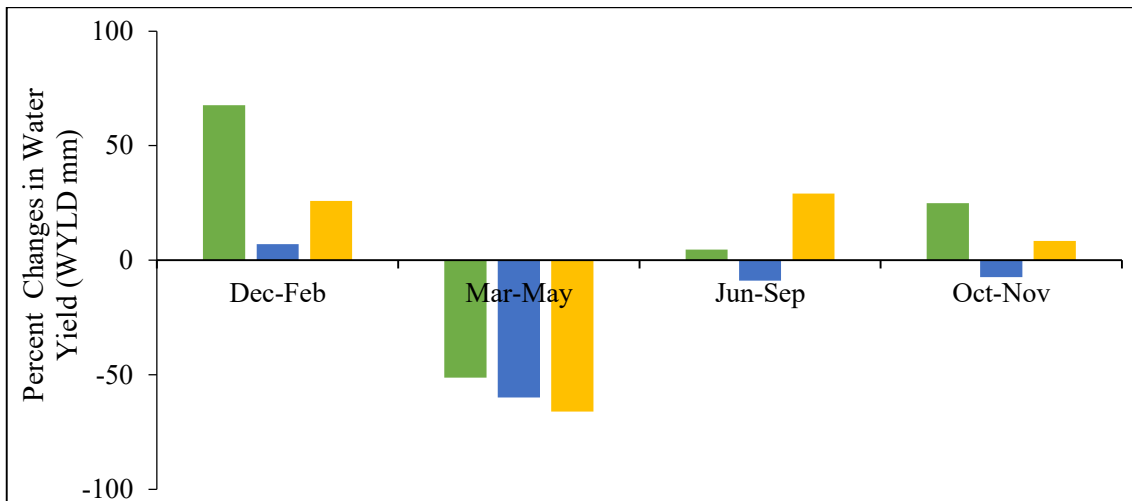


Figure 5.32 Percent changes in water yield (WYLDmm) under RCP 8.5 (dry-cold scenario)

Impact on groundwater contribution

RCP 4.5

Wet-Warm scenario

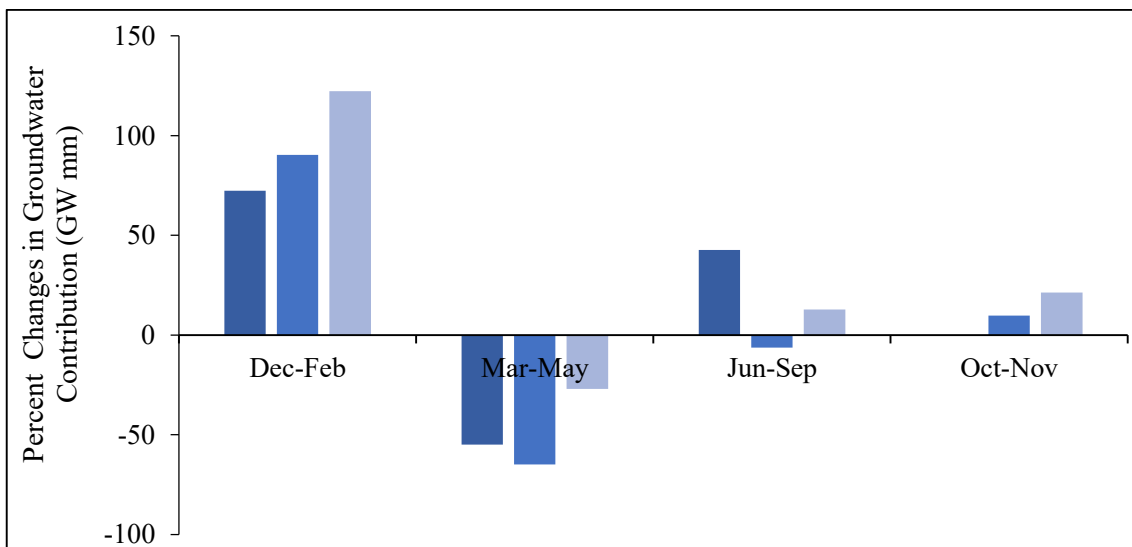


Figure 5.33 Percent changes in groundwater contribution (GWmm) under RCP 4.5 (wet-warm scenario)

Mild changes in the groundwater contribution are observed in the monsoon and post-monsoon period with a maximum increase of 42% and more than 20% respectively. Moderate change is observed in the pre-monsoon period with a maximum decrease of 65%. The maximum increase observed in the dry period ranges between 72% to more than 100% (Figure 5.33).

Dry-Cold scenario

Mild changes in the groundwater contribution are observed in the monsoon and post-monsoon period with a maximum decrease of 19% and 15% respectively. The maximum increase is observed in the dry period which is about 47%. The maximum decrease was observed in the pre-monsoon period which is more than 60% (Figure 5.34).

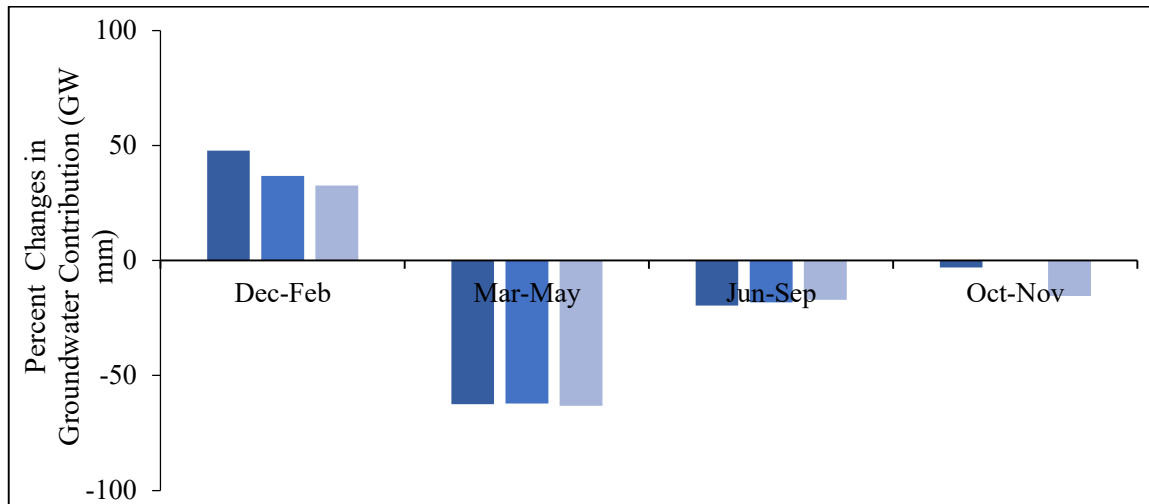


Figure 5.34 Percent changes in groundwater contribution (GWmm) under RCP 4.5 (dry-cold scenario)

RCP 8.5

Wet-Warm scenario

The maximum increase in groundwater contribution is observed in the dry and monsoon period which is more than 50% (Figure 5.35). Moderate change is observed in the pre-monsoon and post-monsoon period with a maximum decrease of 67% and an increase of 52% respectively.

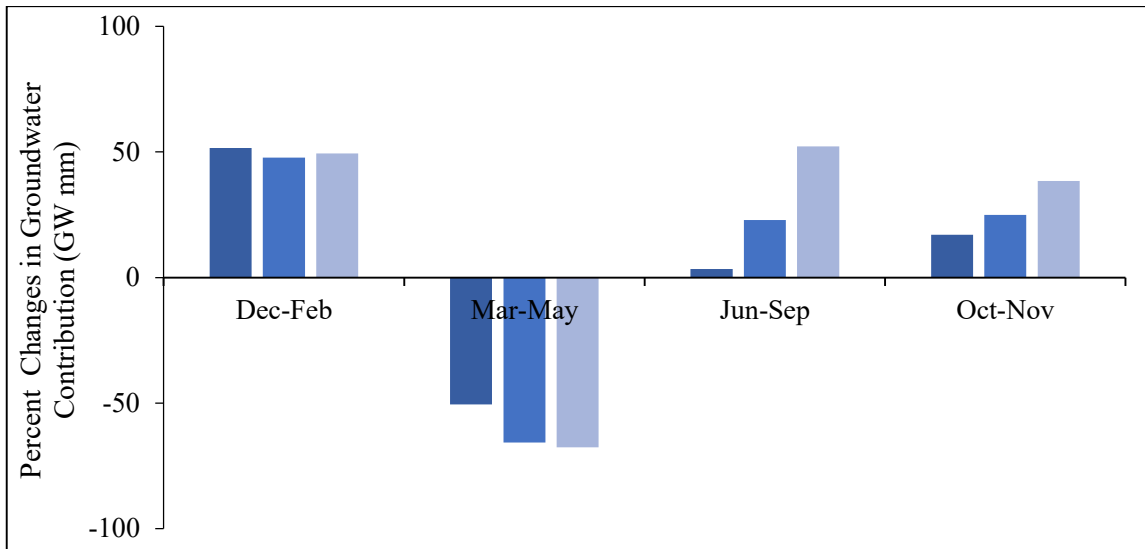


Figure 5.35 Percent changes in groundwater contribution (GWmm) under RCP 8.5 (wet-warm scenario)

Dry-Cold scenario

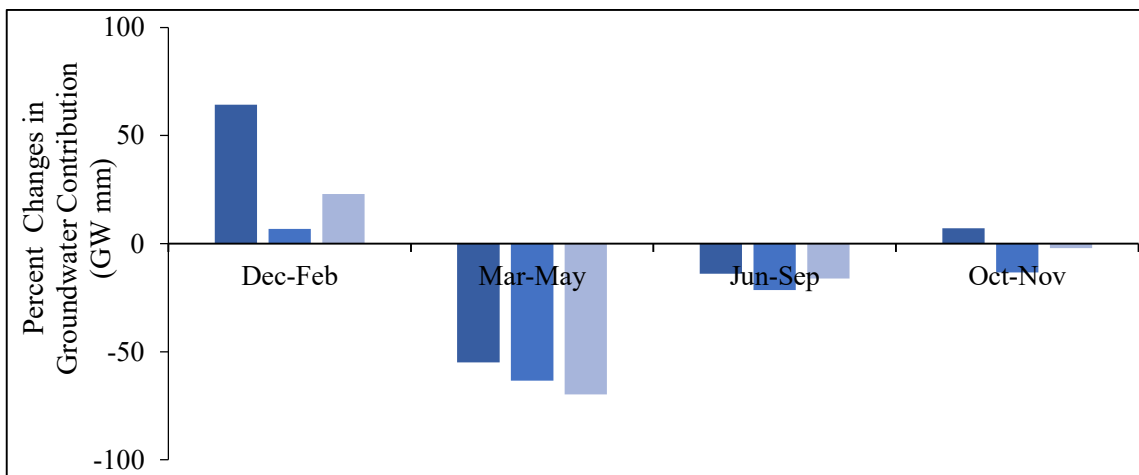


Figure 5.36 Percent changes in groundwater contribution (GWmm) under RCP 8.5 (dry-cold scenario)

Mild changes are observed in the monsoon and post-monsoon period with a maximum decrease of 21% and an increase of 7% respectively. A maximum increase is observed in the dry period which ranges between 7% to 64%. The maximum reduction was observed in the pre-monsoon period which is more than 65% (Figure 5.36).

Impact on percolation

Percolation losses (mm) is usually the least in the dry season of the reference period and increases gradually in pre-monsoon and post-monsoon and then decreases further in post-monsoon. The same pattern is observed in the future period but the amount varies.

RCP 4.5

Wet-Warm scenario

Thus maximum changes indicate large variation in the values with respect to the reference period. Percolation losses increase than previous years in the dry, monsoon, and post-monsoon periods. The maximum increase observed is more than 400%. The least amount of losses are observed in the pre-monsoon period which is more than 60% (Figure 5.37).

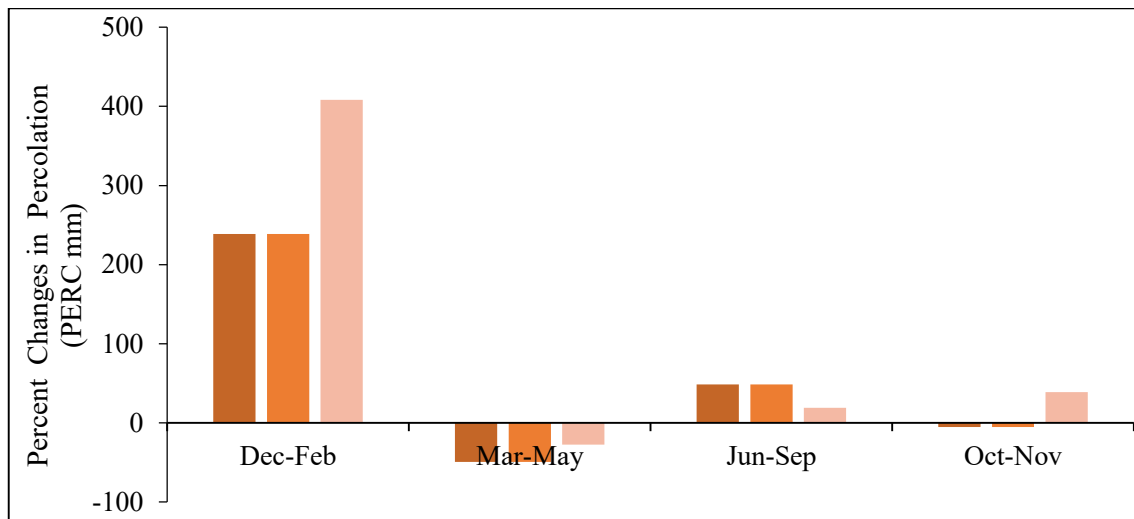


Figure 5.37 Percent changes in percolation (PERCmm) under RCP 4.5 (wet-warm scenario)

Dry-Cold scenario

Maximum changes indicate a large variation in the values with respect to the reference period. Percolation losses increase than previous years in the dry and post-monsoon period. The maximum increase observed is more than 50%. The least amount of losses are observed in the pre-monsoon and monsoon period which is more than 65% (Figure 5.40).

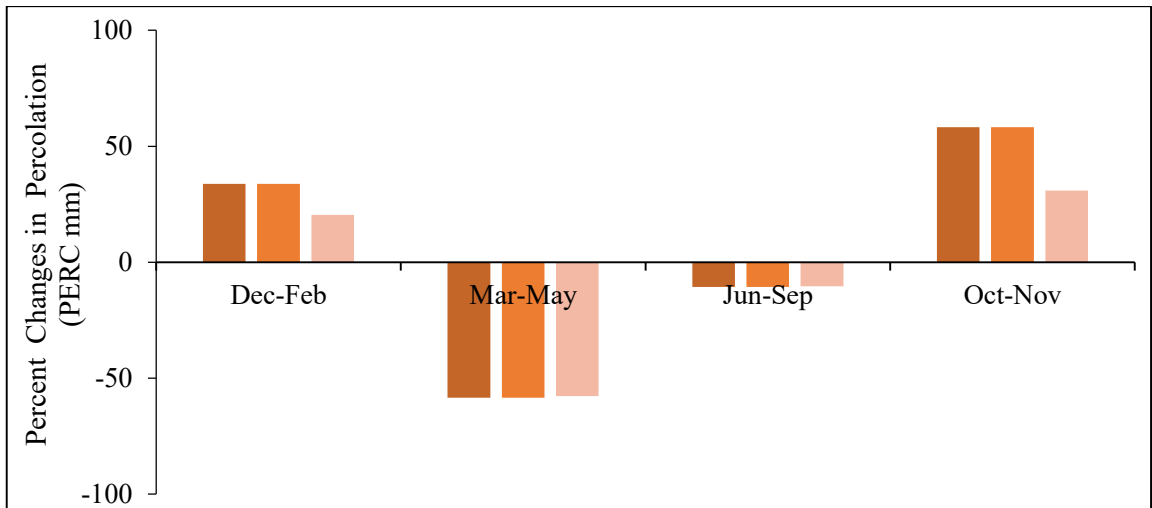


Figure 5.38 Percent changes in percolation (PERCmm) under RCP 4.5 (dry-cold scenario)

RCP 8.5

Wet-Warm scenario

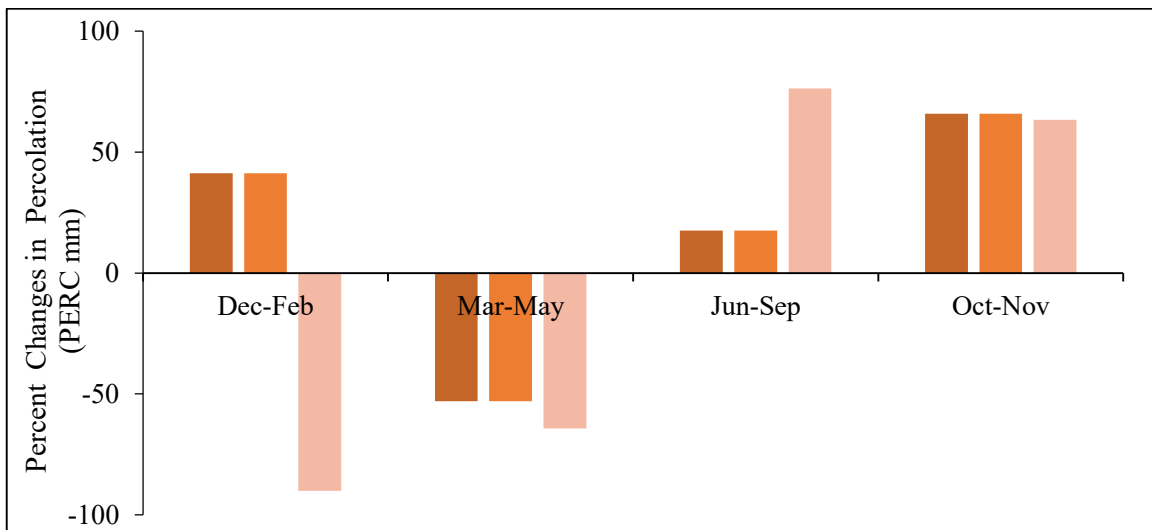


Figure 5.39 Percent changes in percolation (PERCmm) under RCP 8.5 (wet-warm scenario)

Percolation losses increase than previous years in the dry, monsoon, and post-monsoon periods. The maximum increase observed is more than 70%. The least amount of losses are observed in the pre-monsoon period which is more than 60% (Figure 5.38).

Dry-Cold scenario

As similar to RCP 4.5, percolation losses increase than previous years in the dry and post-monsoon period with a decrease in the dry period in the 2080s (about 6.5%). The maximum increase observed is 92% in the post-monsoon of 2020s. The least amount of losses are observed in the pre-monsoon and monsoon period which ranges from 5% to 65% (Figure 5.40).

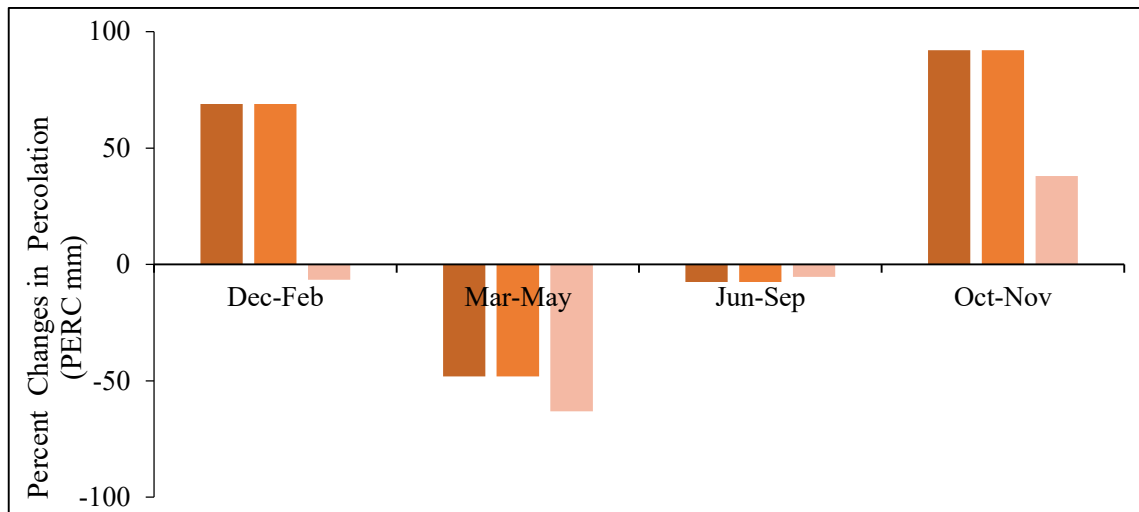


Figure 5.40 Percent changes in percolation (PERCmm) under RCP 8.5 (dry-cold scenario)

Impact on lateral flow

RCP 4.5

Wet-Warm scenario

Contribution from lateral flow (mm) is less in the dry season of the reference period and increases gradually in pre-monsoon and post-monsoon and then decreases further in post-monsoon. The same pattern is observed in the future period but the amount varies. Thus maximum changes indicate large variation in the values with respect to the reference period. Lateral flow increases than previous years in the dry, monsoon, and post-monsoon periods. The maximum increase observed is around 400%. The least amount of losses are observed in the pre-monsoon period which is about 19% (Figure 5.41).

Dry-Cold Scenario

Lateral flow decreases than previous years in the monsoon and pre-monsoon period. The maximum decrease observed is around 62%. Flow contribution increases for dry and post-monsoon periods. The highest amount of lateral flow is observed in the post-monsoon period which about 84 % (Figure 5.42).

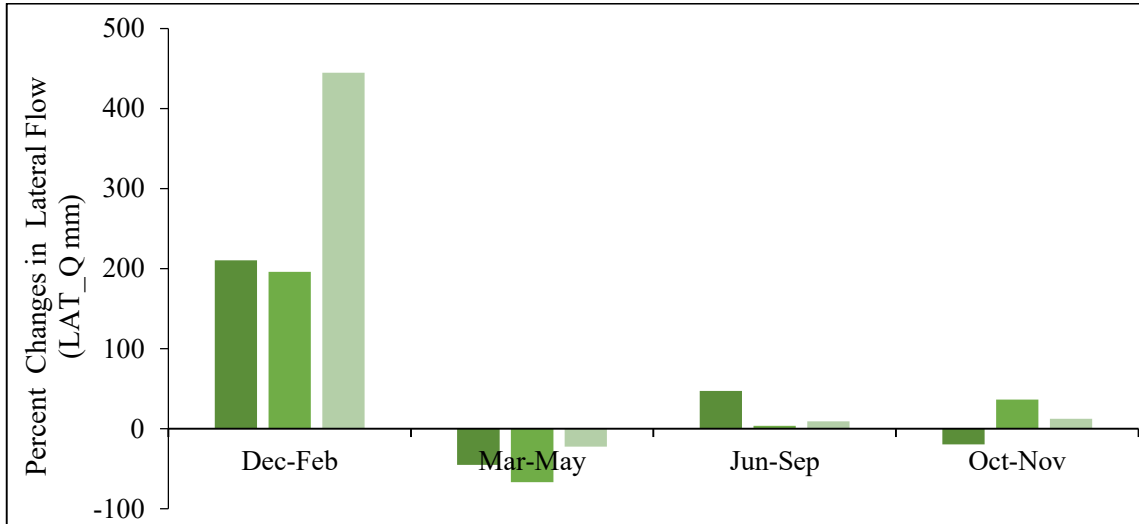


Figure 5.41 Percent changes in lateral flow (LAT_Qmm) under RCP 4.5 (wet-warm scenario)

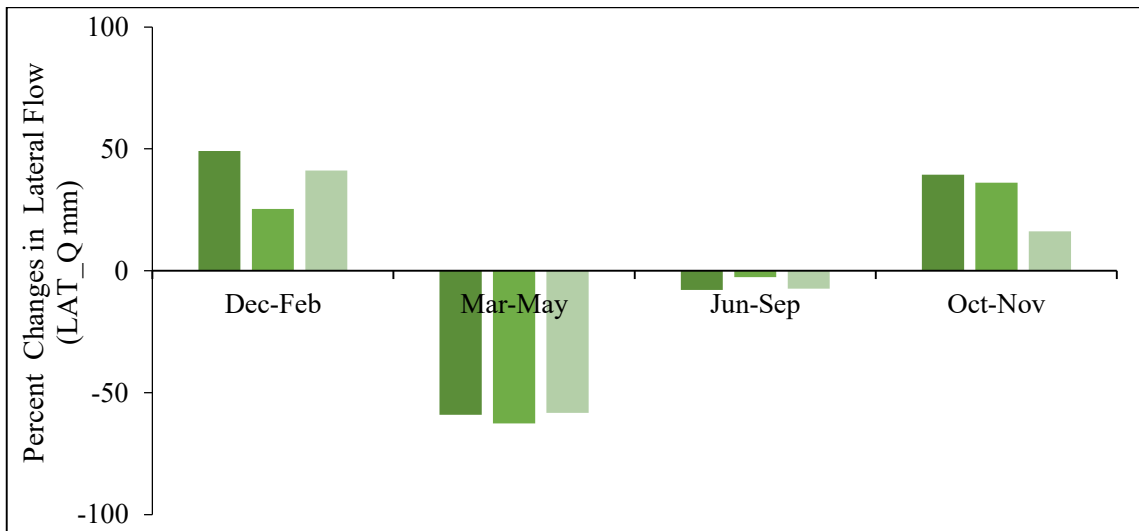


Figure 5.42 Percent changes in lateral flow (LAT_Qmm) under RCP 4.5 (dry-cold scenario)

RCP 8.5

Wet-Warm scenario

Lateral flow increases than previous years in the monsoon and post-monsoon period. The maximum increase observed is around 60%. Flow contribution increases in the 2020s for the dry period and decreases further for the later period. The least amount of flow is observed in the pre-monsoon period which about 84 % (Figure 5.43).

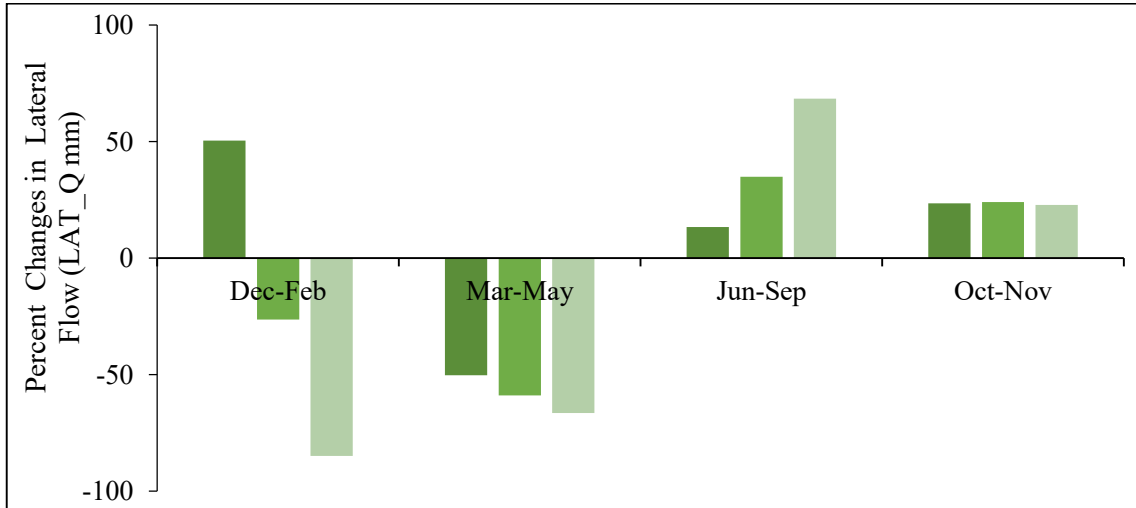


Figure 5.43 Percent changes in lateral flow (LAT_Qmm) under RCP 8.5 (wet-warm scenario)

Dry-Cold scenario

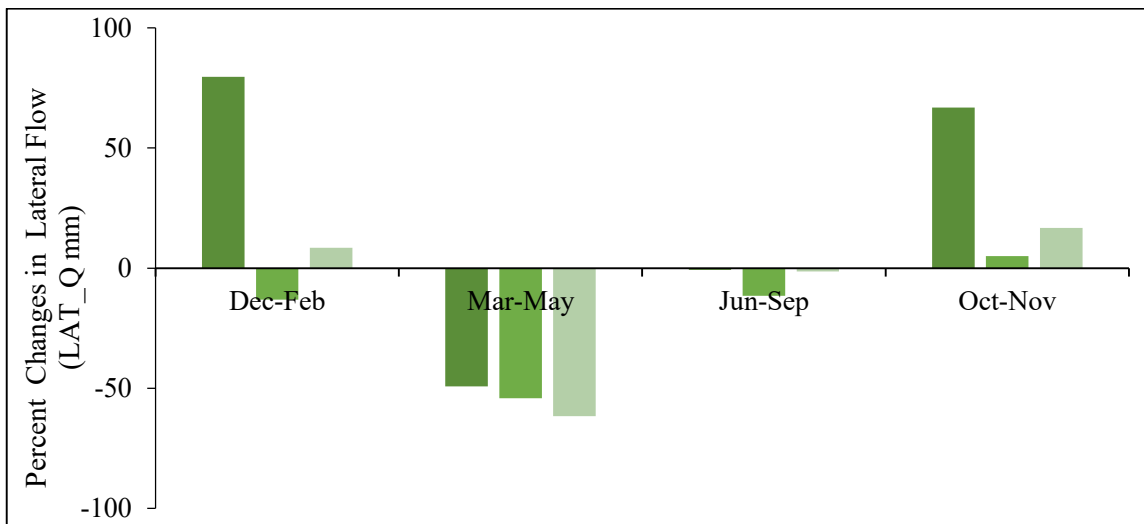


Figure 5.44 Percent changes in lateral flow (LAT_Qmm)

Lateral flow decreases than previous years in the monsoon and pre-monsoon period. The maximum decrease observed is around 61%. Flow contribution increases for the post-monsoon period. The highest amount of lateral flow is observed in the post-monsoon period which about 66 % (Figure 5.44).In the dry period, flow contribution increases to its maximum up to 79% in the 2020s and then decreases by 13% in 2050s.

5.3 Impact on flow due to upstream intervention

Analysis of upstream intervention at the upstream of Amalshid will include a storage reservoir/dam that will follow the reservoir operation strategy set for the Tipaimukh dam (Figure 5.45). As observed data is not available at Amalshid and reservoir location the study will use simulated discharges as the reservoir inflow and discharge at Amalshid. Kushiyara and Surma river receives inflows from the Barak river that enters through Amalshid point in Bangladesh.

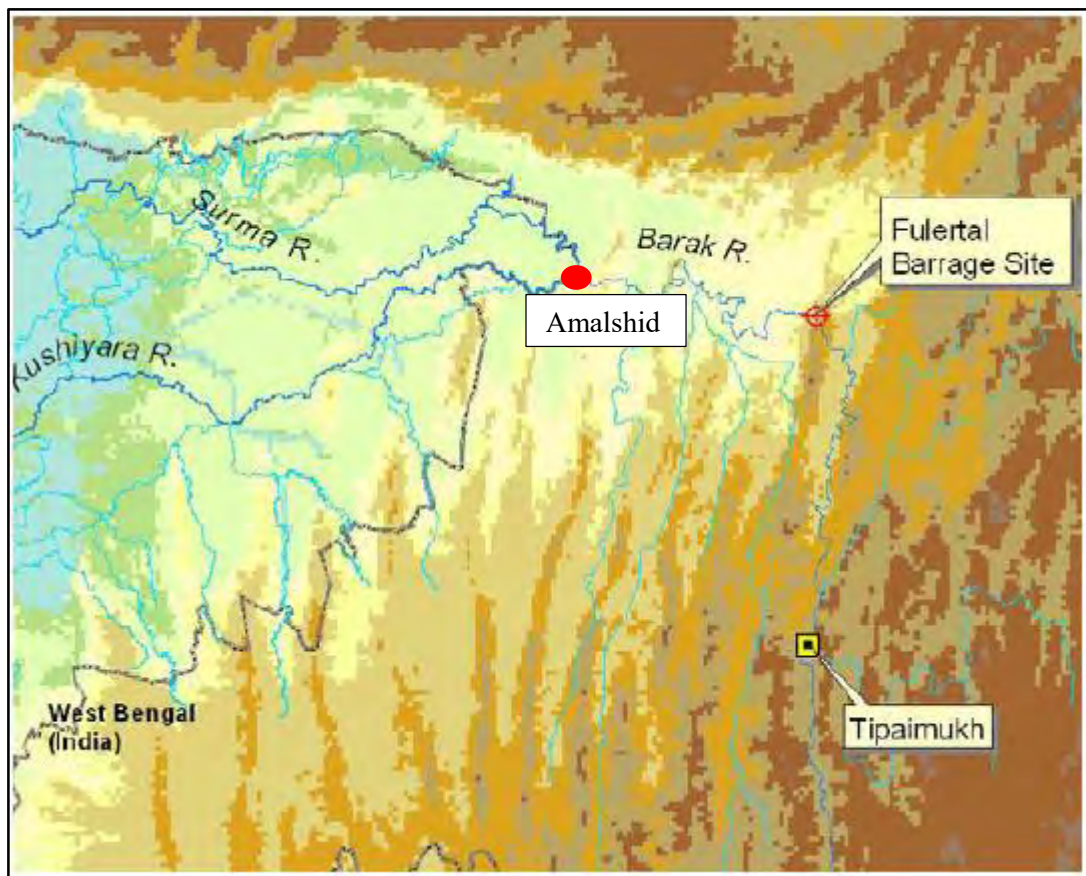


Figure 5.45 Location map of Tipaimukh dam, Fulertal barrage site and Amalshid [57]

Therefore, any changes in the Amalshid discharge indicates subsequent changes in these two rivers. Thus, the present study will estimate the changes in flow at Amalshid point due to the reservoir at Manipur to assess the impact on the Surma and Kushiya River.

5.3.1 Reservoir/Dam location

A storage reservoir/dam is placed downstream of the confluence of the Barak and Tuivai River near Tipaimukh village in Manipur state as shown in Figure 5.46. Probable hydrological change that may happen in the Barak-Surma-Kushiya river system during this reservoir operation scenario will be discussed in this chapter.

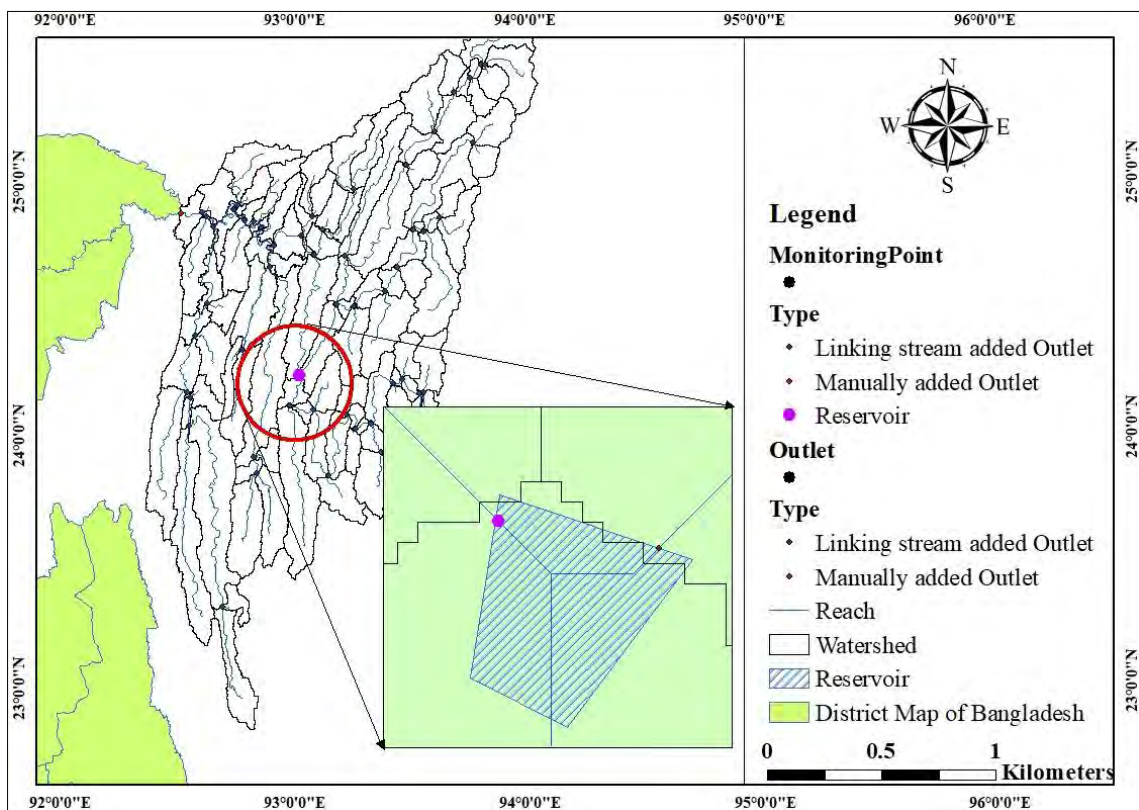


Figure 5.46 Hypothetical reservoir/dam location in the Meghna basin

The collected information from DPR on Tipaimukh Hydro Electric (Multipurpose) Project reveals some salient features of the project, which is found valuable to estimate the probable river flow during the reservoir in full operation. Using those data and information, the Barak River flow at Amalshid point for the post-dam condition has been generated, considering that the pre-dam hydrological events at Amalshid would continue

as same as it had been from 1998 to April 2018 in the future if there is no hydropower project operating on the Barak River.

5.3.2 Reservoir/Dam operation

The main constraint to operate a hypothetical reservoir/dam is the limited amount of data that will act as the basis of all boundary estimation for the upstream intervention scenario. Observed discharge data at Amalshid is available only up to 2002 in Bangladesh and observed discharge at the reservoir/dam location is not readily available in our country. Therefore, the present study used simulated discharge at the reservoir location and at Amalshid (Figure 5.47) which is quite similar to the 10-day averaged observed discharge presented in the previous study in [58].

As the inflow to the reservoir has been generated from 1998 to 2018, the outflow or release from the reservoir has been estimated after fulfilling all the conditions and provisions for the reservoir rule curve collected from the study in [58]. To estimate the possible outflow from the reservoir, outflow simulation code IRESCO 2 was used in SWAT (Figure 5.48). IRESCO 2 is generally used in SWAT to simulate controlled outflow from the reservoir/dam or the target release based on the target storage volume.

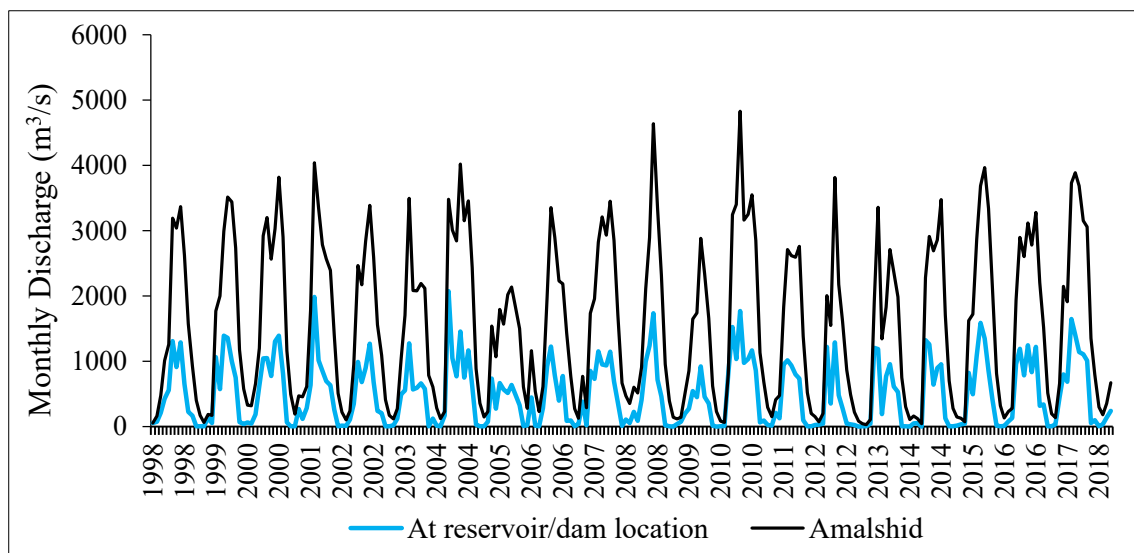


Figure 5.47 Simulated discharge at Amalshid and reservoir/dam location

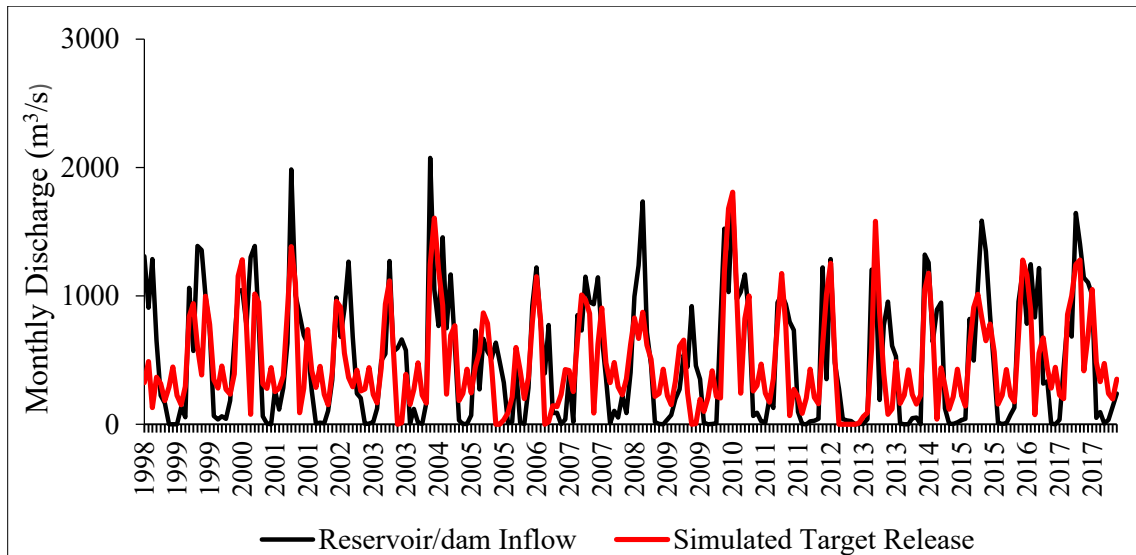


Figure 5.48 Simulated target release from the reservoir/dam

The basic reservoir operation strategy was to store the maximum amount of water for irrigation purposes in the monsoon season and to release the maximum amount of water in the lean season. Target storage volumes are estimated using the rule curve and the area capacity curve. The reservoir/dam is considered to be operational since the start of 1998. Reservoir outflow after fulfilling the demand for water storage in each month was estimated using the simulated inflow for the period of 1998-2018.

5.3.3 Post-Dam river flow at Amalshid (Present State)

Any changes in upstream flow due to flow constriction, diversion, or storage should have an impact on the downstream river. Thus any changes in the Barak river will alter the usual flow pattern of the Surma-Kushiyara river. At first the post-dam flow was simulated keeping the climatic condition same as the developed model of Meghna River basin (1998-2018). The present study found that the alteration of the natural flow of the Barak as well as of the Surma-Kushiyara River at Amalshid would be a large scale one. Post-dam river flow seems to increase in the dry period whereas peak discharge drops subsequently during the monsoon period (Figure 5.49). The reason behind this is related to the dam operation strategy where it has opted that reservoir level in each monsoon month should be maintained at rule curve level and if the unregulated inflows in the reservoir exceed the minimum release for water demands then all the surplus inflows in the reservoir should be stored.

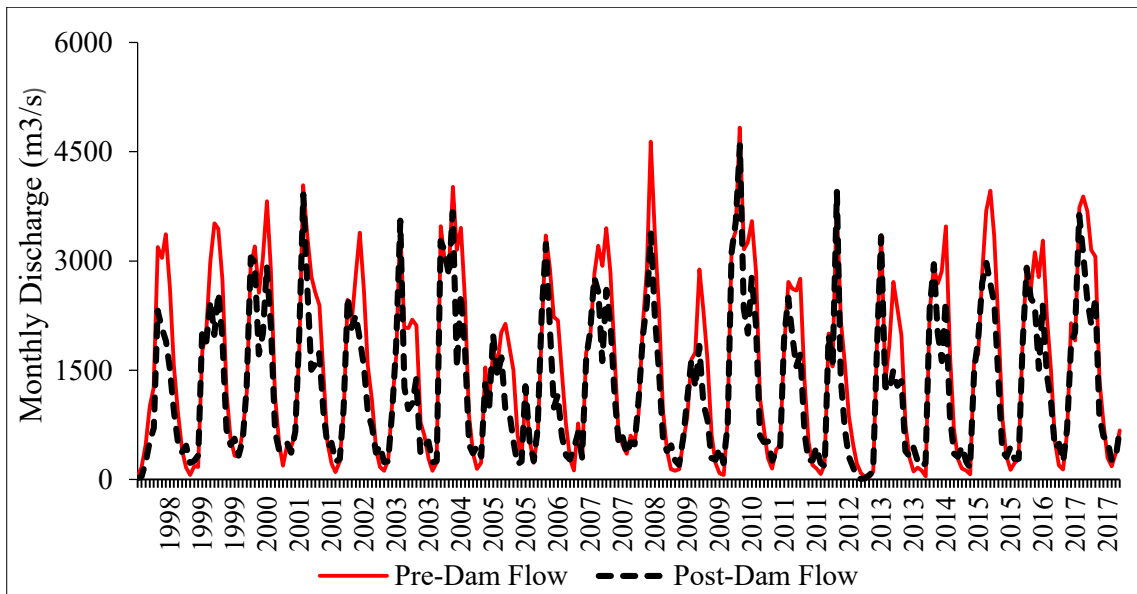


Figure 5.49 Post-dam Amalshid flow (1998-2018)

Generally, a monsoon season is called normal when the total amount of rainfall in the area between June and October is within 10 percent (plus or minus) of the average rain over a long period. Deficit rainfall is when it drops below the margin of 10 percent of the average.

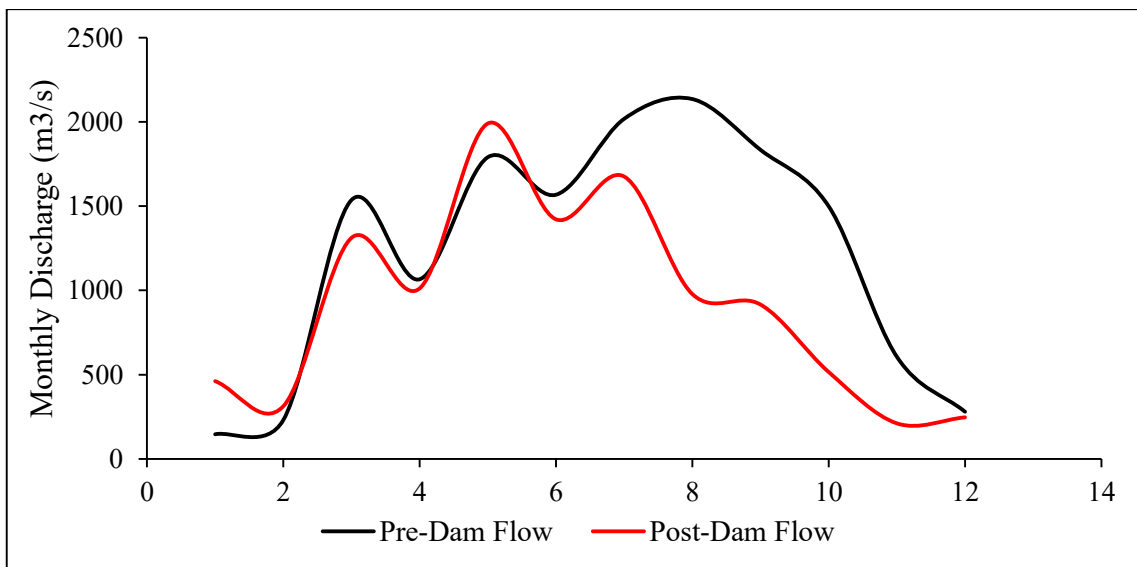


Figure 5.50 Average discharge at Amalshid in driest monsoon year (2005)

Excess rainfall is when it exceeds the average by more than 10 percent. From the analysis, it was found that for the driest monsoon year (2005), Amalshid monsoon flow for the

whole season on average would be substantially reduced due to the reservoir operation (Figure 5.50). Generally July, August, September, and October flow would be reduced on a large scale. In respect of volume, it would be on the average 9% to 65%, respectively.

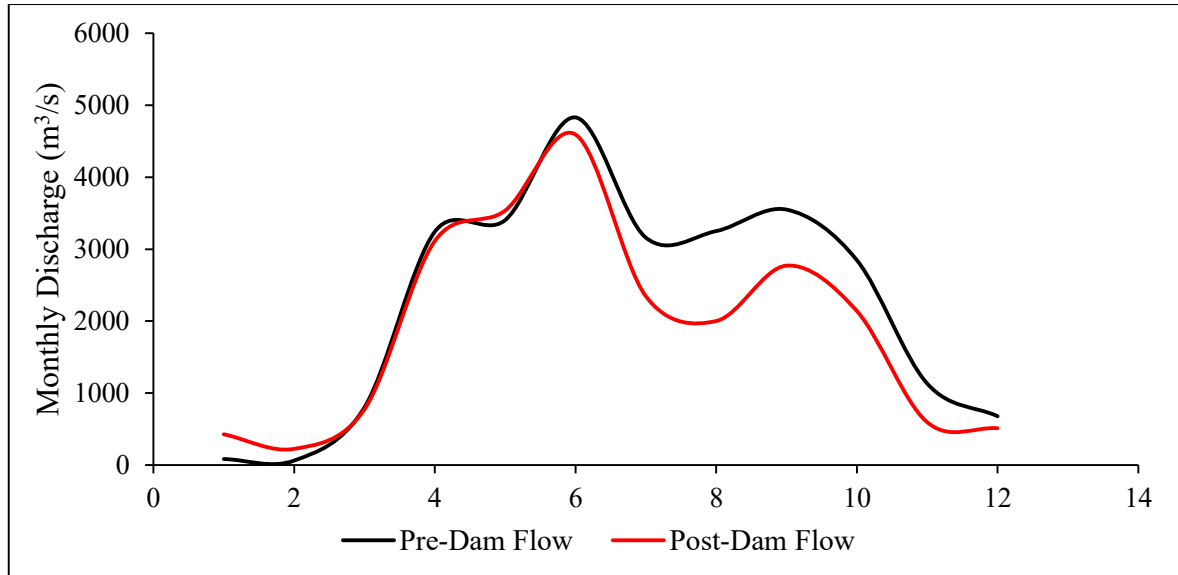


Figure 5.51 Average discharge at Amalshid in average monsoon year (1998)

Table 5.4 Available discharge in the Surma-Kushiyara river system at Amalshid during monsoon, post-monsoon and dry season for pre and post dam condition

Monsoon and Post-monsoon Season		JUN	JUL	AUG	SEP	OCT
Driest Monsoon	Pre-Dam Flow (m ³ /s)	1568.06	2018.77	2135.90	1834.42	1499.46
	Post-Dam Flow (m ³ /s)	1422.00	1676.00	978.20	916.10	515.60
	Increase/Decrease (%)	-9.31	-16.98	-54.20	-50.06	-65.61
Average Monsoon	Pre-Dam Flow (m ³ /s)	4831.40	3160.42	3251.35	3549.63	2846.52
	Post-Dam Flow (m ³ /s)	4593.00	2346.00	2001.00	2771.00	2140.00
	Increase/Decrease (%)	-4.93	-25.77	-38.46	-21.94	-24.82
Dry Season		DEC	JAN	FEB	MAR	
Driest Monsoon	Pre-Dam Flow (m ³ /s)	279.88	146.11	230.45	1536.84	
	Post-Dam Flow (m ³ /s)	246.50	461.30	312.40	1312.00	
	Increase/Decrease (%)	-11.93	215.73	35.56	-14.63	
Average Monsoon	Pre-Dam Flow (m ³ /s)	677.56	82.68	61.25	800.81	
	Post-Dam Flow (m ³ /s)	510.60	426.90	223.80	773.90	
	Increase/Decrease (%)	-24.64	416.35	265.42	-3.36	

Figure 5.51 also shows that dam operation on the Barak River would likely to have more impact in terms of overall monsoon flow reduction in normal monsoon year (1998). It is

found that July, August, September, and October flow would be reduced as much as 4% to 39% which is lower than the volume reduction found for the driest monsoon year that ranges between 9% to 65% approximately (Table 5.4). On the other hand, flow volume during dry season seems to increase in both of this year especially in January, February, and March with a maximum increase more than 200% (Table 5.5). Therefore, it can be concluded that the post-dam scenario would affect more on relatively drier monsoon years than the average monsoon year.

5.3.4 Post-Dam river flow at Amalshid (2050s)

As the reservoir is not constructed yet the current study also includes reservoir operation scenario considering the future climate. To predict near future (2040-2069) changes in the water availability of the stream flow at Amalshid, precipitation and temperature projection by wet-warm scenario and dry-cold scenario was considered. It has been observed from the simulation that if wet-warm scenario (RCP 4.5) prevails flow in dry season and in the month of will July will increase with respect to the pre dam flow (1998-2018) and the range is from 39% to more than 300%. Whereas, in the rest of the months flow at Amalshid seems to be reduced and the maximum predicted reduction is about 75%. Under RCP 8.5 flow increases from 57% to more than 120% in dry season and July and August. Flow tend to reduce within a range of -12% to -60% approximately.

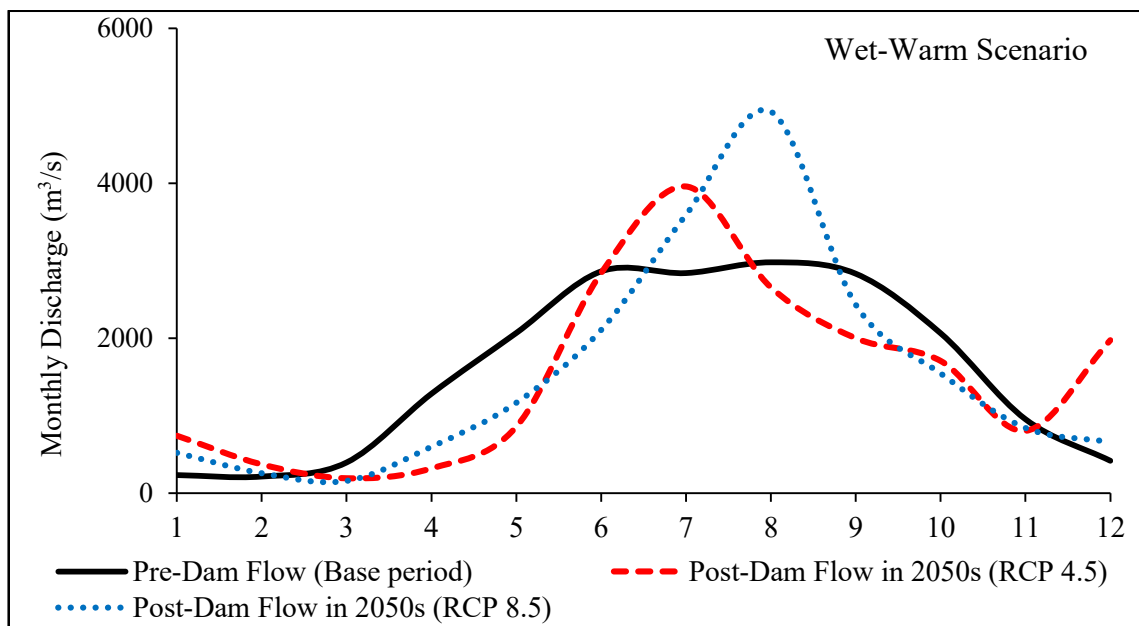


Figure 5.52 Post-dam Amalshid flow (2040-2069) under wet-warm scenario

5.3.5 Summary of the results

The following table summarizes the results of the current study-

Table 5.5 Summary of the results of scenario analyses

Analysis	Category	RCPs	Scenario	Main Results
Impact of Climate Change on Discharge	Mean Monthly Discharge	4.5	Wet-Warm	Mean monthly flow volume is higher than the reference period for each climatic period (2020s, 2050s, and 2080s). The uncertainty in monthly discharge may vary from -200% to 200%.
		4.5	Dry-Cold	Flow volume is quite closer to the base period with a slight increase in peak value over the climatic period. The basin area may experience a change that ranges between -100% to slightly more than 100% in monthly discharge each year over a particular climatic period.
		8.5	Wet-Warm	Flow volume increases gradually during the 2020s, 2050s, and 2080s. Changes in mean monthly flow volume may vary between -250% to > 400%.
		8.5	Dry-Cold	As similar to RCP 4.5, uncertainty in monthly discharge ranges between -100% to more than 100% each year over a particular climatic period.

Impact of Climate Change on Water Balance Components	Changes in Seasonal Flow	4.5	Wet-Warm	Maximum increase in the month of December to February. Seasonal flow may varies in between -50% to 100%.
		4.5	Dry-Cold	Flow decreases in all season. Maximum reduction is about 50%.
		8.5	Wet-Warm	Maximum increase in flow is observed during monsoon season. Seasonal flow may varies from -50% to about 150%
		8.5	Dry-Cold	As similar to RCP 4.5, flow decreases in all season. Maximum reduction is about 50%.
	Evapotranspiration	4.5	Wet-Warm	Evapotranspiration may vary between -25% to >100% with the maximum increase in post monsoon
		4.5	Dry-Cold	Evapotranspiration may vary between -50% to about 100% with the maximum increase in dry season and post monsoon.
		8.5	Wet-Warm	Evapotranspiration may vary between -100% to > 100% with the maximum increase in dry season and post monsoon.
		8.5	Dry-Cold	Evapotranspiration may vary between -100% to about 200% with the maximum increase in dry season and post monsoon.
Water Yield	4.5	Wet-Warm	Water yield may vary between -100% to >200% with the maximum reduction in pre- monsoon.	
	8.5	Dry-Cold	Water yield may vary between >-50% to about 100% with the maximum reduction in pre- monsoon.	

		4.5	Wet-Warm	Water yield may vary between > -50% to > 50% with the maximum reduction in pre- monsoon.
		8.5	Dry-Cold	Water yield may vary between > -60% to > 60% with the maximum reduction in pre- monsoon.
	Groundwater Contribution	4.5	Wet-Warm	Mild changes in the groundwater contribution from >- 60% to > 100 %
		8.5	Dry-Cold	Mild changes in the groundwater contribution from >- 60% to about 50%.
		4.5	Wet-Warm	Moderate change ranges from >-60% to >50%.
		8.5	Dry-Cold	Mild changes from >- 60% to about 100%.
	Percolation	4.5	Wet-Warm	The maximum increase observed is more than 400%. The least amount of losses are observed in the pre-monsoon period which is more than 60%
		8.5	Dry-Cold	Maximum increase more than 50% with maximum reduction between 65%.
		4.5	Wet-Warm	Maximum increase observed is more than 70%. The least amount of losses are observed in the pre-monsoon period which is more than 60%.
		8.5	Dry-Cold	May vary between -65% to 92% approximately.
	Lateral Flow	4.5	Wet-Warm	Maximum lateral flow contribution may vary between 19% to >400%.
		8.5	Dry-Cold	Lateral flow contribution may vary between 62% to 82%.

		4.5	Wet- Warm	Lateral flow contribution may vary between >-80% to >60%.
		8.5	Dry-Cold	Lateral flow contribution may vary between >-50% to >70%.
Impact of Upstream Intervention	Reservoir Operation	-	Base Period	Maximum flow reduction in June to October is more than 60% whereas the increase in flow volume may be more than 200% with the flow diversion scenario.
		4.5	Wet- Warm	Maximum flow may increase in dry season and in July which ranges between 39% to >300% and about 75% of flow may be reduced in other months.
		8.5	Wet- Warm	Maximum flow may increase in dry season and in July and August which ranges between 57% to >120% and about -12% to -60%.

6 CONCLUSION AND RECOMMENDATIONS

6.1 Conclusion

The present study investigated the climate change impact on the hydrology and water balance of the Meghna river basin during the periods the 2020s, 2050s, and 2080s. The study also examined the probable impact on the flow due to the construction of any reservoir on the upstream side. For this purpose, the study used a hydrological model SWAT. Based on the SWAT modeling results, the following conclusions are drawn from this study:

- From the projection of wet-warm and dry-cold scenarios, it was found that the average annual temperature of the basin is expected to increase by 2°C to 4 °C and an increase in the average annual precipitation in the basin of as much as approximately 15% to 26% under RCP 4.5 and 8.5. This synergetic effect of increase in temperature and precipitation will create a stress on the haor basin area downstream and disrupt its ecosystem and biodiversity severely.
- As fish community's lives depending on the type of the water regime, the predicted changes in river discharge under both RCP scenarios will favor one or a few of these communities and other communities will tend to migrate. Thus the reductions in flow under dry-cold scenario by 70%-80% during the driest months will result in loss of habitats for fish and other aquatic organisms. On the other hand, overall increases in flow more than 100% to 200% under wet-warm scenario will may lead an increase in habitat diversity of the basin river system.
- The hydrological regime mainly the lowlands of the Meghna river basin system is suitable to intensive rice growing. The predicted changes in the basin hydrology and the uncertainties involved in the variation of the water balance components due to climate change may have an adverse impact on this dominant cropping pattern. Thus it is needed to initiate further research and development activities to diversify the cropping pattern in this region.

- Peak flow at Amalshid could be greatly affected in the driest monsoon if similar hydrological events occur in the future with a maximum increase in the dry season by >200% and a reduction in the post monsoon by >60%. But to understand the response of a river system due to any change in hydrology or other aspects, it is necessary to characterize the river system and identify the most sensitive variables and parameters. Undoubtedly, the present study has not been in such a position to do so due to the little amount of information and without the validation of model results at the reservoir location.

6.2 Limitations

The study has the following limitations-

- For the model development in SWAT, simulated Amalshid discharge data was divided into Kushiyara and Surma River and given input as point source discharge. Observed discharge data is scarce at Amalshid point which limits the researcher to calibrate the simulated flow at Amalshid point.
- The impact of reservoir operation using SWAT could be best estimated if the with measured monthly volumes and the water level at the downstream of the reservoir were available and the simulated reservoir inflow and Amalshid discharge can be calibrated and validated.

Despite the limitations, the present study is of great importance regarding the assessment of the potential impacts of climate change and upstream intervention in the Meghna river basin. The results of this study can be implemented for the application of best management practices and agro-environmental policies.

6.3 Recommendations

The researcher has a few recommendations that may be considered for further study in the future-

1. Multipoint calibration such as calibration of total discharge at Kushiyara and Surma River can be included to understand the flow behavior of the Surma River under climate change or any other storage scenario. Future studies can extend this study for multipoint calibration in the future if possible and to assess the impact of climate change at Kanairghat station on Surma River.
2. Future studies may assess climate change impact on the haor hydrology within the Meghna river basin area to understand the haor system response to the changing climatic variables. This can be done by simulating runoff at an outlet station far downstream from the Sheola (SW 173) near Bhairab Bazar and including the scenarios of upstream catchments from the present study.
3. In the present study rainfall bias correction was done using observed rainfall from two rain gauge stations. But, eliminating anomalies in rainfall data for the flat terrain like Bangladesh require observed gridded precipitation. Future studies may include bias correction using the gridded observation data using the rainfall product of APHRODITE's (Asian Precipitation - Highly-Resolved Observational Data Integration towards Evaluation). Researcher may try other bias correction technique which provides more accuracy.
4. To understand the wide range of uncertainty of the projected precipitation and temperature, the number of outputs from the RCM model can be increased. Further studies also may include changes in land cover in addition to the climate change scenario.

7 References

Books:

- [1]. Abdul Wazed, “Bangladesher Nadimala (Rivers of Bangladesh, in Bangla)”, Dhaka, 1991; FH Khan, Geology of Bangladesh, University Press Limited, Dhaka, 1991.
- [2]. Haroun Er Rashid, “Geography of Bangladesh”, University Press Limited, Dhaka, 1991.
- [3]. Hugh Brammer, “The Geography of the Soils of Bangladesh”, University Press Limited, Dhaka, 1996.

Periodicals:

- [4]. Ali M. M., Narzis Afiya and Haque Shammi “Impact of Climate Changes on Peak Flow of Upper Meghna Basin”, Journal of PU, Part: B (Science and Engineering); Vol. 3 no.:2; July 2016 pp 54-63; issn: 2224-7610, 2016.
- [5]. Berhanu F. A, “Hydrological Modeling of Large Drainage Basins Using a GIS-Based Hybrid Atmospheric and Terrestrial Water Balance (HATWAB) Model”, Journal of Water Resource and Protection, 4, 516-522, 2012.
- [6]. Gitau F., Gitau W., Mutua F., Bauwens W., “Climate Change Impact on SWAT Simulated Streamflow in Western Kenya” 2009. International Journal of Climatology. 29. 1823 - 1834. 10.1002/joc.1828.
- [7]. Himanshu, Sushil & Pandey, Ashish & Shrestha, Prabin, “Application of SWAT in an Indian River basin for modeling runoff, sediment and water balance”, Environmental Earth Sciences. 76. 3. 10.1007/s12665-016-6316-8, 2016.
- [8]. Javed A.N. B., Jakobsen B., Khan A. S., Bhuiyan S., “Flood Characteristics of Upper Meghna River Basin, Bangladesh” 2010. International Journal of Modelling and Simulation .Volume 30- Issue 4, 2010.
- [9]. Masud, M.B.; Ferdous, J.; Faramarzi, M., “Projected Changes in Hydrological Variables in the Agricultural Region of Alberta, Canada”, Water 2018, 10, 1810, 2018.
- [10]. Mohammed, Khaled & Islam, A.K.M. & Islam, Tarekul & Alfieri, Lorenzo & Khan, Md Jamal Uddin & Bala, Sujit & Das, Mohan. (2018). Future Floods in Bangladesh under 1.5°C, 2°C, and 4°C Global Warming Scenarios. Journal of Hydrologic Engineering. 23. 04018050. 10.1061/(ASCE)HE.1943-5584.0001705.
- [11]. Mondal, M. S., Islam, A. S., Haque, A., Islam, A., Biswas, S., & Mohammed, K. (2018). Assessing high-end climate change impacts on floods in major rivers of Bangladesh using multi-model simulations. Global Science and Technology Journal, Australia, 6(2), 1–14.
- [12]. Nowreen, Sara & Murshed, Sonia & Islam, A. & Bhaskaran, Bhaski & Hasan, M. (2014). Changes of rainfall extremes around the haor basin areas of Bangladesh using multi-member ensemble RCM. Theoretical and Applied Climatology. 119. 10.1007/s00704-014-

1101-7.

Articles from published conference proceedings:

- [13]. Abbas, Nahla & Wasimi, Saleh & Al-Ansari, Nadhir & Baby, Sultana, “Recent Trends and Long-Range Forecasts of Water Resources of Northeast Iraq and Climate Change Adaptation Measures”, *Water*. 10. 1-19. 10.3390/w10111562, 2018.
- [14]. Abera, Fikru & Asfaw, Dereje & Nigussie, Agizew & Melesse, Assefa, “Climate Change Impact on the Hydrology of Tekeze Basin, Ethiopia: Projection of Rainfall-Runoff for Future Water Resources Planning”, *Water*. 10.1007/s41101-018-0057-3 , 2018 .
- [15]. Abouabdillah, Aziz & Oueslati, Ons & De Girolamo, Anna & Lo Porto, Antonio, “Modeling the impact of climate change in a Mediterranean catchment (Merguellil, Tunisia)”, *Fresenius Environmental Bulletin*, 2010.
- [16]. Alipour, Maryam & Hosseini, Majid, “Simulation of surface runoff in Karaj dam basin, Iran”, *Applied Water Science*. 8. 10.1007/s13201-018-0782-y, 2018.
- [17]. Arnold, Jeff & Moriasi, Daniel & Gassman, Philip & Abbaspour, Karim & White, Michael & Srinivasan, Raghavan & Santhi, Chinnasamy & Harmel, R. & van Griensven, Ann & Van Liew, Michael & Kannan, Narayanan & Jha, Manoj, “SWAT: Model use, calibration, and validation”,55. 10.13031/2013.42256, 2012.
- [18]. Bajracharya, Ajay & Bajracharya, Sagar & Shrestha, Arun & Maharjan, Sudan, “Climate change impact assessment on the hydrological regime of the Kaligandaki Basin, Nepal”, *The Science of the total environment*. 625. 837-848. 10.1016/j.scitotenv.2017.12.332, 2018.
- [19]. Asaduzzaman, M., & Rahman, M. M., “Impacts of Tipaimukh Dam on the Down-stream Region in Bangladesh: A Study on Probable EIA”,*Journal of Science Foundation*, 13(1), 3-10, 2016.
- [20]. Brouziyne, Y., Abouabdillah, A., Bouabid, R. et al., “SWAT manual calibration and parameters sensitivity analysis in a semi-arid watershed in North-western Morocco”, *Arab J Geosci* 10, 427, 2017.
- [21]. Chavoshian, Ali & Ishidaira, Hiroshi & Takeuchi, Kuniyoshi & Yoshitani, Junichi, “Hydrological Modeling of Large-scale Ungauged Basin Case Study: Ayeyarwady (Irrawaddy) Basin, Myanmar”, 2007.
- [22]. Dhaubanjari, Sanita & Pandey, Vishnu & Bharati, Luna., “Climate futures for Western Nepal based on regional climate models in the CORDEX-SA”, *International Journal of Climatology*. 40. 10.1002/joc.6327, 2019.
- [23]. Durieux, Laurent & Arino, O. & Frédéric, Achard & Ranera, F. & Gross, Dorit & Bicheron, P. & Latham, J. & Defourny, Pierre & Vancutsem, Christelle & Plummer, Stephen, “GLOBCOVER - A Global Land Cover Service”, 2006.
- [24]. Evans, Jason. CORDEX - An international climate downscaling initiative. 2705-2711, 2011.

- [25]. Gassman, Philip & Reyes, Manuel & Green, C. & Arnold, Jeff, “Soil and Water Assessment Tool: Historical Development, Applications, and Future Research Directions, The Transactions of the ASABE”. 50. 10.13031/2013.23637, 2007.
- [26]. Ghimire, Shreta & Choudhary, Anubhav & Dimri, A P, “Assessment of the performance of CORDEX-South Asia experiments for monsoonal precipitation over the Himalayan region during present climate: part I”, *Climate Dynamics*. 10.1007/s00382-015-2747-2, 2015.
- [27]. Ghoraba, Shima, “ Hydrological modeling of the Simly Dam watershed (Pakistan) using GIS and SWAT model”, *Alexandria Engineering Journal*. 18. 10.1016/j.aej.2015.05.018, 2015.
- [28]. Hunink, Johannes & Immerzeel, W.W. & Droogers, Peter & Kauffman, J. & van Lynden, Godert, “Impacts of Land Management Options in the Upper Tana, Kenya using the Soil and Water Assessment Tool – SWAT”, *Environmental and Experimental Botany - ENVIRON EXP BOT*, 2011.
- [29]. Islam, M.S., Islam, M.N. “Environmentalism of the poor: the Tipaimukh Dam, ecological disasters and environmental resistance beyond borders”. *Bandung J of Global South* 3, 27, 2016.
- [30]. Jain, Sharad & Jain, Sanjay & Jain, Neha & Xu, Chong-Yu, “Hydrologic modeling of a Himalayan mountain basin by using the SWAT model”, *Hydrology and Earth System Sciences Discussions*. 1-26. 10.5194/hess-2017-100, 2017.
- [31]. Jakobsen, Flemming & Hoque, A.K.M. & Paudyal, Guna & Bhuiyan, Md. , “Evaluation of the Short-Term Processes Forcing the Monsoon River Floods in Bangladesh”, *Water International*. 30. 389-399. 10.1080/02508060508691880, 2005.
- [32]. Khan, Asim Jahangir. *Selecting and Downscaling a Set of Climate Models for Projecting Climatic Change for Impact Assessment in the Upper Indus Basin (UIB)*. *Climate*. 6. 89. 10.3390/cli6040089, 2018.
- [33]. Kim, Nam & Lee, Jeong & Kim, Ji. , “Assessment of Flow Regulation Effects by Dams in the Han River, Korea, on the Downstream Flow Regimes Using SWAT”. *Journal of Water Resources Planning and Management*. 138. 24-35. 10.1061/(ASCE)WR.1943-5452.0000148, 2012.
- [34]. Leta, Olkeba T. & El-Kadi, Aly & Dulaiova, Henrieta, “Impact of Climate Change on Daily Streamflow and Its Extreme Values in Pacific Island Watersheds”. *Sustainability*. 10. 2057. 10.3390/su10062057, 2018.
- [35]. Luo, Min & Liu, Tie & Meng, Fanhao & Duan, Yongchao & Frankl, Amaury & Bao, Anming & De Maeyer, Philippe, “Comparing Bias Correction Methods Used in Downscaling Precipitation and Temperature from Regional Climate Models: A Case Study from the Kaidu River Basin in Western China”. *Water*, 2018.
- [36]. Masood M., Yeh P. J.-F., Hanasaki N., and Takeuchi K. “Model, “Study of the

Impacts of Future Climate Change on the Hydrology of Ganges–Brahmaputra–Meghna Basin”, 2015. *Hydrology and Earth System Sciences*, 19, 747–770.

[37]. Mearns, Linda & Hulme, Mike & Carter, Timothy & Leemans, Rik & Lal, Murari & Whetton, Penny & Hay, Lauren & Jones, Roger & Kittel, Timothy & Smith, J & Wilby, Robert, “Climate scenario development”, 2001.

[38]. Meng, Xianyong & Wang, Hao & Cai, Siyu & Wu, Hongjing & Ji, Xiaonan & Wang, Jianhua., “Hydrological modeling in the Manas River Basin using soil and water assessment tool driven by CMADS. *TEHNICKI VJESNIK-TECHNICAL GAZETTE*”. 24. 525-534. 10.17559/TV-20170108133334, 2017.

[39]. Mehan, Sushant & Kumar, Sandeep & Neupane, Ram, “SWAT Model Calibration, Validation and Parameter Sensitivity Analysis using SWAT-CUP”, 2015.

[40]. Mishra, Yogendra & Nakamura, Tai & Babel, Mukand & Ninsawat, Sarawut & Ochi, Shiro. “Impact of Climate Change on Water Resources of the Bheri River Basin, Nepal”. *Water*. 10. 220. 10.3390/w10020220, 2018.

[41]. M. M. Ali, A. Narzis and S. Haque, “Evaluation of Climate Change Scenarios of Upper Meghna River Basin using Hydrologic Modeling system (HEC-HMS)”, 2nd International Conference on Advances in Civil Engineering 2014 (ICACE), CUET, Chittagong, Bangladesh, 2014.

[42]. Moriasi, Daniel & Arnold, Jeff & Van Liew, Michael & Bingner, Ron & Harmel, R.D. & Veith, Tamie, “Model Evaluation Guidelines for Systematic Quantification of Accuracy in Watershed Simulations. *Transactions of the ASABE*”. 50. 10.13031/2013.23153, 2007.

[43]. Narzis, A; Haque, S and Ali, M.M , “Climate Change Scenario: Impact on Upper Meghna River Basin and Flow of Sylhet Region Using a Hydrological Model in HEC-HMS”, International conference on Climate Change in relation to Water and Environment (I3CWE), Department of Civil Engineering, DUET - Gazipur, Bangladesh, 2015.

[44]. Nazari-Sharabian, Mohammad & Taheriyoun, Masoud & Ahmad, Sajjad & Karakouzian, Moses & Ahmadi, Azadeh, “Water Quality Modeling of Mahabad Dam Watershed-Reservoir System under Climate Change Conditions, Using SWAT and System Dynamics”. *Water*. 11. 1-16. 10.3390/w11020394, 2019.

[45]. Neitsch, Susan & Arnold, Jeff & Kiniry, James & Williams, J.R. & King, Kevin, “SWAT theoretical documentation”, *Grassland*. 494. 234-235, 2005.

[46]. Prajapat, D.K., Lodha, J. & Choudhary, M., “ A spatiotemporal analysis of Indian warming target using CORDEX-SA experiment data”, *Theor Appl Climatol* 139, 447–459 <https://doi.org/10.1007/s00704-019-02978-7>, 2020.

[47]. Ramaraju, Anirudh & Mittapalli, Giridhar, “Digital Elevation Model Generation using SRTM, 2015.

[48]. Sharmin, Shuchita, “ The Tipaimukh Dam: A Threat for Bangladesh”, Dhaka

University Journal of Development Studies. 01. 261-270, 2010.

- [49]. Shiferaw, Henok & Berhe, Amdom & G., Tesfay Gebretsadkan & Abraha, Amanuel. “Modelling hydrological response under climate change scenarios using SWAT model: the case of Ilala watershed, Northern Ethiopia”, *Modeling Earth Systems and Environment*. 10.1007/s40808-018-0439-8, 2018.
- [50]. Shivhare, Nikita & Singh, Sarदार & Dwivedi, S.B. (2018), “A Comparison of SWAT Model Calibration Techniques for Hydrological Modeling in the Ganga River Watershed”, *Engineering*. 4. 10.1016/j.eng.2018.08.012, 2018.
- [51]. Tarek, Mehedi Hasan & Hassan, Adil & Bhattacharjee, Joy & Choudhury, Sayedul & Badruzzaman, Abu, “Assessment of TRMM data for precipitation measurement in Bangladesh. *Meteorological Applications*”, 24. 10.1002/met.1633, 2017.
- [52]. Uddin, Ekram & Akter, S & Uddin, Muhammad & Diganta, Mir Talas, “Trend Analysis, Variations and Relation Between Discharge and Rainfall: a Study on Kushiya River”, 2018.
- [53]. Van Liew, Michael & Arnold, Jeff & Bosch, David, “Problems and Potential of Auto-Calibrating a Hydrologic Model”, *Transactions of the American Society of Agricultural Engineers*. 48. 10.13031/2013.18514, 2005.
- [54]. Vuuren, Detlef & Edmonds, Jae & Kainuma, Mikiko & Riahi, Keywan & Thomson, Allison & Hibbard, Kathy & Hurtt, George & Kram, Tom & Krey, Volker & Lamarque, Jean-François & Masui, Toshihiko & Meinshausen, Malte & Nakicenovic, Nebojsa & Smith, Steven & Rose, Steven. The representative concentration pathways: an overview. *Climatic Change*. This issue. *Climatic Change*. 109. 5-31. 10.1007/s10584-011-0148-z., 2011.
- [55]. Wang, Yufei & Wen, Xin & Fang, Guohua & Tan, Qiaofeng & Tian, Yu & Wang, Chao & Wang, Hao, “Effects of damming and climatic change on the eco-hydrological system: A case study in the Yalong River, southwest China”, *Ecological Indicators*. 10.1016/j.ecolind.2018.07.039, 2018.
- [56]. Wickel, B. & Lehner, B. & Sindorf, Nikolai, “HydroSHEDS: A global comprehensive hydrographic dataset”, *AGU Fall Meeting Abstracts*, 2007.
- Reports:*
- [57]. FAO AQUASTAT, “Trans boundary River Basins – Ganges-Brahmaputra-Meghna River Basin”, Food and Agriculture Organization of the United Nations (FAO), Rome, Italy, 2011.
- [58]. Japan International Cooperation Agency, “Preparatory Planning Study for Meghna River Basin Management in the People’s Republic of Bangladesh”, Infrastructure Development Institute - Japan Yachiyo Engineering Co., Ltd., 2011.
- [59]. Khan S. A., Masud S. Md. and Palash W., “Hydrological Impact Study of Tipaimukh Dam of India on Bangladesh”, Institute of Water Modelling (IWM), 2005.
- [60]. Water Resources Systems Division National Institute of Hydrology, “Hydrology and

Water Resources Information System for India”, Jalvigyan Bhawan, Roorkee - 247 667, India.

Theses:

- [61]. Alam S., “Impact of Climate Change on Future Flow of Brahmaputra River Basin using SWAT Model”. M.Sc. Engg. Thesis, Bangladesh University of Engineering & Technology (BUET), Dhaka, Bangladesh, 2015.
- [62]. Haque, S. and Narzis, N., “Climate change Scenario of Upper Meghna River Basin using a Hydrological Model in HEC-HMS”. B.Sc. Engg. Thesis, Bangladesh University of Engineering & Technology (BUET), Dhaka, Bangladesh, 2014.
- [63]. Khan I., “Effect in the Water Balance of the Teesta River Basin due to Different Climate Changes and Upstream Development” 2018. M.Sc. Engg. Thesis, Bangladesh University of Engineering & Technology (BUET), Dhaka, Bangladesh.
- [64]. Rahaman, A. (2019). Climate Anomalies of Bangladesh using Statistically Downscaled Climate Projections for Representative Concentration Pathways (RCPs). M.Sc. Engg. Thesis, Bangladesh University of Engineering & Technology (BUET), Dhaka, Bangladesh.
- [65]. Rahat S. H., “Impact Assessment of Future Climate scenario on the Upper Meghna Basin using HEC-HMS” B.Sc. Engg. Thesis, Bangladesh University of Engineering & Technology (BUET), Dhaka, Bangladesh. 2016.
- [66]. Rahman, MM. (2017). Modelling climate change impacts on the water regimes of the river-wetland systems in the data-scarce transboundary Upper Meghna River Basin (Bangladesh and India).
- [67]. Setegn, G. S., “Modelling Hydrological and Hydrodynamic Processes in Lake Tana Basin, Ethiopia” PhD Thesis, KTH, School of Architecture and the Built Environment (ABE), Land and Water Resources Engineering, Hydraulic Engineering, Stockholm, 2010.